



Bsc. Thomas Rabensteiner

**Extension and Validation of an Expert-Tool for the
Assessment and Adjustment of Powertrain Systems**

Submitted in Partial Fulfillment of the Requirements for the Degree of
Master of Science

Master's programme - Mechanical Engineering and Business Economics

Graz University of Technology
Faculty of Mechanical Engineering and Economic Sciences

Institute of Automotive Engineering
Member of Frank Stronach Institute

Supervisors:

Univ.-Doz. Dipl.-Ing. Dr. techn. Arno Eichberger

Dipl.-Ing. Mario Vockenhuber

Graz, 16.05.2013

Restricted access until 16.05.2015

Acknowledgement

This thesis has been undertaken by order of Magna Powertrain, with support of the Institute of Automotive Engineering.

Particularly, I would like to express my sincere thanks to my company supervisor Dipl.-Ing. Mario Vockenhuber for welcoming me into his project and his professional support throughout the creation of this thesis.


Furthermore, I would also like to thank my university supervisor Univ.-Doz. Dipl.-Ing. Dr. techn. Arno Eichberger, who has supported my work by means of his experienced advices in our meetings.

Finally, I would like to thank my parents Anneliese and Gerhard, who are always there for me and encouraged me throughout my work on this thesis. Of course, I also have to thank my sisters Martina and Julia, who have been very entertaining flat mates during my years of study in Graz.

Statutory Declaration


Ich erkläre an Eides statt, dass ich die vorliegende Arbeit selbstständig verfasst, andere als die angegebenen Quellen/Hilfsmittel nicht benutzt, und die den benutzten Quellen wörtlich und inhaltlich entnommenen Stellen als solche kenntlich gemacht habe.

Graz, am.....16/5/2013.....


.....
(Unterschrift)

I declare that I have authored this thesis independently, that I have not used other than the declared sources / resources, and that I have explicitly marked all material which has been quoted either literally or by content from the used sources.

.....16/5/2013.....
date


.....
(signature)

Abstract

During the last decades, four-wheel drive systems have changed from pure mechanical traction systems, which were mainly designed for off-road use, to complex mechatronic solutions. Due to the possibility of 4WD systems to provide a positive impact on the vehicle's driving behavior, they are more and more applied for everyday road traffic.

The variety of different transfer case systems is huge. On this point, different OEMs rely on distinct concepts. Generally, transfer case systems can be classified into active, semi-active or passive systems. Most of Magna Powertrain's transfer case concepts rely on an active torque distribution by means of an externally controlled multi-plate wet clutch. This technology can be considered as the company's core competence.

This thesis deals with the analysis and evaluation of externally controlled transfer case systems for road tests and simulations. First designs of engineers base on their expert knowledge and their experience. A vehicle will not be released for series production until the driving dynamical adjustment is completed. During the development phase engineers that integrate the customer's requirements, bear the responsibility. The engineer affects the direction of the adjustment and has to rely as well on his subjective driving impressions as on returned objective assessment criteria from road tests or simulations.

Since the adjustment of drivetrain systems in the mechatronic environment of modern motor vehicles requires expert knowledge and experience, Magna Powertrain took the attempt to integrate specific knowledge of the fields pre-adjustment, analysis and fine-tuning into an applicable expert-tool. Within the design and adjustment stage of a four-wheel drive system, conflicting goals occur between traction, driving dynamics, comfort, system load and efficiency requirements. Therefore, the evaluation of the assessment criteria within the expert-tool has been classified according to these adjustment goals.

To optimize the quality of the achieved development- and adjustment progress, the driving states the expert-tool extracts have been extended by assessment criteria and substitution calculations. Assessment criteria have been found for different driving states, such as braking or cornering. Furthermore, substitution calculations, such as the determination of the steering tendency or an approach to quantify binding in the drivetrain have been implemented within the scope of this thesis.

Kurzfassung

Im Laufe der letzten Jahrzehnte haben sich Allradantriebskonzepte von rein mechanischen, zu komplizierten mechatronischen Traktionssystemen weiterentwickelt. War früher vor allem die Erhöhung der Geländegängigkeit Zweck eines Allradantriebs, so finden Allradantriebe heute, aufgrund ihrer Möglichkeit das Fahrverhalten positiv zu beeinflussen, auch immer mehr Anwendung im alltäglichen Straßenverkehr.

Eine hohe Anzahl an technisch unterschiedlichen Allradsystemen bestimmt den Markt. Jeder OEM vertraut auf unterschiedliche Antriebskonzepte. Generell jedoch, können Verteilergetriebe in aktive, semi-aktive und passive Systeme eingeteilt werden. Die meisten Verteilergetriebekonzepte bei Magna Powertrain beruhen auf einer aktiven Momentenverteilung über eine extern regelbare Lamellenkupplung. Diese Technologie kann als Kernkompetenz der Firma betrachtet werden.

Die vorliegende Diplomarbeit befasst sich mit der Analyse und Bewertung von Verteilergetrieben im Rahmen des Fahrversuchs sowie der Simulation. Erste Auslegungen durch den Ingenieur beruhen oft auf Fachwissen und Erfahrung. Ein Fahrzeug wird erst dann für die Serie freigegeben, wenn die Abstimmung nach vielfältigen Kriterien abgeschlossen ist. Die Verantwortung in der Entwicklung tragen Ingenieure, die die Interessen des Kunden in die Fahrzeugkonzeption integrieren. Der Ingenieur beeinflusst die Richtung der Abstimmung und muss sich auf seine subjektiven Fahreindrücke sowie aus Signalen extrahierte objektive Bewertungsgrößen aus Fahrversuchen bzw. Simulationen verlassen können.

Da die Aufgabe der Abstimmung von Antriebsstrangsystemen im Gesamtumfeld vernetzter mechatronischer Systeme moderner Kraftfahrzeuge hohes Fachwissen und Erfahrung erfordert, wurde bei Magna Powertrain spezifisches Wissen aus den Bereichen Vorabstimmung, Analyse und Feinabstimmung in ein anwendbares Expertentool integriert. In der Entwicklungs- und Abstimmungsphase eines Allradkonzepts treten Konflikte zwischen den Auslegungszielen Traktion, Fahrdynamik, Komfort, Systembelastung und Effizienz auf. Aus diesem Grund wurde die Auswertung der Bewertungskriterien hinsichtlich dieser Ziele klassifiziert.

Um die Analysetiefe und Qualität der Entwicklung bzw. Abstimmung zu optimieren, wurde das Expertentool im Rahmen dieser Diplomarbeit um geeignete Bewertungskriterien und Modellrechnungen erweitert bzw. wurden bestehende Bewertungskriterien validiert. Bewertungskriterien wurden zum Beispiel für die Fahrzustände Bremsen und Kurvenfahrt hinzugefügt. Des Weiteren wurden dem Experten-tool Ersatzrechnungen, wie zum Beispiel eine Möglichkeit zur Berechnung der Steuertendenz oder ein Ansatz zur Quantifizierung von Verspannungen im Antriebsstrang, im Rahmen dieser Arbeit hinzugefügt.

Table of Contents

Acknowledgement	iii
Statutory Declaration	v
Abstract	vii
Kurzfassung	ix
Table of Contents	xi
Abbreviations	xiii
Symbols	xv
1 Introduction	1
1.1 Magna Powertrain	1
1.2 Motivation	1
1.3 Project Description	3
2 Fundamentals	5
2.1 Linear Single-Track Vehicle Model	5
2.2 Circle of Forces	9
2.3 Four-Wheel Drive Systems	12
2.3.1 System Classification	14
2.3.2 Externally Controlled Multi-Plate Clutch	16
2.3.3 Active Dynamic Stability Control	20
2.3.4 Steering Tendencies	21
2.3.5 Active Traction Control	22
2.3.6 Adaption to ESP	22
3 Assessment of Driving States and Maneuvers	25
3.1 Driving Maneuvers	26
3.1.1 Steady-State Circular Driving Behavior	28
3.1.2 Non-Steady-State Steering Conditions	34
3.2 Classification of Driving States	38
3.3 Stability/Agility	43
3.3.1 Stability	44
3.3.2 Agility	46
4 Implementation of Substitution Calculations	47
4.1 Current Yaw Rate	48
4.2 Target Yaw Rate	48
4.3 Steering Tendency	49

4.4	Side Slip Angle	50
4.4.1	Side Slip Rate Estimation	51
4.4.2	Luenberger Observer	53
4.4.3	Kalman Filter	55
4.5	Effective Torque Distribution	56
4.6	Binding	57
4.7	Adaption of the Graphical User Interface in Matlab	61
5	Implementation of new Assessment Criteria	63
5.1	Standstill	64
5.2	Driveaway	68
5.3	Upshift	72
5.4	Downshift	74
5.5	Braking	77
5.6	Acceleration	81
5.7	4WDASR	84
5.8	Cornering	87
5.9	Turning into a Curve	90
6	Summary	91
	List of Figures	93
	List of Tables	95
	Bibliography	97

Abbreviations

Abbreviation	Full text
4WD	Four-Wheel Drive
4WDASR	Four-Wheel Drive Anti-Slip Regulation
ABS	Anti-Lock Control
ASR	Anti-Slip Regulation
ATC	Active Torque Control
AWD	All-Wheel Drive
CCC	Center Coupling Control
CoG	Center of Gravity
DSC	Dynamic Stability Controller
ESC	Electronic Stability Control
ESP	Electronic Stability Program
GUI	Graphical User Interface
HIL	Hardware in the Loop
LSD	Limited Slip Differential
NHTSA	National Highway Traffic and Safety Administration
OEM	Original Equipment Manufacturer
SUV	Sport Utility Vehicle
TCS	Traction Control System
veDYNA	TESIS DYNAware GmbH Driving Dynamics-Software

Symbols

Matrices

<i>Symbol</i>	<i>Unit</i>	<i>Description</i>
A	-	System matrix
B	-	Input matrix
C	-	Output matrix
D	-	Feedthrough matrix
I	-	Identity matrix
K	-	Gain matrix
$P_{\theta,k}$	-	Measurement noise covariance matrix
$P_{x,k}$	-	Estimation error covariance matrix
$P_{\xi,k}$	-	System noise covariance matrix

Vectors Latin Symbols

<i>Symbol</i>	<i>Unit</i>	<i>Description</i>
r	m	Radius vector in CoG
u	-	Input vector
v	m/s	Velocity vector in CoG
v_f	m/s	Velocity vector front axle
v_r	m/s	Velocity vector rear axle
x	-	State vector
\hat{x}	-	Estimation of the state vector
\hat{x}^-	-	Predicted state
\tilde{x}	-	Estimation error
y	-	Output vector

Vectors Greek Symbols

<i>Symbol</i>	<i>Unit</i>	<i>Description</i>
θ_k	-	Measurement noise
ω	°/s, rad/s	Angular velocity vector in CoG
ξ_k	-	System noise

Variables Latin Symbols

<i>Symbol</i>	<i>Unit</i>	<i>Description</i>
a_n	m/s ²	Radial acceleration
a_t	m/s ²	Tangential acceleration
a_x	m/s ²	Longitudinal acceleration
a_y	m/s ²	Lateral acceleration
br	-	Brake pedal
c_α	N/°, N/rad	Cornering stiffness
cl	-	Clutch opening
C	1/s	Constant term
EG	°·s ² /m	Self-steering gradient:
f	Hz	Sampling rate
f_{corr}	-	Correction term
$gear$	-	Inserted gear
F_G	N	Weight force
F_R	N	Friction force
F_{SO}	-	Spinout criterion
F_t	N	Inertial force
g	m/s ²	Gravitational acceleration
h	m	Height of the CoG
i_{axle}	-	Axle ratio
i_S	-	Steering ratio
i_{sync}	-	Gear box ratio
J	kg·m ²	Moment of inertia
l	m	Vehicle length
l_f	m	Distance between CoG and front axle
l_r	m	Distance between CoG and rear axle
$lock_{sr}$	%	Overlocking time
$lock_{srmean}$	%	Overlocking torque
m	kg	Vehicle mass
M_S	Nm	Steering moment
M_ψ	Nm	Yaw moment
n_{idle}	rpm	Idle speed
n_{mot}	rpm	Engine speed
O	-	Velocity pole
P_{cl}	kW	Cutch power
p_{br}	Pa	Braking pressure
R	m	Curve radius
sl_{curve}	-	Kinematic curve slip
s	m	Course deviation, Braking distance
S	%	Locking value
t	s	Time

th	%	Throttle opening
T	Nm	Torque
T_d	Nm	Drag torque
T_{gb}	Nm	Torque after gear box
T_{high}	Nm	Torque on high traction surface
T_{low}	Nm	Torque on low traction surface
T_{max}	Nm	Maximum clutch capacity
T_{mot}	Nm	Engine torque
T_t	Nm	Target torque
TB	$^{\circ}\cdot s, rad\cdot s$	TB value
TBR	-	Torque bias ratio
TSR	-	Torque split ratio
u	m	Arclength
U	%	Overshoot value
v	m/s	Velocity
v_x	m/s	Longitudinal velocity
v_y	m/s	Lateral velocity
W	J	Work
W_{cl}	J	Clutch work
x_{dis}	-	Torque distribution
x_{over}	-	Overlocking

Variables Greek Symbols

<i>Symbol</i>	<i>Unit</i>	<i>Description</i>
α	$^{\circ}, rad$	Tire slip angle
β	$^{\circ}, rad$	Side slip angle
$\dot{\beta}$	$^{\circ}/s, rad/s$	Side slip rate
γ	$^{\circ}, rad$	Angle total force
δ	$^{\circ}, rad$	Steering angle
δ_A	$^{\circ}, rad$	Ackermann steering angle
δ_S	$^{\circ}, rad$	Steering wheel angle
ε	-	Model design parameter
φ	$^{\circ}, rad$	Roll angle
κ	1/m	Curvature
κ_{corr}	1/m	Corrected curvature
μ	-	Coefficient of friction
μ_{util}	-	Friction utilization
ω	$^{\circ}/s, rad/s$	Angular velocity
ω_z	$^{\circ}/s, rad/s$	Yaw rate
$\dot{\omega}_z$	$^{\circ}/s^2, rad/s^2$	Yaw acceleration
ψ	$^{\circ}, rad$	Yaw angle

Indices

<i>Symbol</i>	<i>Description</i>
$(\cdot)^-$	Prediction step Kalman filter
$(\cdot)_c$	Current
$(\cdot)_{\text{calc}}$	Calculated
$(\cdot)_{\text{est}}$	Estimated
$(\cdot)_f$	Front
$(\cdot)_i, (\cdot)_j, (\cdot)_k$	Control variables
$(\cdot)_{\text{max}}$	Maximum value
$(\cdot)_{\text{mean}}$	Mean value
$(\cdot)_{\text{min}}$	Minimum value
$(\cdot)_r$	Rear
$(\cdot)_{\text{sim}}$	Simulated
$(\cdot)_{\text{stat}}$	Steady-state condition
$(\cdot)_t$	Target
$(\cdot)_{\text{tot}}$	Total
$(\cdot)_x$	Longitudinal direction
$(\cdot)_y$	Lateral direction
$(\cdot)_z$	Vertical direction

1 Introduction

With increasing prosperity, the number of four-wheel drive vehicles that represent first-class driving comfort and driving dynamics has increased constantly over the last years. If you trust predictions this movement will continue and the demand will even increase. Especially the boom in sales of SUVs, which are nearly entirely equipped with a four-wheel drive system, contributes to the rise of four-wheel drive vehicles on the roads of this world. In 1979 only 10 000 four-wheel drive vehicles were sold in Germany. According to [30], the number of sold 4WD vehicles increased up to 130 000 by 2002 and the upswing is still continuing. As statistics from the website of the German Federal Motor Transport Authority confirm, the number of four-wheel drive vehicles is still growing rapidly. In 2009 around 2 million four-wheel drive vehicles were registered in Germany [7]. This equaled 4.88 % of all registered passenger cars. In 2012 already 2.95 million 4WD vehicles have been registered, which equaled already 6.8 % [8]. Manufacturers have recognized this movement and try to meet the customers' needs. Today, no OEM can afford not having a 4WD model in its vehicle portfolio. The automotive manufacturer BMW even indicates that the number of vehicles sold, that are equipped with their AWD system X-Drive, reaches already 50 % of the total number of sales [2].

1.1 Magna Powertrain

This thesis has been undertaken by order of Magna Powertrain. Magna International Inc. is an international supplier for the automotive industry. With its various subsidiaries Magna International is capable to manufacture a whole vehicle. Its subsidiary Magna Powertrain develops and produces mechanically and electronically controlled drivetrain systems. At the plant in Lannach/Austria transfer cases are designed and manufactured. The development and production of externally controlled multi-plate clutches belongs to the company's core competencies.

1.2 Motivation

To meet the demand of high quality driving comfort and driving dynamics the requirements on a transfer case system increase with the expectations. Furthermore, modern four-wheel drive vehicles have to face environmental standards concerning efficiency and fuel consumption. To satisfy these expectations a consensus between driving comfort, traction, driving dynamics and efficiency has to be found. Therefore, an appropriate adjustment of the vehicle's transfer case system is indispensable.

The variety of different transfer case systems is huge. On this point, different OEMs trust on distinct concepts. Magna Powertrain offers a wide range of different transfer cases with various torque distribution alternatives to their customers. Most of these concepts rely on a torque distribution between the front and the rear axle by an externally controlled multi-plate wet clutch. This technology can be seen as the company's core competence.

Within the adjustment and implementation phase of an electronically controlled transmission case, the vehicle controller has to be programmed and adapted corresponding to the customer's preferences. First designs are mostly based on expert knowledge that is provided by the experience of engineers.

During the development stage, simulations and test drives are undertaken in order to test the performance of the powertrain system. A vehicle is not released for series production before a proper tuning with regard to driving dynamics is completed. The engineer influences the direction of the adjustment and has to rely on his subjective driving impressions and the available objective assessment criteria he has at his disposal. Especially objective assessment criteria concerning system load or efficiency are becoming increasingly important as the test driver cannot perceive their magnitude and impact.

Therefore, the adjustment of a powertrain system requires expert knowledge and experience. At Magna Powertrain an attempt has been undertaken to create an expert software tool that integrates specific knowledge within the field of pre-adjustment, analysis and fine tuning. In the system design process the tool can ideally be used for the evaluation of early vehicle simulations, for test bench evaluations and of course for the evaluation of real road test drives. The software is based on Matlab, Simulink and Microsoft Excel. Easy handling for the user is ensured by an easy manageable graphical user interface. The tool should support inter-divisional working as the tool can be used from earliest development stages up to entirely developed series operation. The tool can be helpful to document the development progress of the distinct stages. In addition, the tool has been kept easy to extent for further modifications. Information about the integration of the expert-tool into the development environment of a modern vehicle can be found in earlier publications concerning the expert-tool, as for example in [34].

To support the developing engineer with non-perceivable intelligence the software returns information in the fields driving dynamics, efficiency, system load, comfort and traction. Figure 1.1 shows the integration of the expert-tool within the layout and development process. The fine-tuning process, as well as the whole tuning process of a transfer case system can be considered as a loop. As seen in Figure 1.1 the evaluation results of simulations and test drives are depending on the setup, which in turn depends on expert-knowledge of experienced engineers.

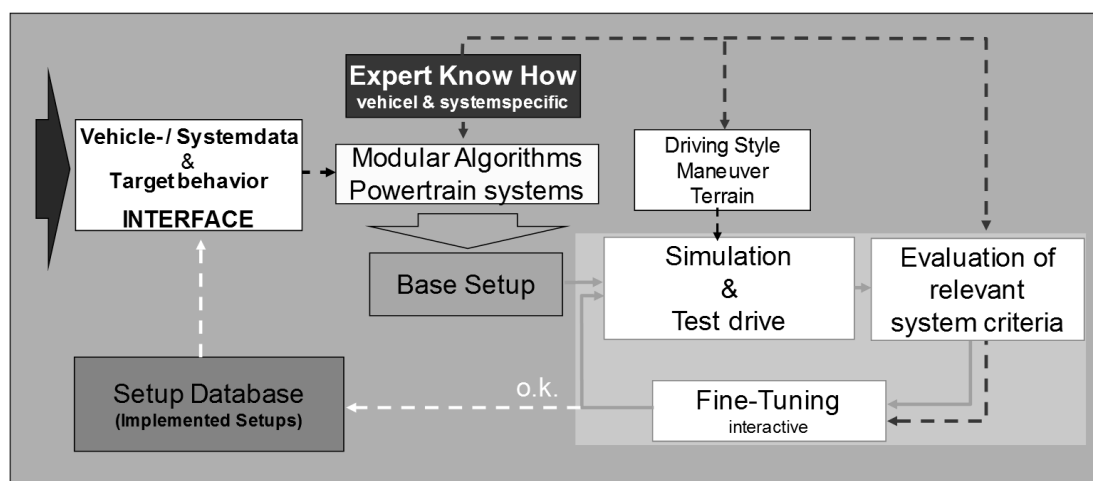


Figure 1.1: Configuration and environment of the expert-tool [34]

The output quality of the software depends on the assessment criteria. After a carried out analysis, vehicle specific setup and logic parameters can be modified according to the results. The modification and developing process can therefore be considered as a loop as shown in Figure 1.1. A meaningful and high-quality output is of high importance and contributes to a fast development. The goal of this thesis was to extent the expert-tool with additional assessment criteria and substitution calculations.

1.3 Project Description

The output quality of the expert-tool depends on the provided assessment criteria. The main goal of this master thesis was to extend the already existing expert-tool by finding new assessment criteria for the analysis of a simulation or a road test. A further task was to verify the existing assessment criteria.

As the tool can be used for the evaluation of real road tests, as well as for the evaluation of simulation data, the verification task includes the control of the available input parameters. For standard road tests, input signals are very often not available by default or have not been measured, because the effort or the costs exceed the gain. However, sometimes certain data signals can easily be reconstructed by vehicle model substitution calculations. To prevent errors, a task was the implementation of substitution calculations for input parameters that have not been measured, but can be recalculated. Therefore, substitution calculations concerning driving dynamics, such as the calculations of the yaw rate ω_z or the side slip angle β have been implemented. Also transfer case specific substitution calculations, such as the determination of binding in the drivetrain have been implemented within this thesis.

Furthermore, guidance values for the newly added assessment criteria had to be found from simulations, driving tests or literature entries. During the work on these points, the Matlab graphical user interface of the software had to be adapted according to the modifications. A further goal of the thesis was to prepare the software for the introduction of internal operations.

Within the design and adjustment stage of a four-wheel drive system, conflicting goals occur between traction, driving dynamics, comfort, system load and efficiency requirements. This justifies the assessment criteria classification for the evaluation according to these categories. Furthermore, the criteria have been distinguished according to their origin. Therefore, the criteria have been classified into driver-, vehicle- and system-related criteria. The output criteria have been classified according to these categories as listed in Table 1.1.

An efficient 4WD system has to be compact and light in weight at the expense of the maximum system load. A more compact clutch will reach its torque peak values sooner, which results in an earlier thermal shutdown. Weight reduction in order to improve the vehicle's efficiency, affects the traction, as well as the driving dynamic performance [34].

Table 1.1: Assessment criteria classification

Operation Criteria		Driving Criteria		
Efficiency	System load	Vehicle dynamics	Comfort	Traction
System-related		Vehicle-related	Driver-related	

It is important to distinguish between operation-relevant criteria that are subjectively not noticeable and driving-relevant criteria that are subjectively noticeable by the driver. In contrast to the objective evaluation of the vehicle's drivability by reproducible criteria that depends on subjective impression, it is for example less complicated to determine the vehicle's fuel consumption or exhaust emissions that follow well established standards or legal requirements. A very common method for the evaluation of subjective driving impressions is to evaluate a sequence of relevant driving maneuvers by the

implementation of a rating system that bases on the subjective assessment of experienced test drivers. An example of a method for a subjective rating system can be found in [11].

Operation-relevant criteria are of high importance as the test driver cannot recognize and rate the effects he cannot feel. On the other hand, it is of high importance to convert subjectively noticeable impact on the driving behavior into physical assessment criteria. Within the scope of this thesis, criteria have been found and evaluated for these areas.

The analysis of a road test or a simulation always relies on the available measurement data. For a simulation nearly every desired data signal will be available. On the other hand, only data which has actually been measured is available for the evaluation of a real road test. However, very often a signal has not been measured and is needed for the evaluation. In this case many signals can be reproduced by available signals and substitution calculations that follow the kinematic relations of vehicle models as for example the linear single track model. If a physical connection cannot be indicated with simple equations, the reproducibility gets more complex or is not possible at all. An example for such a challenge is the retroactive calculation of the side slip angle β . For an accurate reconstruction sophisticated observation techniques as the Kalman filter or the Luenberger observer have to be applied to receive a high-quality data signal. Within the scope of this thesis the software has been extended by queries that evaluate the reproducibility of a nonexistent signal and the related substitution calculations.

2 Fundamentals

This thesis deals with the search for new assessment criteria to evaluate transfer cases with the focus on externally controlled multi-plate clutch systems. The scope of work does not only request criteria concerning the system itself, but also driver- and vehicle-related criteria. Therefore, not only the understanding of a transfer case system, but also to understand fundamental driving dynamics is important. To describe the dynamic behavior of a vehicle, dynamic vehicle models have been created. A famous vehicle model for lateral dynamics is the so called linear single-track model.

2.1 Linear Single-Track Vehicle Model

The linear single-track model, or also called bicycle model, is a simple vehicle model for the description of lateral vehicle dynamics. According to [10], the model was defined by Dr. Riekert and Dr. Schunk in 1940. It describes the vehicle's reaction on a steering input. Because of its simplifications and assumptions it is only valid within the linear range of driving dynamics. As seen in Figure 2.1 the limited linear operating range results due to a declining characteristic curve of the lateral tire force F_y as a function of the tire slip angle α . In [22], Pfeffer explains the reason for the limitation of the linear operating range. The lateral tire force results from lateral deformation of the tire's wheel tread. This deformation demands a relative movement in lateral direction between the tire's belt and the road surface. This deformation is caused by the tire slip angle. The tire profile is deformed in the tire contact patch as long as the non-positive connection is sufficient. This is the case for lateral accelerations beneath 3 - 4 m/s^2 on dry road surfaces. At higher lateral accelerations the tire profile begins to slip on the road. Within this range, the simplification to calculate the lateral force F_y , that affects the tire, can be made by introducing the cornering stiffness c_α :

$$F_y = c_\alpha \cdot \alpha . \quad (2.1)$$

As seen in Figure 2.1 this linear tire model is only valid for small tire slip angles. Due to the characteristic curve of the declining cornering stiffness the linear bicycle model is furthermore only valid up to the lateral acceleration of approximately 4 m/s^2 . At this threshold, many vehicles leave the linear range. Some still show linear behavior up to a boundary of 6 m/s^2 . Due to the reason that a vehicle stays beneath the boundary value of 4 m/s^2 in the most driving situations the model is broadly used at industrial applications and even for the observation of online driving dynamics in driver assistance systems. The range above 6 m/s^2 is only reached in extreme situations as race driving or in situations with accident risk in normal road traffic [25].

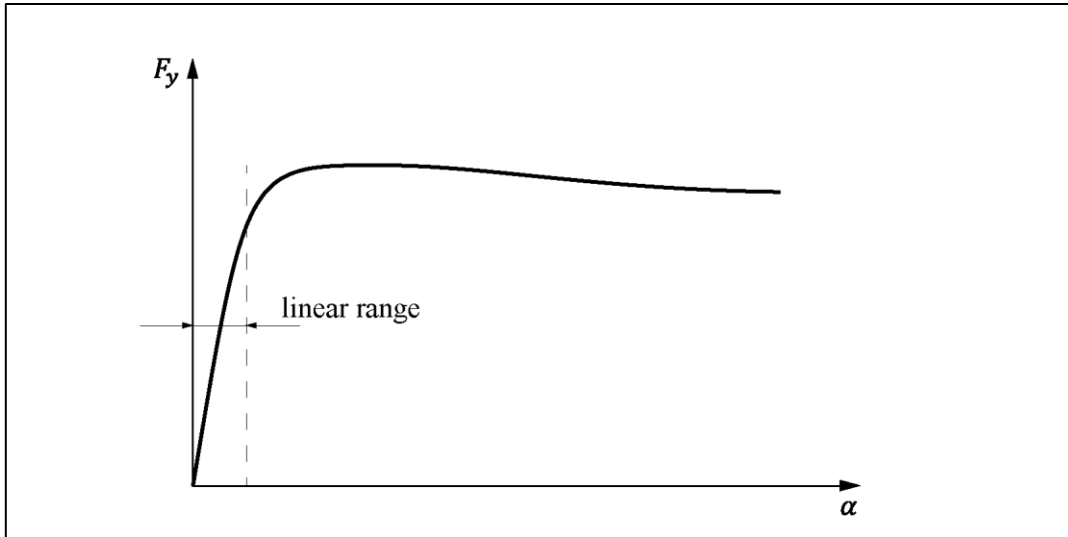


Figure 2.1: Typical characteristic of the lateral force F_y over the tire slip angle α

The big advantage of this model is that the number of degrees of freedom is reduced, but the analysis results within the linear driving range are not affected significantly. To derive the model, the following assumptions have to be made: [10], [28]

- The driving speed v is constant and the tangential acceleration a_t consequently is zero:

$$a_t = \frac{dv}{dt} = 0 . \quad (2.2)$$

- The center of gravity is located on the height of the road and the total mass m is centralized in the center of gravity.
- Front and rear wheels are combined to one wheel in the middle of the axle. (bicycle model)
- Pneumatic trails are neglected.
- The wheel load distribution is constant.
- Roll and pitch rotations are not possible due to the center of gravity's position and the constant wheel load distribution between the front and the rear axle. Vertical movements are neglected as well.
- No longitudinal forces on the tire:

$$F_{xf} = 0 , \quad (2.3)$$

$$F_{xr} = 0 . \quad (2.4)$$

- Due to the simplification concerning the center of gravity, differences concerning the wheel load do not occur between the inner and the outer side of the vehicle. It is not necessary to divide between inner and outer side anymore.
- The equations of motion are linearized for small angles. Linearizing considerations are valid for angles up to 3° to 4° . This means the trigonometric functions turn into:

$$\sin \alpha \approx \alpha , \quad (2.5)$$

$$\tan \alpha \approx \alpha , \quad (2.6)$$

$$\cos \alpha \approx 1 . \quad (2.7)$$

- As shown in Figure 2.1 linear wheel characteristics are assumed. After the threshold of 3° to 4° the wheel characteristic curve shows a declining slope and the assumption becomes defective.

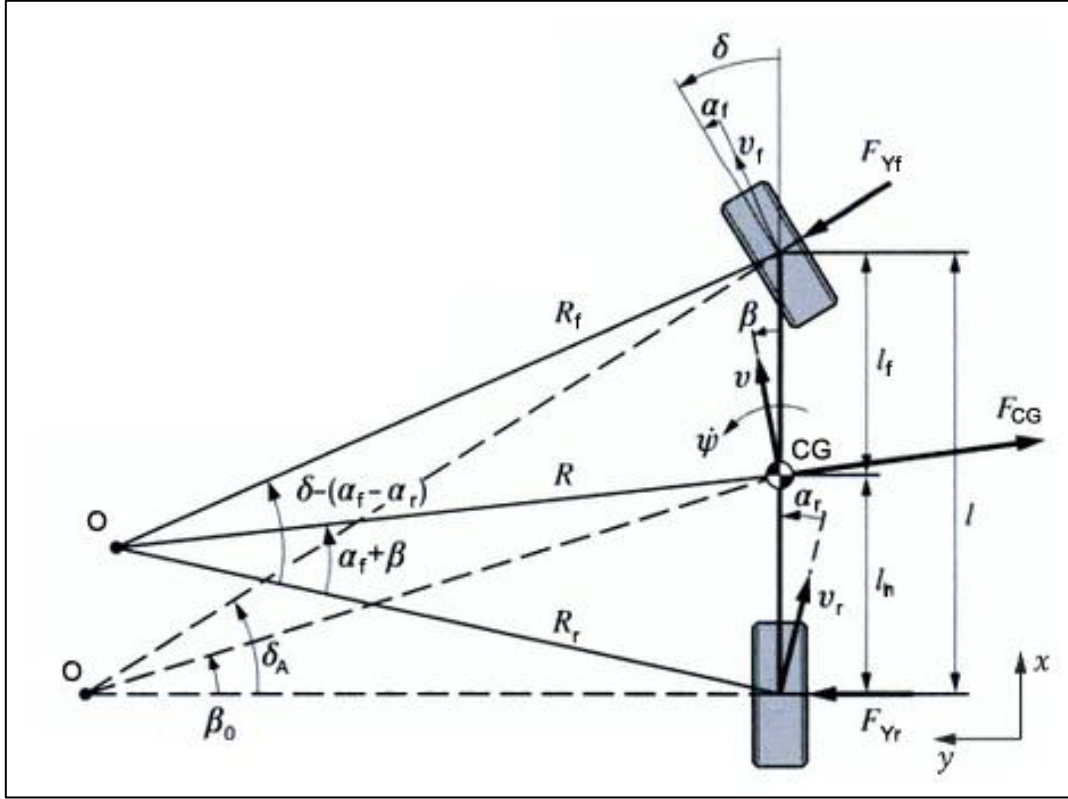


Figure 2.2: Kinematic relations of the bicycle model, modified from [25]

Due to the first two limitations the degrees of freedom are limited to the yaw rate ω_z and the side slip angle β . The yaw rate or yaw velocity ω_z is the angular speed around the z axis. The side slip angle is the angle between the longitudinal axis of the vehicle and the current direction of motion in the vehicle's center of gravity. The side slip angle provides a statement about the controllability of the vehicle.

Now the equations of motion can be derived from the kinematic and kinetic correlations according to Figure 2.2. Therefore, a fixed coordinate system in the center of gravity of the model has to be imagined, where the x -axis points in the direction of the longitudinal vehicle axle of the model, and the y -axis points to the left in Figure 2.2, perpendicular to the longitudinal axis. The vehicle's velocity vector \mathbf{v} in the center of gravity can be expressed as

$$\mathbf{v} = \begin{bmatrix} v \cdot \cos \beta \\ v \cdot \sin \beta \\ 0 \end{bmatrix}. \quad (2.8)$$

By extending equation 2.8 by the influence of the yaw rate ω_z , the velocity vectors for the combined front and rear wheels \mathbf{v}_f and \mathbf{v}_r can be found:

$$\mathbf{v}_f = \mathbf{v} + \boldsymbol{\omega} \times \mathbf{r}_f = \begin{bmatrix} v \cdot \cos \beta \\ v \cdot \sin \beta \\ 0 \end{bmatrix} + \begin{bmatrix} 0 \\ 0 \\ \omega_z \end{bmatrix} \times \begin{bmatrix} l_f \\ 0 \\ 0 \end{bmatrix} = \begin{bmatrix} v \cdot \cos \beta \\ v \cdot \sin \beta + l_f \cdot \omega_z \\ 0 \end{bmatrix}, \quad (2.9)$$

$$\mathbf{v}_r = \mathbf{v} + \boldsymbol{\omega} \times \mathbf{r}_r = \begin{bmatrix} v \cdot \cos \beta \\ v \cdot \sin \beta \\ 0 \end{bmatrix} + \begin{bmatrix} 0 \\ 0 \\ \omega_z \end{bmatrix} \times \begin{bmatrix} -l_r \\ 0 \\ 0 \end{bmatrix} = \begin{bmatrix} v \cdot \cos \beta \\ v \cdot \sin \beta - l_r \cdot \omega_z \\ 0 \end{bmatrix}. \quad (2.10)$$

In addition, the kinematic equations for \mathbf{v}_f and \mathbf{v}_r can be expressed by the front tire slip angle α_f , the rear tire slip angle α_r and the steering angle δ according to the correlations of Figure 2.2. The velocities \mathbf{v}_f and \mathbf{v}_r then read

$$\mathbf{v}_f = \begin{bmatrix} v_f \cdot \cos(\delta - \alpha_f) \\ v_f \cdot \sin(\delta - \alpha_f) \\ 0 \end{bmatrix}, \quad (2.11)$$

$$\mathbf{v}_r = \begin{bmatrix} v_r \cdot \cos \alpha_r \\ -v_r \cdot \sin \alpha_r \\ 0 \end{bmatrix}. \quad (2.12)$$

The tire slip angles α_f and α_r are the angles between the velocity vector of the wheel's contact patch and the wheel's peripheral direction. Uniting the equations 2.9 and 2.11 as well as 2.10 and 2.12 and dividing the x and y terms provides the expressions

$$\tan(\delta - \alpha_f) = \frac{v \cdot \sin \beta + l_f \cdot \omega_z}{v \cdot \cos \beta}, \quad (2.13)$$

$$-\tan \alpha_r = \frac{v \cdot \sin \beta - l_r \cdot \omega_z}{v \cdot \cos \beta}, \quad (2.14)$$

where l_f is the distance between the CoG and the front axle and l_r equals the distance between the rear axle and the CoG. After linearizing, the tire slip angles finally read

$$\alpha_f = \delta - \beta - \frac{l_f \cdot \omega_z}{v}, \quad (2.15)$$

$$\alpha_r = -\beta + \frac{l_r \cdot \omega_z}{v}. \quad (2.16)$$

To set up the equations of motion, the normal acceleration a_n , which is the centripetal acceleration in the curve, has to be defined by dividing the squared vehicle velocity v by the curve radius R :

$$a_n = \frac{v^2}{R}. \quad (2.17)$$

The radius R can be determined by means of geometric circle relations. Therefore, the infinitesimal arc length du is divided by the infinitesimal angle change $d(\beta + \psi)$. Attention has to be paid to insert the side slip angle β and the yaw angle ψ in radian:

$$R = \frac{du}{d(\beta + \psi)}, \text{ with} \quad (2.18)$$

$$v = \frac{du}{dt}. \quad (2.19)$$

Uniting the equations 2.17, 2.18 and 2.19 delivers

$$a_n = \frac{v^2}{R} = v^2 \cdot \frac{d(\beta + \psi)}{du} = v^2 \cdot \frac{d(\beta + \psi)}{v \cdot dt} = v \cdot (\dot{\beta} + \omega_z). \quad (2.20)$$

Now the equations of motion can be formed:

$$m \cdot \dot{v}_x = m \cdot a_n \cdot \sin \beta + m \cdot a_t \cdot \cos \beta = F_{xf} \cdot \cos \delta - \sin \delta \cdot F_{yf} + F_{xr}, \quad (2.21)$$

$$m \cdot \dot{v}_y = m \cdot a_n \cdot \cos \beta + m \cdot a_t \cdot \sin \beta = F_{xf} \cdot \sin \delta + \cos \delta \cdot F_{yf} + F_{yr}, \quad (2.22)$$

$$J \cdot \dot{\omega}_z = F_{xf} \cdot \sin \delta \cdot l_f + F_{yf} \cdot \cos \delta \cdot l_f - F_{yr} \cdot l_r. \quad (2.23)$$

By linearizing and inserting the equations 2.15, 2.16 and 2.20 into the equations 2.21 and 2.22, 2.23 the final forms of the equations of motion can be obtained.

In addition, the other assumptions that have been made for the simple single-track model have to be taken into account. This means that the tangential forces F_{xf} and F_{xr} as well as the tangential acceleration a_t can be set to zero due to a constant driving speed as provided in equation 2.2. By assuming the steering angle δ and side slip angle β to be very small, equation 2.21 equals zero and the equations 2.22 and 2.23 read

$$m \cdot v \cdot (\dot{\beta} + \omega_z) = F_{yf} + F_{yr}, \quad (2.24)$$

$$J_z \cdot \dot{\omega}_z = F_{yf} \cdot l_f - F_{yr} \cdot l_r. \quad (2.25)$$

Equation 2.1 can be applied to replace the front and the rear lateral wheel force. At last the tire slip angles provided in equation 2.15 and 2.16 have to be inserted and the equation of motion for the lateral direction can be written as

$$m \cdot v \cdot (\dot{\beta} + \omega_z) = c_{af} \cdot \left(\delta - \beta - \frac{l_f \cdot \omega_z}{v} \right) + c_{ar} \cdot \left(-\beta + \frac{l_r \cdot \omega_z}{v} \right). \quad (2.26)$$

The principle of momentum is defined as

$$J_z \cdot \ddot{\psi} = c_{af} \cdot l_f \cdot \left(\delta - \beta - \frac{l_f \cdot \omega_z}{v} \right) - c_{ar} \cdot l_r \cdot \left(-\beta + \frac{l_r \cdot \omega_z}{v} \right). \quad (2.27)$$

2.2 Circle of Forces

The circle of forces is a graphical representation of the total force distribution on a tire. The total force F_{tot} on the wheel is split up in a lateral force component F_y and longitudinal component F_x as shown in Figure 2.4. The total force that is supplied by the engine to the axles cannot exceed the maximum frictional force that the wheel is able to transfer to the road due to the law of friction. If the total force F_{tot} reaches this limit value, slip will grow at first and change over to total sliding when exceeding the value. The major conclusions of the circle of forces are that the longitudinal and lateral forces on the wheel depend on each other and the resulting total force, which a tire is able to transfer to the road, is limited by the coefficient of friction μ of the road surface. Furthermore, it is obvious that maximum longitudinal acceleration and deceleration are only feasible at straight ahead driving.

The circle of forces can be explained by means of the dynamic wheel load distribution. Therefore, a quasi-static moment of an accelerated vehicle delivers the moment equilibriums of the front and rear axle of a vehicle as shown in Figure 2.3. The moment equilibriums read

$$\sum M_f = 0 = (l_f + l_r) \cdot F_{Gr} - l_f \cdot F_G - m \cdot a \cdot h, \quad (2.28)$$

$$\sum M_r = 0 = (l_f + l_r) \cdot F_{Gf} - l_r \cdot F_G + m \cdot a \cdot h, \quad (2.29)$$

where F_{Gr} and F_{Gf} equal the weight forces on the axles. The force F_G equals the total vehicle's weight force and h is the height of the vehicle's center of gravity. Rearranging the equations provides the dynamic wheel load distributions for the front and the rear axle:

$$F_{Gf} = \frac{l_r \cdot F_G - m \cdot a \cdot h}{l_f + l_r}, \quad (2.30)$$

$$F_{Gr} = \frac{l_f \cdot F_G + m \cdot a \cdot h}{l_f + l_r}. \quad (2.31)$$

The equations show that the load on the front axle F_{Gf} decreases with the acceleration a . On the contrary, the weight force on the rear axle F_{Gr} increases with the acceleration. This justifies the standard torque distribution of many transfer case systems that distribute more torque to the rear axle by default.

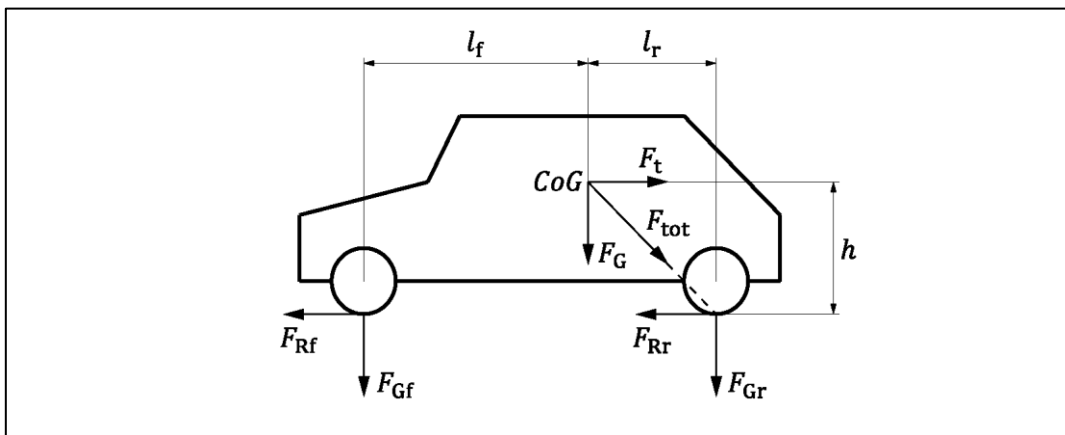


Figure 2.3: Forces while accelerating (simplified case)

As intimated by the dynamic wheel load distribution, the position of the vehicle's center of gravity has a significant influence on longitudinal and lateral vehicle dynamics. In acceleration situations, a high located center of gravity causes a high dynamic wheel load distribution from the front to the rear axle. Hence, the 4WD is limited in the torque transfer to the street on the front axle at acceleration events. In braking situations the inverse effect occurs and load depending on the height of the center of gravity is distributed from the rear to the front axle which usually already has to carry the weight of the heavy engine. With regard to the declining brake characteristic curve, the brake power is not rising linearly with the applied load, thus longer braking distances result [30]. Therefore, the design engineer's challenge is to install heavy parts as low as possible. Furthermore, it is tried to oppose a high center of gravity by a wide track gauge. This affects especially 4WD vehicles, as many 4WD vehicles are SUVs or off-road vehicles that are traditionally built high. Due to the combination of more weight and a

higher center of gravity, SUVs accordingly have longer braking distances than standard passenger cars.

In the special case of Figure 2.3 the total force F_{tot} points in an angle of exactly 45° to the rear wheel's contact patch. Due to this simplification it is assumed that the wheel load is fully distributed to the rear axle and F_{Gf} equals zero:

$$F_{\text{Gr}} = F_{\text{G}} = m \cdot g . \quad (2.32)$$

The horizontal balance of forces according to the principle of linear momentum provides:

$$F_{\text{Rr}} = F_{\text{t}} = m \cdot a , \quad (2.33)$$

with the friction force F_{Rr} :

$$F_{\text{Rr}} \leq \mu \cdot F_{\text{G}} = \mu \cdot m \cdot g . \quad (2.34)$$

Combining equation 2.33 and 2.34 delivers:

$$a \leq \mu \cdot g . \quad (2.35)$$

The maximum possible acceleration thus is limited by the laws of physics and cannot exceed the frictional limit that is provided in equation 2.35. The maximum coefficient of friction for ideal conditions is 1. Only special off-road wheels that dig into the ground or very sticky racing wheels can exceed the value of 1. Therefore, the maximum possible acceleration a_{max} can be assumed by:

$$a_{\text{max}} = g . \quad (2.36)$$

The same result of equation 2.36 for the maximum acceleration applies also for the maximum deceleration $-a_{\text{max}}$. This natural limit applies for two-wheel drive vehicles as well as for four-wheel drive vehicles.

However, the friction coefficient that results from the interaction between tire and road surface varies a lot and depends additionally on the wheel slip as the friction quality decreases with increasing wheel slip. Concluding, it can be said that the knowledge of the present friction coefficient would allow an improved adjustment of the four-wheel drive torque supply. This would have enormous impact on the performance of the four-wheel drive system. However, a permanent online monitoring of the friction coefficient can be considered as one of the last unsolved problems within the field of automotive engineering. A lot of research is done on this field, as for example in [29].

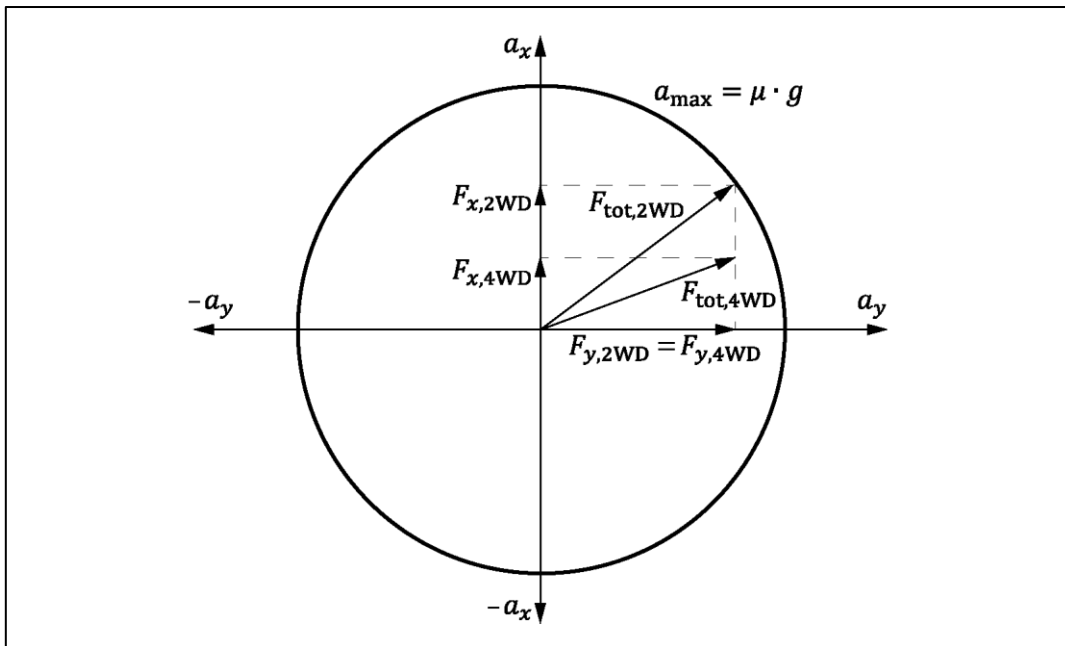


Figure 2.4: Circle of forces

In Figure 2.4 an illustration of a circle of forces is provided that compares the forces on a wheel of a 2WD and a 4WD. The resulting total force of the two-wheel drive $F_{tot,2WD}$ reaches the current maximum possible acceleration a_{max} . The graphic shows that the components $F_{x,2WD}$ and $F_{y,2WD}$ would not reach the limit by themselves. The circle of forces, which is exhibited in Figure 2.4, demonstrates the advantage of a four-wheel drive system. At the moment the total force of the two-wheel drive $F_{tot,2WD}$ reaches the physical acceleration limit, the 4WD would still have a safety margin at his disposal, as the longitudinal power is assumed to be divided by 50 % among the axles in the example of Figure 2.4. Therefore, it is possible to transfer more power to the road with a 4WD than with a conventional two-wheel drive vehicle.

In contrast, no advantage is provided by a four-wheel drive powertrain in braking situations, since a standard braking system always brakes all four wheels. This may surprise and irritate the driver as a 4WD vehicle climbs even steep streets easily upwards, but provides no advantage in braking situations.

Nevertheless, there is still an advantage of the 4WD during coasting. In these situations the torque that is absorbed from the road by the engine is divided between both axles. This means one axle absorbs less longitudinal forces and has more space left for the absorption of lateral forces in critical driving situations. Especially on low friction surfaces a 4WD vehicle provides the advantage to prevent the axles from overbraking as a single powered axle could overbrake and lose stability easier as a result of too much engine resistance that is led to the axle.

2.3 Four-Wheel Drive Systems

Four-wheel drive systems can look back on a long tradition within the automotive industry. As explained by means of the circle of forces the advantage of distributing torque to all four wheels is to provide more traction to the road. As seen in Figure 2.5 the 4WD can distribute more torque to the road, if the torque transfer is limited by the friction availability. If the supplied power of the engine

could be transferred to the road by two wheels as well, the curves would reach the same maximum traction force. Off-road vehicles often require this additional torque supply. Moreover, also vehicle dynamics can be improved by the presence of a four-wheel drive system. This explains the expansion of 4WD systems for standard road transport vehicles. Also the increasing popularity of sport utility vehicles contributes to the rise of vehicles equipped with a 4WD in road traffic.

The different origins of the curves in Figure 2.5 can be explained by the multi-pass-effect. In normal forward motion on off-road surfaces, such as sandy roads, the front wheels compact the surface and provide a surface with an improved friction coefficient to the rear wheels. A rear-wheel drive can take advantage of this condition, whereas a front-wheel drive requires more wheel slip to obtain traction. The origin of the 4WD curve is located between the origins of the front drive curve and the rear drive curve, as it is assumed that the power is distributed to both axles and thus the effect cannot be utilized completely by the rear axle [30].

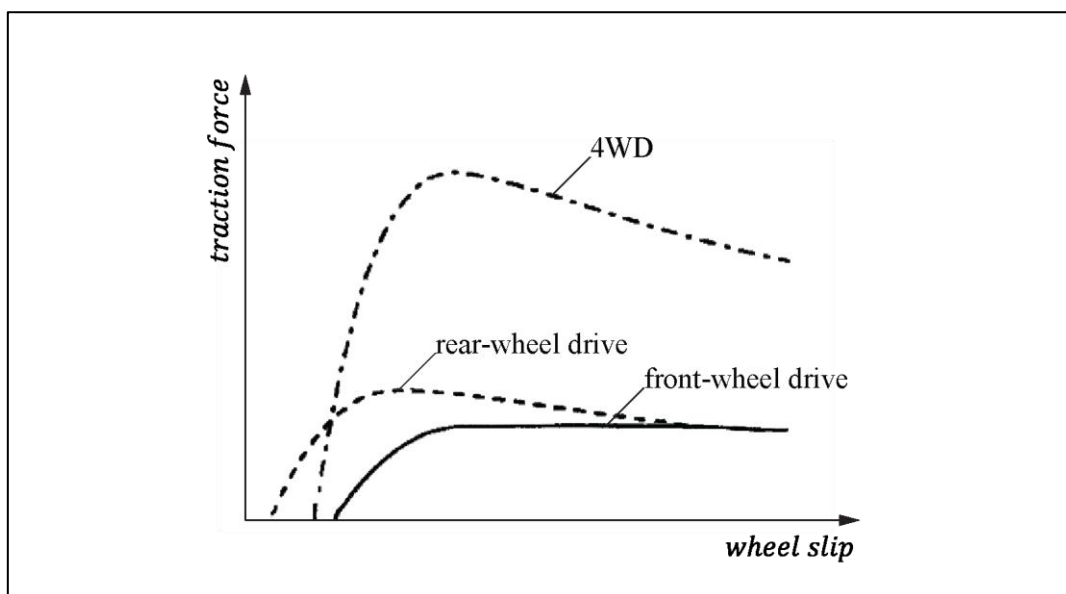


Figure 2.5: 2WD and 4WD traction performance on off-road surface, modified from [30]

Established abbreviations for a vehicle with four powered wheels are 4x4, 4WD or AWD. The first number of the abbreviation 4x4 stands for 4 wheels and the second number determines the number of powered wheels. The definitions 4WD and AWD have to be distinguished. In [18], 4WD systems are described as systems that have an additional low-range gear at their disposal and are designed for off-road use. Part time 4WD systems can be manually engaged and provide a rigid connection between the axles. Permanent 4WD systems provide a permanent connection between the axles by means of for example a center differential. Furthermore, [18] indicates that AWD systems only have high-range gear ratios at their disposal. It is said that an AWD vehicle is one with an on-demand transfer case that occasionally sends power to the secondary axle. Many SUVs were originally developed from passenger car platforms. The AWD systems were adapted to work for the platform, rather than being designed specifically for the vehicle. That is why the term AWD usually describes powertrain systems with a transverse engine and an on-demand transfer case system. The Torsen differential is an example for a permanent AWD system, as a permanent connection between the axles exists, but an extra reduction gear is not available. At Magna Powertrain the term 4WD is used to describe transfer case systems for longitudinally mounted engines. The term AWD describes transfer case systems that comply with transverse engine related transfer case systems. In this thesis, the terms AWD and 4WD are used interchangeably to describe a vehicle with four powered wheels.

The existence of a power distribution to the second axle provides many advantages in traction and driving dynamics. Nevertheless, the additional equipment parts do not only affect a higher total price of the vehicle, but also the weight. This extra weight yields in additional fuel consumption. According to [33] the installation of a four-wheel drive system raises the weight of the vehicle between 60 to 120 kg in general. It is indicated in [33] that a weight increase of 100 kg yields in an additional fuel consumption of about 0.2 to 0.5 l/100 km. Furthermore, additional losses of the torque distribution to the secondary axle have to be taken into account with regard to fuel consumption.

An open differential, which is the basic transfer case layout, provides a permanent 50 % torque distribution between the axles. Due to its basic functional principle, an open differential has disadvantages in driving situations in which one axle has no traction available or a dynamic torque distribution could improve the vehicle's driving behavior. From the driving dynamics point of view a variable torque distribution is more flexible and allows to adapt the torque distribution according to the driving situation. On a dry asphalt surface a vehicle can reach its theoretical best traction by distributing torque to the axles according to the dynamic wheel load distribution. Table 2.1 gives an overview of general advantages a 4WD system can provide. In chapter 2.3.1, a brief overview of different 4WD systems with the main focus on externally controlled transfer cases is provided.

Table 2.1: Advantages of 4WD Systems [14]

#	Advantage/Objective
1	Traction improvement
2	Reduction of understeering in acceleration situations
3	Improvement of the cornering ability
4	Increase of the maximum lateral acceleration
5	Inverse ESP, Torque Vectoring
6	Impact on load changes

2.3.1 System Classification

Four-wheel drive systems generally can be classified into active, semi-active or passive systems. Active systems in general base on the principle of actuated multi-plate clutches which are actuated by a vehicle controller. The actuation can be electro-mechanically, hydraulically or magnetorheologically. An example for an active system is Magna Powertrain's ATC differential which is better known under the BMW's label X-Drive. The ATC differential represents a system that distributes torque by means of an externally controlled clutch. The functionality of such systems is discussed in detail in chapter 2.3.2. Passive systems do not require external energy for actuation. The distributed torque arises as a result of internal friction in the system. A famous representative of this transfer case group is the Torsen differential which is the heart of the Audi Quattro 4WD. Basically, the Torsen differential provides the functionality of an open differential. The locking effect of these systems arises due to the bad efficiency of the worm gears that balance a rotational speed difference between the axles. An essential advantage of passive systems in comparison to active systems is that an additional external control unit for regulation is not needed. The torque distribution among the axles is defined entirely by

a characteristics curve respectively the default locking torque. Semi-active systems represent a mixture between active and passive transfer case systems. The specialty of these systems is the ability to switch into an active condition during a passive coupling behavior according to a given characteristics curve [34].

There is a huge amount of different four-wheel drive systems. Nearly every vehicle manufacturer trusts in a different technical concept. A classification according to the systems' mechanical functionalities can quickly get confusing. Jürgen Stockmar [30] gives a compact overview of different four-wheel drive solutions and distinguishes four-wheel drive systems into four general groups. Table 2.2 provides a full overview of these four groups and the common systems on the market.

Table 2.2: Four-wheel drive systems [30]

4WD/AWD					
		on-demand		Permanent	
		manual	automatic		
1	Determined power split	Rigid positive clutch	Rigid shifting multi-plate clutch	Central differential	
2	Variable power split given by the system			Torsen differential	Viscous Coupling Unit
3	Variable power split between given boundaries		Externally controlled multi-plate clutch	Controlled multi-plate self-locking differential	Viscomatic, Haldex
4	Selectable variable power split		Torque Vectoring		

A 4WD system can be considered as a permanent system if there is a constant positive or non-positive connection between the axles. The amount of distributed torque is not significant for the definition. Systems as the Viscous clutch or the Torsen differential are examples for permanent four-wheel drive systems.

On the other hand, on-demand four-wheel drive systems connect the axles automatically or manually as requested. An example for an on-demand system is the BMW X-Drive system that is based on an ATC transfer case that is manufactured by Magna Powertrain. An image of the ATC transfer case is provided in Figure 2.6. The advantage of such a system is that a multi-plate wet clutch distributes the torque between the axles depending on the required demand and the connection can be cut off immediately when desired.

Very sophisticated on-demand systems are torque vectoring systems that use an inverse ESP effect to influence the vehicle's stability by generating a yaw moment. This technology is used by the manufacturers Audi, BMW, Honda or Mitsubishi [30]. ESP opposes under- or oversteering events by generating a yaw moment with selective braking actions and engine torque interventions. Torque vectoring does the same by selectively distributing torque separately to all four wheels. The advantage is that no energy is dissipated by braking. This can as well be a disadvantage in situations with accident risk, as kinetic energy is not taken out, but is added to the system. The individual torque distribution is enabled by electronically controlled clutches and additional transmissions on the axles.

As this thesis mainly deals with the assessment of on-demand external controlled clutch systems this transfer case type is explained in detail in the following chapters.

2.3.2 Externally Controlled Multi-Plate Clutch

The core product among the transfer case systems at Magna Powertrain is the externally controlled multi-plate clutch. An illustration of Magna Powertrain's ATC transfer case is provided in Figure 2.6. Magna Powertrain's on-demand transfer case systems are based on a torque distribution via a clutch. The standard built in clutch can be categorized as a non-positive multi-plate wet clutch with an electromechanical actuation. The applied force on the clutch has to generate a friction moment that is equivalent to the torque that is desired to be transmitted.

The system is sold to OEMs as for example BMW where the system is promoted and famous under the name X-Drive. BMW advertises with the benefits of the best possible traction at difficult road surfaces, more driving safety and excellent vehicle dynamics up to border areas due to a variable power distribution between the axles.

Since 4WD vehicles are getting more popular for on-road use, development activities focus not only on traction improvement, but also on on-road safety and handling improvement. Handling can be understood as the performance of the driver/vehicle system [13].

In comparison to other systems that react torque sensing or according to the rotational speed difference, the advantage of an externally controlled multi-plate clutch is that the system recognizes the driver's request due to his input signals, such as the throttle pedal position or the steering wheel angle, and the system is able to apply a pre-controlled torque to the clutch before slip even occurs. Referring to [33], the pre-controlled target torque T_t is a function of the throttle valve opening th , the engine torque T_{mot} , the velocity v_x , the steering wheel angle δ_S and the lateral acceleration a_y :

$$T_t = f(th, T_{mot}, v_x, \delta_S, a_y) . \quad (2.37)$$

The connection process between the two cardan shafts by the transfer case is called locking. The axle that is connected permanently to the gear box and delivers steadily power to the road is defined as the primary axle. According to the OEM's distribution concept the primary axle can be the front or the rear axle. Logically, the secondary axle is the other axle and is defined as the axle that can be connected to the torque distribution on demand. Depending on the request of the vehicle controller the distributed torque to the secondary axle T_{sec} can be adjusted variably from 0 up to the maximum clutch capacity T_{max} . If the clutch is opened, the whole torque is transferred to the primary axle.

Vehicle and driver input parameters determine the desired locking torque that the vehicle controller applies. The advantage of an externally controlled transfer case system is that it can take corrective action before the electronic stability control has to come into action. An externally controlled clutch transfer case system therefore serves as an additional vehicle dynamic control system and can play an important role concerning driving safety.



Figure 2.6: Active Transfer Case 450 [15]

The work W that stresses the clutch occurs due to the applied torque T and difference of the rotational speeds of the axles $\Delta\omega$ and is defined by:

$$W = T \cdot \Delta\omega . \quad (2.38)$$

This means that the clutch only works when there is a difference in rotational speeds. The torque distribution among the axles can be defined by the torque bias ratio TBR , which can be obtained by dividing the torque that is effectively distributed to the high traction axle T_{high} , by the torque that is effectively distributed to the low traction axle T_{low} :

$$TBR = \frac{T_{\text{high}}}{T_{\text{low}}} . \quad (2.39)$$

Furthermore, the torque distribution among the axles can be defined by the locking value S :

$$S = \frac{T_{\text{high}} - T_{\text{low}}}{T_{\text{high}} + T_{\text{low}}} . \quad (2.40)$$

According to developing engineers the quantitative measurement of the friction utilization μ_{util} correlates very well with the system availability. To evaluate the friction utilization μ_{util} , T_{max} is set in relation to $T_{\text{sec,max}}$:

$$\mu_{\text{util}} = \frac{T_{\text{max}}}{T_{\text{sec,max}}} , \quad (2.41)$$

where T_{max} is the maximum torque the transfer case clutch is able to provide and $T_{\text{sec,max}}$ equals the maximum deliverable torque to the secondary axle with regard to the wheel load distribution and the current friction coefficient. To calculate $T_{\text{sec,max}}$ according to equation 2.42 the static wheel load $F_{G,\text{sec}}$ for the secondary axle is calculated at first. To determine the maximum deliverable torque, $F_{G,\text{sec}}$ is multiplied with an ideal friction coefficient of 1 and with the wheel radius r_{dyn} . Furthermore, the maximum torque of the secondary axle has to be divided by the axle ratio to be comparable to T_{max} :

$$T_{\text{sec,max}} = \frac{\mu_{\text{max}} \cdot F_{G,\text{sec}} \cdot r_{\text{dyn}}}{i_{\text{axle}}} . \quad (2.42)$$

If the friction utilization of equation 2.41 reaches a value beyond 1, the transfer case system is available to deliver the maximum possible amount of torque $T_{\text{sec,max}}$ to the secondary axle. According to test engineers, problems occur if the friction utilization μ_{util} reaches values beneath approximately 0.7. If the calculated value is below this threshold the transfer case system availability performs very poorly, as the system is not designed for maximum load utilization. The availability of a transfer case is usually defined as the amount of starting maneuvers the vehicle is able to master before the system shuts down due to overheating. Naturally, it is an important requirement to keep the number of downtimes as low as possible. On the other hand, it would be nice to build the transfer case as small and cheap as possible. Nevertheless, due to a small construction, the transfer case system is not capable to store a high quantity of heat and has to shut down earlier due to overheating. A consensus between customer wishes and a technical optimum has to be found. With regard to vehicle dynamics a slipping clutch enables great driving performance, but the load on the clutch is huge. For development purposes the overheating of the system is controlled by a thermal post calculation [9]. The thermal post calculation returns the clutch stress factor which describes the heat of the clutch in percent. Normally, the system has to shut off and thus is not available, if the clutch stress factor reaches a threshold of approximately 90 %. The system is not available until the clutch has cooled down and the stress factor decreases beneath a predefined threshold. A typical customer requirement for an on-demand 4WD system would be that the system masters three or five straight racing starts before the system shuts down.

An explanation for the correlation of the friction utilization and the system availability can be found in the extremely increasing loads on smaller dimensioned clutch plates due to a full utilized capacity. Roughly speaking, one could say that the chance of problems with the load spectrum increases with a poor friction utilization.

The magnitude of the available clutch capacity T_{max} depends on the OEM's requirement, thus the costs and the vehicle's target group. For the most driving situations where traction is required a friction utilization of 40 to 60 % is enough to satisfy the requirements. For a full traction drive a friction utilization of 100 % is necessary [33]. Due to the non-necessity of full traction utilization in the most standard driving situations, so called light four-wheel drive systems are disposed to capture the market. The torque capacity of a light four-wheel drive clutch is downsized on purpose to be more efficient [34].

The centerpieces of an externally controlled multi-plate wet clutch system are the multi-plate wet clutch, the actuator and the control unit.

Multi-Plate Wet Clutch

The externally controlled multi-plate wet clutch system, which is provided in Figure 2.6, has a rigid connection between the main shaft and the primary axle. The multi-plate clutch is mounted on the primary axle. The clutch redirects torque from the primary axle that is brought to the secondary by a belt, a gear drive or as in the example of Figure 2.6 by a transmission chain with pivoting pins. An oil pump located on the main shaft in the transfer case supplies lubricating oil and coolant to the clutch.

Passive lubrication concepts can replace an oil pump and increase the efficiency of the transfer case system.

Actuator

The actuator closes or opens the clutch. At the ATC clutch, which is exhibited in Figure 2.6, this happens via a spread mechanism with a ball ramp system. The generated axial force provides the desired locking torque of the clutch. In Figure 2.6 the actuation is executed electro-mechanically. The movement of a direct-current motor is transferred to the spread mechanism via a worm gear. The actuation can also be hydraulically or magnetorheologically. The adjustment speed can be regulated. An incremental sensor in the actuator detects the adjustment speed and the position of the actuator shaft. This data is necessary to control and regulate the clutch. High adjustment speeds and high accuracy are a demand for the fulfillment of dynamic driving requirements. During quick actuations, high current peaks may occur. On the other hand, the current demand is low to hold a stationary torque value [5].

Furthermore, [33] indicates that the actuation speed can have influence on the sensed driving comfort. Too fast actuation interventions can be noticeable as shifting jolts which lead to a loss of comfort. On the contrary, too slow actuation interventions can be noticeable as dynamic losses, as they affect the subjective feeling of traction.

Control Unit

The control unit regulates the target torque T_t that the clutch applies. Within the software of the transfer case control unit characteristic curves of the target torque are stored. These pre-control values are applied according to the driver's input parameters and the current driving situation. The extent of the control system depends on technical considerations, the level of complexity, required adaptations and cost considerations [17]. Adjustment speed and accuracy define the quality of the control unit and thus of the transfer case.

A multi-plate clutch cannot operate without protection against overheating. Therefore, temperature sensors and monitoring calculation models observe the clutch and turn off the transfer case in critical conditions.

In Figure 2.7 the rough layout of BMW's X-Drive concept is provided. The dynamic stability control consists out of the three control loops brake-management, engine-management and longitudinal torque management. The DSC controller calculates the required target torque $T_{t,DSC}$ according to the drivers input signals and the current driving situation considering driving dynamics. The input signals that influence the calculation of the pre-control torque are the throttle valve position th , engine torque T_{mot} , engine speed n_{mot} , driving speed v_x , gear position or steering wheel angle δ_S . Furthermore, different tire circumferences are considered. The calculated target torque $T_{t,DSC}$ is led to the transfer case control unit. The pre-control torque $T_{t,DSC}$ that is suggested by the characteristic pre-control curve is additionally corrected according to the influence of the following factors:

- Gearbox oil temperature
- Clutch wear

- Load on the actuator

In addition, the transfer case control unit returns the information about the corrected pre-control torque to the DSC including further calculated and measured data.

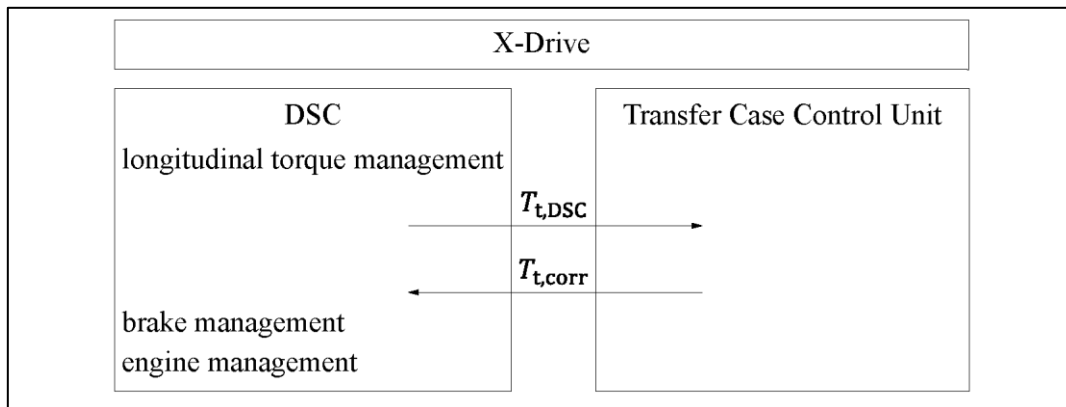


Figure 2.7: Functionality of the BMW's DSC control loops

The dynamic stability and traction control observes the slipping behavior of the axles and tries to keep the vehicle stable. The transfer case system is able to lower under- or oversteering tendencies by dynamic torque distributions between the axles, as discussed in chapter 2.3.4. The vehicle controller observes the current vehicle movement by means of a yaw rate sensor and detects deviations with regard to the driver's intended direction. In case of deviations the vehicle controller reacts with longitudinal torque distributions. Furthermore, the vehicle controller tries to achieve optimum traction by dynamic torque distributions according to the current driving conditions. Therefore, the vehicle controller evaluates signals as the yaw rate ω_z , lateral acceleration a_y , steering wheel angle δ_s or rotational wheel speeds ω_i .

Moreover, the system detects different tire circumferences due to different wear of the tires and balances the difference in rotational speeds by allowing the clutch to slip and by reducing the locking torque.

The requirements on an externally controlled multi-plate wet clutch system consider the improvement of traction, driving dynamics and efficiency. Therefore, the requirements on an externally controlled system exceed the requirements of a conventional mechanical differential which mainly aims on the best possible traction.

2.3.3 Active Dynamic Stability Control

The advantage of having an electronically controlled transfer case system installed is the external controllability. The electronic stability program has a further tool at its disposal that can be applied for stability measures.

The BMW's X-Drive concept exists out of the three control loops brake-management, engine-management and longitudinal torque management. The latter is provided by the electronic transfer case system. First of all the X-Drive DSC system tries to conduct stability measures with the longitudinal torque management, thus the transfer case. Brake management and engine management

do not react before the longitudinal torque management. This means less brake and engine reactions, which additionally has positive effects on efficiency and driving comfort [5].

2.3.4 Steering Tendencies

A vehicle oversteers if the rear axle cannot provide enough lateral guidance according to the theory of the circle of forces. The vehicle tends to drift. If oversteering is detected by the vehicle controller an electronic transfer case system is able to react on this condition by distributing more torque to the front axle. The rear axle is discharged from drive torque and is able to absorb more lateral force. The vehicle gains lateral guidance back again and stabilizes as seen in Figure 2.8. As provided in the oversteering example of Figure 2.8 the front axle, which is the secondary axle in this example, receives up to 65 % of the provided engine torque while stabilizing the vehicle. According to [5], the distribution of 65 % is actively not adjustable and results from the current slip and traction conditions on the wheels.

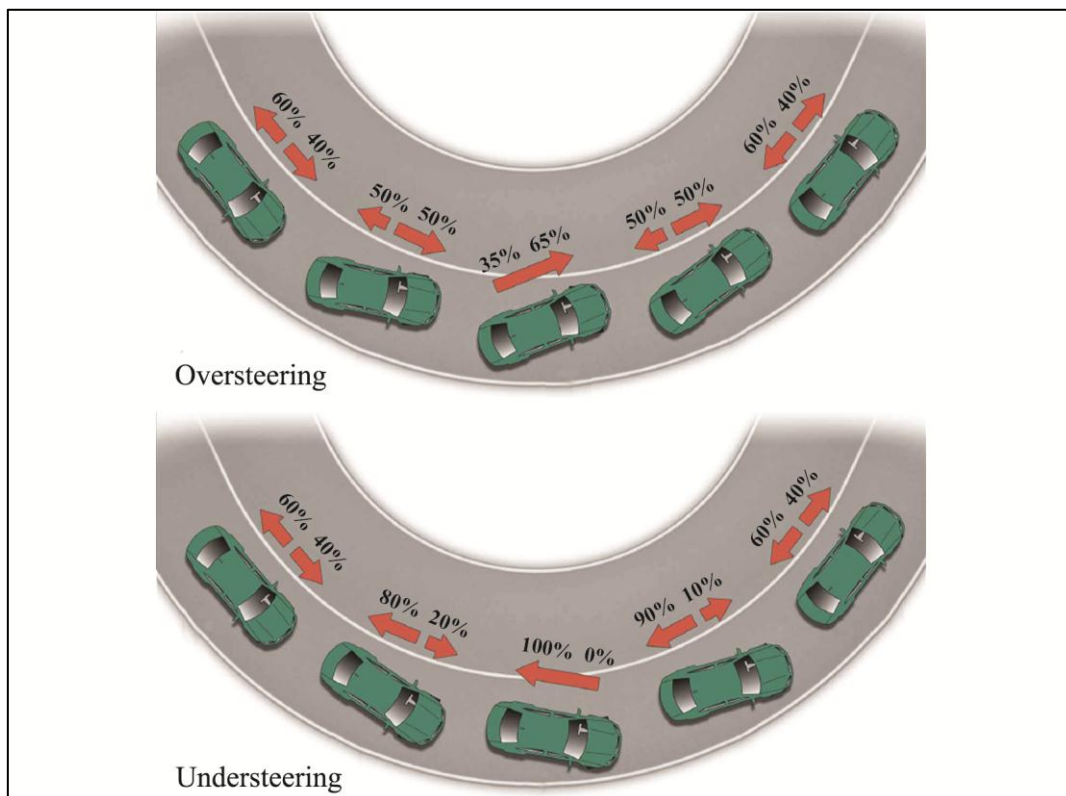


Figure 2.8: Oversteering and understeering, modified from [13]

A vehicle understeers if the vehicle does not follow the exact drivers wish, but tends to drive straight ahead while cornering. If the driving dynamics controller detects understeering the transfer case system will try to distribute more drive torque to the rear axle. According to the theory of the circle of forces the front axle is now able to absorb more lateral force F_y and the vehicle stabilizes again. As provided in the understeering example of Figure 2.8 up to 100 % of the engine torque may be distributed to the rear axle by completely opening the clutch. At the end of the curve in the understeering example of Figure 2.8, where the vehicle should be stable again, the torque is split up according to the standard distribution again.

2.3.5 Active Traction Control

The amount of torque that can be distributed to the road with an open differential is determined by the friction availability of the low friction axle. If one axle stands on ice and thus has no friction available, the axle will spin and cannot distribute torque to the road. In addition, also no power can be distributed by the other axle that stands on a high traction surface, as the differential cannot support itself on the low friction side. Therefore, only the same amount of torque that is distributed by the low traction axle to the road can also be applied by the other axle.

The mechanical solution to this problem is a limited slip differential or a locking differential. A locking differential represents the special case of a limited slip differential that is able to provide a 100 % locking value S by means of for example a manually engageable claw coupling. If needed, an electronically controlled transfer case system is able to provide the functionality of a locking differential by providing a rigid connection between the axles by closing the clutch completely.

Therefore, maximum traction performance can be reached in starting conditions by applying a high amount of torque to the clutch and enabling a rigid connection between the axles. The transfer case system then has the function of a locked differential and provides optimum traction in sophisticated 4WD situations. A further advantage of the system is the non-necessity of a brake action to transfer torque to the other axle, in the case that one axle is slipping.

2.3.6 Adaption to ESP

Due to the prevention of axle speed differences by a 100 % locking differential, synergetic effects between this transfer case system and an additional ESP support cannot be provided. However, an open differential or a self-locking device as the Torsen differential can be combined with an ESP system and is not bothered in its functionality by the ESP's selective brake interventions. As the Torsen differential is a torque sensing differential, an ESP system can secure the lock functionality of the system by targeted brake interventions onto the slipping axle. The same applies for the open differential. By braking the slipping axle, torque can still be distributed to the high friction axle [13].

Nevertheless, an externally controlled transfer case system provides the ideal conditions for the combination with an ESP system. Additionally to targeted brake interventions and engine interventions, the current vehicle dynamic conditions can be influenced by longitudinal torque distributing measures between the axles. However, the optimum synergetic effects among an ESP system and a 4WD drivetrain can be achieved with a torque vectoring system, as an individual torque distribution is not only possible between the two axles, but between all four wheels.

If an axle passes beyond the peak point of optimum tire slip, the axle loses traction and the vehicle can get instable. According to [17], three alternatives are feasible to control the vehicle:

- 1.) Torque distribution between the wheels/axles
- 2.) Control of the applied torque from the engine to the drivetrain
- 3.) Regulation of the traction on the wheels via controlled brake interventions

The control concept of an ESP system usually exists out of the two control loops engine management and brake management. An externally controlled transfer case system extends the control concept with

a further control loop, the longitudinal torque management. The ESP calculates the target torque for the secondary axle and forwards it to the transfer case control unit that applies the target torque to the clutch [5]. According to Fischer et al. [5], the longitudinal torque management control loop is executed at first. Only if the instability risk cannot be opposed by a targeted torque distribution measure, the engine and brake management control loops are executed. By means of this additional control loop the number of engine and brake interventions by the ESP can radically be reduced. In case of an individual brake intervention the ESP tries to oppose under- or oversteering by generating a yaw moment. Therefore, the curve inner rear wheel is braked in case of understeering or the curve outer front wheel in case of oversteering. The targeted brake intervention generates a yaw moment that leads the vehicle back into its desired position.

The combination of an ESP system and a 4WD system presumes some requirements to secure a clean operation. To prevent unintended torque transfers between the axles due to brake interventions, a quick reaction behavior of the transfer case control unit at individual brake interventions on single wheels is required. Therefore, the clutch has to be opened by the transfer case control unit immediately if the ESP orders to open the clutch. Additionally, overbraking of the rear axle has to be prevented. In [13] and [33] it is stated that the clutch has to be opened within 100 ms at corresponding situations. Nevertheless, the transfer case clutch should only be opened on request of the ESP. A system with a clutch to the rear axle can always open the clutch as the vehicle is stabilized by reducing power from the rear wheels. On the other hand, the clutch should not always be opened at systems with a clutch to the front axle, as the whole power would be shifted entirely to the rear wheels and a high risk of instability is likely to arise. The reason for this measure to avoid instability is discussed in chapter 3.3.1. In the worst case the vehicle would spin out. At these systems the torque is held or reduced to a lower level, depending on the ESP's wish.

The Haldex clutch is able to release the axles in the case of braking situations immediately and interrupt the torque distribution. Electronically controlled clutches receive a signal from the vehicle controller in dangerous brake situations to open the clutch. Braking stability is explained more detailed in chapter 3.3.1.

3 Assessment of Driving States and Maneuvers

The vehicle's driving behavior assessment can be done by evaluating the subjective assessment impressions of experienced test engineers on the one hand, or by evaluating objective assessment criteria of the test drive on the other hand. In the design and tuning phase, objective measurement assessment methods are becoming more and more important. However, as driving behavior in its entirety affects us as humans, subjective evaluation as well is still of high importance for final precision tuning [11]. Nevertheless, especially the importance of objective assessment criteria within vehicle drivability evaluations is growing. With the growing stage of development, the differences in progress get smaller and thus harder to evaluate without the help of objective assessment criteria. Manufacturers as well as customers are therefore interested in an objective vehicle performance comparison. As very complex driving situations may occur in daily road traffic, it is essential to select the right driving maneuvers for the assessment. Therefore, a driving maneuver catalog according to the Design Verification Plan is carried out within the company's internal adjustment phase. The DVP contains maneuvers that cover many possible driving situations of the vehicle's field of application in road traffic.

Subjective Assessment Methods and Criteria

The subjective vehicle assessment by test engineers belongs to standard assessment methods before series release. Subjective test methods evaluate the interaction between driver and vehicle [11]. The term driving behavior describes the relation between driver, vehicle and the surrounding environment [23]. The difficulty of subjective driving assessment is the complicated comparability of subjective statements. Therefore, it is necessary to have distinct definitions for default driving properties and to quantify subjective assessment results via a classification system. A distinct understanding of particular driving situations is important for the success of subjective comparisons with different test drivers. Normally, the quantification of subjective impressions is done by means of a rating scale. The test driver has to rate the sensed driving experience. Very common is the so-called ATZ-scale with a fragmentation from 0 to 10. Usually 10 would be the best and 0 the worst rating value [11]. Each grade needs to have an exact verbal definition for every possible condition that is likely to arise for the currently evaluated criterion or driving state. Only then the test driver is able to distinguish between the different steps. The problem that arises with this kind of rating systems is that each driver can have a different subjective understanding of the single grade definitions.

An example for a condition that can be recognized easily by the driver's subjective impression is binding in the drivetrain, which is explained in chapter 4.6. Nevertheless, binding is more difficult to measure or quantify by means of an objective assessment criterion. In this thesis, a possibility to detect binding via measured variables is introduced.

Objective Assessment Methods and Criteria

For the objective analysis of a road trial, more sophisticated measuring and analysis techniques than for a subjective assessment process are needed.

According to [11], objective test methods can generally be divided into two groups:

- Closed-loop methods and criteria
- Open-loop methods and criteria

Road trials are classified analogous to the definitions of open- and closed-loop maneuvers. At a closed-loop maneuver the driver controls the vehicle by longitudinal and lateral guidance. A closed loop maneuver therefore describes a test drive that assesses the concurrence, thus the interaction among driver and vehicle. Closed-loop measurements are primarily carried out to evaluate the interaction between the vehicle that represents a controlled system and the human as the controller. Closed-loop tests are primarily carried out for the assessment of stability and steerability [10].

On the other hand, the aim of an open-loop method is to minimize or eliminate the driver's influence on the vehicle's reaction behavior. Only the vehicle's response behavior is of importance. Open loop tests are driving tests with given inputs for the steering wheel, the throttle pedal and the brake pedal. These components are controlled by a mechanism at an open-loop test. The big advantage of such a test is that due to the given input parameters the maneuver is better and easier to reproduce than a closed-loop test.

Open-loop tests are very common in standardization, as it is of high importance to eliminate the driver's varying influence as much as possible [11].

According to this description, testing the vehicle's steady-state circular driving behavior with a given steering angle would be an open loop test, but can be transferred into a closed-loop test easily by assigning a driver to steer the vehicle along the given circular path. Consequently, if not standardized, many maneuvers are not automatically assigned to a specific group, but can be carried out as a closed- or an open-loop maneuver. Furthermore, the output of the same maneuver can either be subjective impressions or objective assessment criteria [23].

3.1 Driving Maneuvers

To receive information about the vehicle's reaction behavior in extraordinary and extreme driving situations, a vehicle has to run through a wide range of different driving maneuvers from first design stages until the final series release. There is a group of driving maneuvers that were able to establish themselves over the years and have been standardized. Table 3.1 provides examples of well-known standard ISO tests for the evaluation of the vehicle's lateral dynamic behavior.

Table 3.1: Examples of ISO-standard tests for the assessment of lateral dynamics

ISO-Standard	Test
3888-1	Test track for a severe lane-change manoeuvre – Part 1: Double lane-change
3888-2	Test track for a severe lane-change manoeuvre – Part 2: Obstacle avoidance
4138	Steady-state circular driving behavior
7401	Lateral transient response test methods
7975	Braking in a turn
9816	Power-off reaction of a vehicle in a turn
12021-1	Sensitivity to lateral wind – Part1: Open-loop test method using wind generator input
13674-1	Test method for the quantification of on-centre handling – Part 1: Weave test
17288-1	Free-steer behavior – Part 1: Steering-release open-loop test method

Within the fine tuning phase the requirements on the driving behavior depend strongly on the different manufacturer's demands. With regard to the design of specific product groups as transfer case systems, a wide varying range of different company internal driving maneuvers is imaginable. Most of them are not standardized. Table 3.2 provides a list of possible driving maneuvers to assess the performance of a transfer case system. Important terms in this context are μ -split and μ -jump. A μ -split surface describes a road surface that has two different coefficients of friction for each longitudinal side of the vehicle. On the other hand, a μ -jump maneuver is defined by having one axle on a surface with a high friction coefficient and one axle on a low traction surface.

Table 3.2: Examples of specific maneuvers for the transfer case assessment

#	Maneuver
1	Full load acceleration on μ -high from 0 to 100 km/h
2	Full load acceleration with racestart on μ -high from 0 to 100 km/h
3	Full load acceleration on μ -high with maximum steering angle
4	Full load acceleration on μ -jump
5	Full load acceleration with racestart on μ -jump
6	Full load acceleration on μ -jump with maximum steering angle
7	Starting with 50 % throttle pedal and turned right
8	Starting with 100 % throttle pedal and turned right
9	Quasi-steady-state circular test with slow acceleration up to the limit

An important parameter concerning assessment criteria is the delay between the driver's perception and the appearance of an interruption, thus the driver's reaction time on an obstacle on the road or on

an error of the vehicle system. In [24] it is said that the reaction time depends on the conditions, but is at least 0.3 s. In [23] the normal reaction time is specified with 1 s.

Assessment criteria can be classified according to different categories. Within the expert-tool the classification has been undertaken according to Table 1.1. Furthermore, the categories have been divided according to their causation. This can be the driver himself, the vehicle or the transfer case system. The impact on a criteria category can have multiple causations. Therefore, the category efficiency can be influenced by an efficient driver, an efficient vehicle or an efficient transfer case system. On the other hand, the driver has no direct influence on the system load. Table 3.3 provides an overview of the influential factors for each assessment category of Table 1.1.

Table 3.3: Influential factors on assessment categories

	Driver	Vehicle	Transfer Case System
Comfort		X	X
Efficiency	X	X	X
Traction	X	X	X
Vehicle Dynamics		X	X
System Load		X	X

Within the scope of this thesis driver-, vehicle- and system-related assessment criteria, that describe the categories comfort, efficiency, traction, vehicle dynamics and system load, had to be found. Criteria concerning vehicle dynamics can be found in standardized road tests for lateral dynamics. Standardized assessment criteria are related to default and reproducible driving maneuvers as for example the steady-state circular test that is discussed in chapter 3.1.1. The vehicle's reaction with regard to a defined input is evaluated. Further examples for non-steady state steering inputs are provided in chapter 3.1.2.

Criteria that take the driver's reaction time into account, normally concern the vehicle's safety. Very often criteria are specified to assess the behavior of a driving assistance system. The sine with dwell test, which is discussed in chapter 3.1.2.3, provides a possibility to assess the ESP's functionality.

Criteria that take the system load into account are unusual for standardization as they concern company internal and product related data. Therefore, they are usually not freely accessible, but can rather be found in company internal documents.

3.1.1 Steady-State Circular Driving Behavior

Testing the steady-state circular driving behavior is the oldest standardized ISO test [11]. The maneuver is usually undertaken to determine the vehicle's self-steering behavior. This determination can be carried out with two different methods [27]. At the first method, the vehicle is held at a constant steering angle δ while raising the velocity v . The inconstant value of the radius R can be determined. At the second method the self-steering behavior is determined by driving a constant radius R while raising the velocity v . The inconstant value of the steering angle demand δ will result. Both

methods are suitable to determine the self-steering behavior of the vehicle. However, the second method is more common in literature and also suggested in ISO 4138. The evaluation of this test provides the vehicle's self-steering behavior as shown in Figure 3.1. In addition to the under- or oversteering behavior of the vehicle, the test returns the vehicle's critical or characteristic speed. Table 3.4 provides an overview of possible criteria to test the vehicle's steady-state circular driving behavior. All criteria are defined as a function of the lateral acceleration $f(a_y)$.

Table 3.4: Assessment criteria to evaluate steady-state circular driving behavior according to [23]

<i>Criterion</i>	<i>Symbol</i>
Steering angle	δ
Steering moment	M_S
Roll angle	φ
Side slip angle	β
Tire slip angle difference	$\Delta\alpha$
Steering angle difference	$\delta - \delta_A$
Steering angle ratio	$\frac{\delta}{\delta_A}$
Yaw rate amplification factor	$\frac{\omega_z}{\delta_S}$
Lateral acceleration amplification factor	$\frac{a_y}{\delta}$
Self-steering gradient	$\frac{d\delta}{da_y}$

By driving the vehicle at a constant radius R and at a constant velocity v the following simplifications can be considered according to the theory of the bicycle model that has been discussed in chapter 2.1:

$$\beta = \text{const.} , \quad (3.1)$$

$$\dot{\beta} = 0 , \quad (3.2)$$

$$\omega_z = \text{const.} , \quad (3.3)$$

$$\dot{\omega}_z = 0 . \quad (3.4)$$

As provided in Figure 2.2 the lateral move can be seen as a rotation around the velocity pole O . Due to equation 3.2, equation 2.18 can be rewritten and the velocity in the center of gravity can be determined according to:

$$v = \omega_z \cdot R . \quad (3.5)$$

The simplifications of the equations 3.1, 3.2, 3.3, 3.4 and 3.5 allow to rewrite the equations 2.26 and 2.27 as

$$\frac{m \cdot v^2}{R} = F_{yf} + F_{yr} , \quad (3.6)$$

$$l_f \cdot F_{yf} = l_r \cdot F_{yr} . \quad (3.7)$$

The lateral wheel forces read

$$F_{yf} = \frac{m \cdot v^2}{R} \cdot \frac{l_f}{l} , \quad (3.8)$$

$$F_{yr} = \frac{m \cdot v^2}{R} \cdot \frac{l_r}{l} . \quad (3.9)$$

By inserting equation 2.1 in the equations 3.8 and 3.9, the tire slip angles can be expressed as

$$\alpha_f = \frac{m}{c_{\alpha f}} \cdot \frac{l_r}{l} \cdot \frac{v^2}{R} , \quad (3.10)$$

$$\alpha_r = \frac{m}{c_{\alpha r}} \cdot \frac{l_f}{l} \cdot \frac{v^2}{R} . \quad (3.11)$$

Now the tire slip angle difference can be introduced:

$$\Delta\alpha = \alpha_f - \alpha_r = \frac{m}{l} \cdot \left(\frac{l_r}{c_{\alpha f}} - \frac{l_f}{c_{\alpha r}} \right) \cdot \frac{v^2}{R} . \quad (3.12)$$

As seen in equation 3.12, a four-wheel drive system influences the self-steering tendency by the weight of the transfer case that dislocates the vehicle's center of gravity. Furthermore, it influences the steering tendency from the driving dynamics point of view as a yaw moment can be created by shifting power to the secondary axle.

By inserting equation 2.16 in equation 2.15 the steering angle δ reads

$$\delta = \frac{\omega_z}{v} \cdot l + \alpha_f - \alpha_r . \quad (3.13)$$

The steering angle demand can be expressed as:

$$\delta = \delta_A + \Delta\delta = \delta_A + \Delta\alpha . \quad (3.14)$$

Equation 3.15 contains the Ackermann angle δ_A which can be derived from the geometric relations of Figure 2.2:

$$\tan \delta_A \approx \delta_A = \frac{l_f + l_r}{R} . \quad (3.15)$$

Now the equations 2.17, 3.5 and 3.12 can be inserted in equation 3.13:

$$\delta = \frac{l}{R} + \frac{m}{l} \cdot \left(\frac{l_r}{c_{\alpha f}} - \frac{l_f}{c_{\alpha r}} \right) \cdot a_y . \quad (3.16)$$

The Ackermann angle δ_A equals the total steering angle demand if the lateral slip is zero, thus the wheels are free of lateral forces. The correction steering angle $\Delta\delta$ depends on the lateral acceleration

a_y and equals the angle the driver has to apply additionally to the Ackermann angle δ_A to compensate the tire slip angle difference $\Delta\alpha$. Equation 3.14 includes the definition of the self-steering gradient EG :

$$EG = \frac{m}{l} \cdot \left(\frac{l_r}{c_{af}} - \frac{l_f}{c_{ar}} \right). \quad (3.17)$$

The self-steering gradient EG can be assumed as a constant term within the linear operating range. The vehicle's self-steering behavior is defined by the steering angle δ that depends on the lateral acceleration:

$$\delta = \delta_A + EG \cdot a_y. \quad (3.18)$$

The vehicle's steering behavior can be described by means of the tire slip angle difference $\Delta\alpha$ according to Olley [27]:

$$\Delta\alpha = \alpha_f - \alpha_r \begin{cases} < 0, & \text{oversteering} \\ = 0, & \text{neutral} \\ > 0, & \text{understeering} \end{cases} \quad (3.19)$$

Nevertheless, this method is only restrictedly applicable to evaluate the self-steering behavior. A disadvantage of this method is that the tire slip angles are complex to measure. Furthermore, no consideration is shown for the steering activity δ . The method is only valid for small lateral acceleration values. At high lateral acceleration values, the relation between $\Delta\alpha$ and δ is no longer valid, due to high lateral wheel forces and their non-linear behavior over a_y .

Therefore a situation might arise, in which according to Olley understeering is detected, but the steering demand decreases. An example is provided in Figure 3.1. The signs of $\Delta\alpha$ and $d\delta/da_y$ are unequal. Therefore, it is better to describe the steering behavior by means of the self-steering gradient EG . The self-steering gradient EG is defined in ISO 4138 as:

$$EG = \frac{1}{i_s} \cdot \frac{\partial \delta_S}{\partial a_y} - \frac{\partial \delta_A}{\partial a_y}, \quad (3.20)$$

where δ_S is the by the driver applied steering wheel angle and i_s is the steering ratio. With this method, the steering activity δ is considered. The self-steering gradient EG can be seen as the inclination of the curve in Figure 3.1.

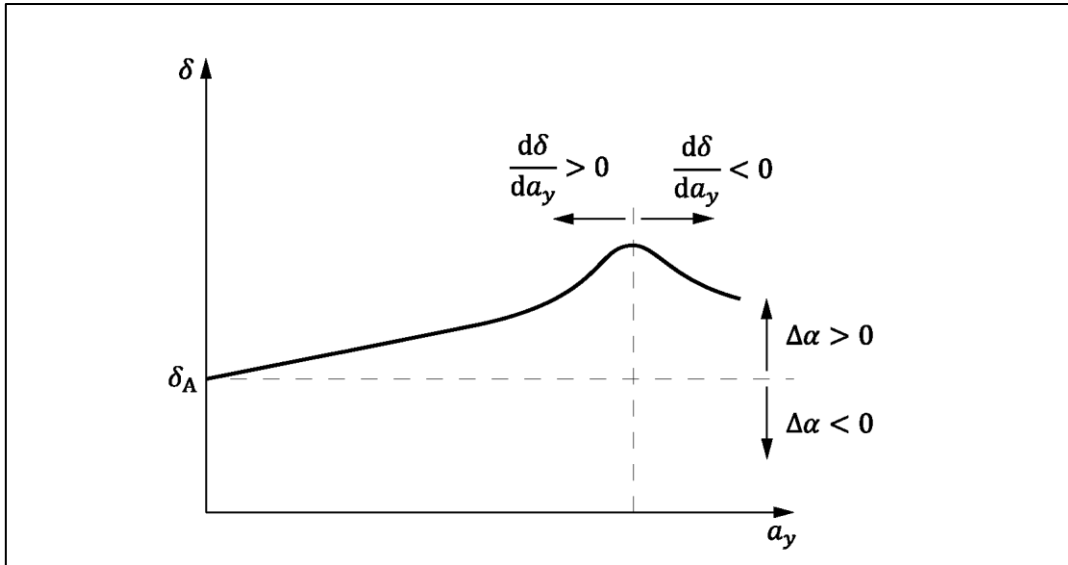


Figure 3.1: Steering tendency according to the self-steering gradient and the tire slip angle difference

The self-steering gradient EG can be considered as constant up to a lateral acceleration of $0.4g$. After exceeding this threshold, the self-steering gradient EG varies as a function of a_y . The steering behavior can be classified according to the sign of EG . As the Ackermann angle δ_A is a constant term at the steady-state circular test that is carried out with a constant radius R , the Ackermann angle δ_A does not have to be considered in the differential equation 3.20:

$$EG = \frac{d\delta}{da_y}. \quad (3.21)$$

The steering behavior can be determined as follows:

$$EG \begin{cases} < 0, & \text{oversteering} \\ = 0, & \text{neutral} \\ > 0, & \text{understeering} . \end{cases} \quad (3.22)$$

Another important criterion to evaluate the steady-state circular test, is the yaw amplification factor. The yaw amplification factor can be obtained by dividing the yaw rate ω_z by the steering angle δ . Moreover, the obtained equation can be simplified by applying the equations 2.17, 3.5 and 3.17. The yaw rate amplification factor then reads

$$\left(\frac{\omega_z}{\delta}\right)_{\text{stat}} = \frac{v}{l + EG \cdot v^2}. \quad (3.23)$$

The yaw amplification factor is an essential criterion, as the driver expects the yaw rate to rise proportional to the applied steering angle. The maximum yaw amplification can be seen as a criterion that describes the agility impression of a vehicle at mean velocities [27]. Figure 3.2 provides the slopes of the curves of the yaw amplification factor as a function of the self-steering gradient EG .

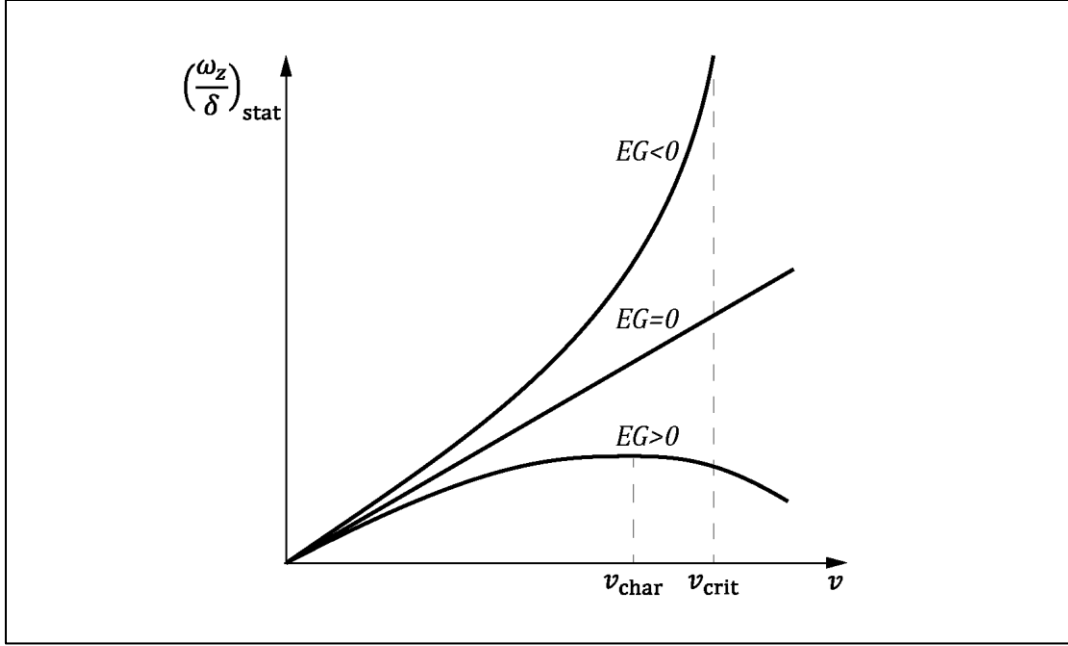


Figure 3.2: Yaw rate amplification factor over velocity

The yaw amplification stays low for an understeering vehicle. The characteristic velocity v_{char} can be determined by differentiating equation 3.23 and determining the velocity at which the slope is zero:

$$\frac{d}{dv} \left(\frac{\omega_z}{\delta} \right)_{\text{stat}} = \frac{l + EG \cdot v^2 - 2 \cdot EG \cdot v^2}{(l + EG \cdot v^2)^2} = 0. \quad (3.24)$$

The characteristic velocity v_{char} then reads

$$v_{\text{char}} = \sqrt{\frac{l}{EG}}. \quad (3.25)$$

According to [10] and [27] the range of the characteristic speed can be between 65 and 125 km/h. The knowledge of the characteristic speed of a vehicle can be very helpful in further dynamic considerations and calculations. At speed values around the characteristic velocity v_{char} , a vehicle shows the highest steering sensitivity [10]. The characteristic speed v_{char} can be determined for understeering vehicles.

On the other hand, the critical velocity v_{crit} can be evaluated for oversteering vehicles. As seen in Figure 3.2 the yaw amplification increases progressively with the vehicle velocity and heads towards infinity at the critical velocity. To determine the critical velocity, the denominator in equation 3.24 has to be set to zero and the pole can be determined. The critical velocity can then be written as

$$v_{\text{crit}} = \sqrt{-\frac{l}{EG}}. \quad (3.26)$$

3.1.2 Non-Steady-State Steering Conditions

This subchapter deals with the conventional steering inputs for open-loop maneuvers that are used for the evaluation of the vehicle's steering behavior [10]. Figure 3.3 provides an overview of common maneuvers. In order not to go beyond the scope of this thesis, only some of the maneuvers are described more detailed. Detailed descriptions can be found in [23] and [16].

The interaction between the vehicle and the driver can be considered as a control system, where the vehicle is the controlled system and the driver is the controller. To meet the requirement for stability, the vehicle defines the constraints for the driver's driving style. The aim is to determine the transmission behavior of the technical control system. To describe the non-steady state steering characteristics, different steering wheel angle functions, as listed in Figure 3.3, are suggested in [23] and [10] in order to evaluate the system response. Assessment criteria are defined for the separate functions. A very common maneuver is the so-called steering step input.

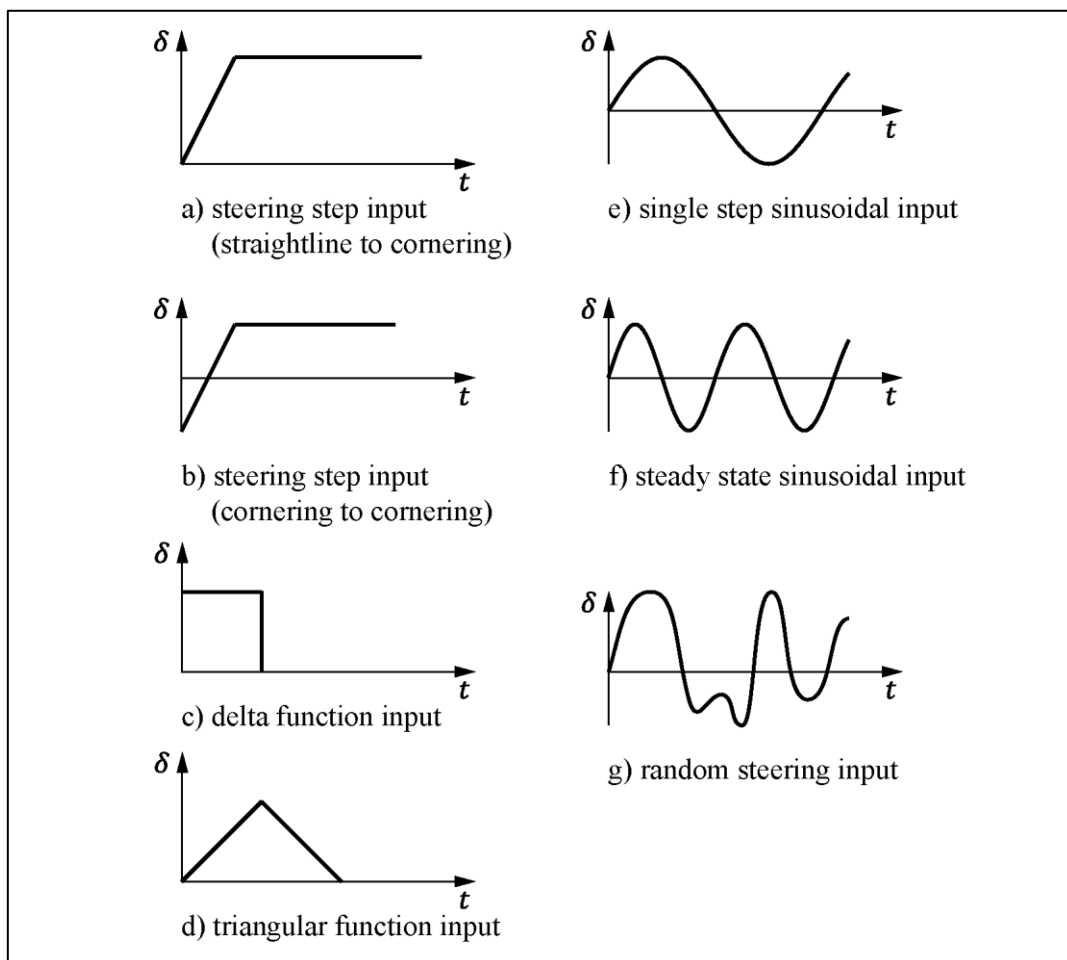


Figure 3.3: Non-steady-state steering inputs

Steering Step Input (Straightline to Cornering)

The steering step input is an open-loop maneuver for objective assessment. At a speed of approximately 80 km/h [25] the test vehicle's straight-ahead drive is interrupted by a short and quick steering action that ends at a given amplitude which is held for about 6 s [23]. The variables lateral acceleration a_y and yaw rate ω_z can follow this fast steering wheel variation only with delay. The

steering speed should be between 200 °/s and 500 °/s [23]. The steering amplitude should be selected in such a way that the lateral acceleration a_y is around 4 m/s² [25]. The throttle pedal should be kept constant during the maneuver. The maneuver is standardized in ISO 7401. Criteria for this maneuver are defined in [23] and [16].

To reduce the influence of different steering speeds, the reference point for the delay times t_{in} is the point at which the steering angle equals 50 % of the aimed amplitude as seen in Figure 3.4.

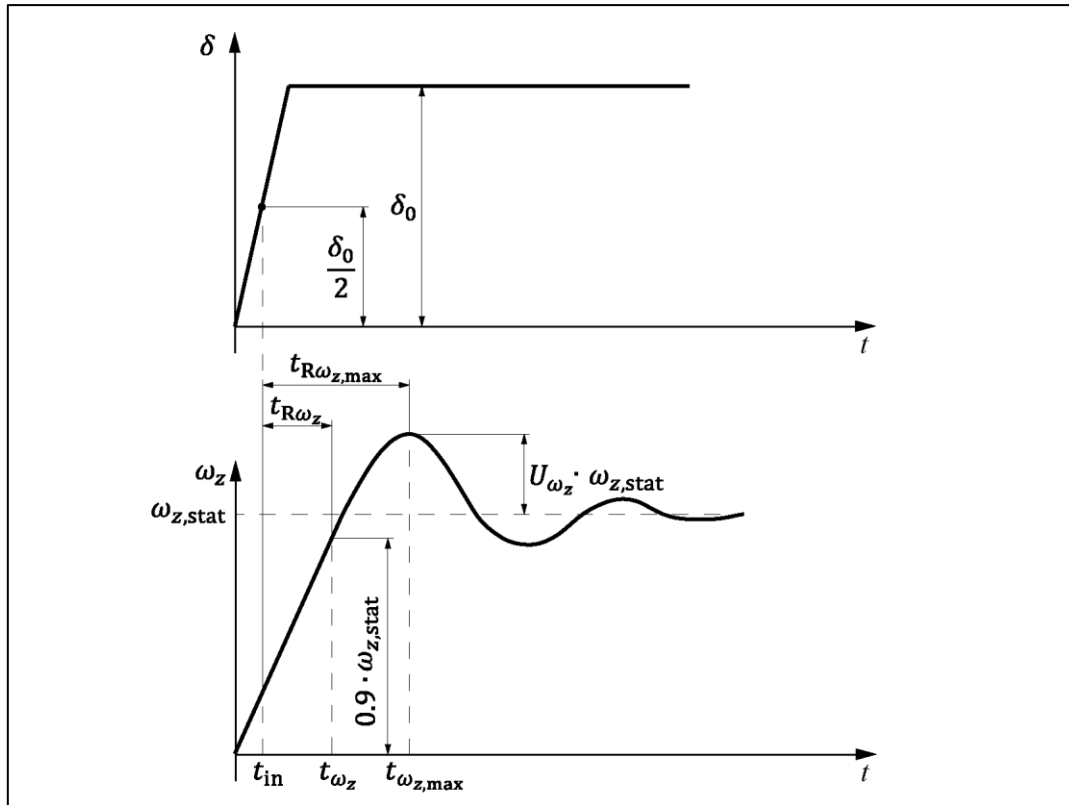


Figure 3.4: Steering step input

Table 3.5 provides an overview of possible criteria that can be evaluated for the steering step maneuver according to [23]. An interesting criterion is the so called TB value. According to [23], the TB value correlates very well with the subjective sensation of the test driver. Steady-state variables, such as the steady state side slip angle β_{stat} and the steady-state lateral acceleration $a_{y,stat}$, refer to their steady-state value that results subsequently to the actuation when the overshooting is faded away. Figure 3.4 provides the response time of the yaw rate $t_{R\omega_z}$ and the peak-response time of the maximum yaw rate $t_{\omega_{z,max}}$. The response time of the lateral acceleration t_{Ra_y} and peak-response time of the maximum lateral acceleration $t_{Ra_{y,max}}$ are evaluated the same way, according to the progress of the lateral acceleration a_y .

On the one hand, the vehicle should not react too slowly on the steering input. On the other hand, the overshoot reactions should not be too high [25]. A fast reaction causes a negative strong overshooting. Moreover, a fast reaction behavior indicates higher understeering at the steady-state circular test [23].

Table 3.5: Criteria and reference values for the steering step input according to [23]

Criterion	Symbol	Unit	Reference values
Response Time of ω_z	$t_{R\omega_z} = t_{\omega_z} - t_{in}$	s	0.10...0.20 [24]
Peak-Response Time $\omega_{z,max}$	$t_{R\omega_{z,max}} = t_{\omega_{z,max}} - t_{in}$	s	0.20..0.50 [24] 0.33...0.50 [16]
Response Time of a_y	$t_{Ra_y} = t_{a_y} - t_{in}$	s	
Peak-Response Time $a_{y,max}$	$t_{Ra_{y,max}} = t_{a_{y,max}} - t_{in}$	s	
TB value	$TB = t_{R\omega_{z,max}} \cdot \beta_{stat}$	°s	0.10...0.90 [24] (-0.04)+0.17...0.53 [16]
Overshoot of ψ	$U_{\omega_z} = \frac{\dot{\psi}_{max}}{\dot{\psi}_{stat}}$	%	1.20...1.80 [24] 13...17 [16]
Overshoot of a_y	$U_{a_y} = \frac{a_{y,max}}{a_{y,stat}}$	%	
Gain factor	$\left(\frac{\omega_z}{\delta}\right)_{stat}$	1/s	0.20...0.30 [16]

According to [16], good driving behavior can be determined if the gain factor is high and the peak-response time $t_{R\omega_{z,max}}$ is low. A high gain factor indicates strong and quick vehicle reactions on the steering wheel input. However, a high gain factor also causes massive vehicle reactions already at very small steering motions. Furthermore, the gain factor should also not be too small so that the driver does not have to carry out big steering motions. A high $t_{\omega_{z,max}}$ value indicates a slowly reacting vehicle, and accordingly a low $t_{\omega_{z,max}}$ value indicates a quickly reacting vehicle. In summary it can be said that the objective delay criteria have a high correlation with the driver's subjective evaluations. According to [23], $t_{R\omega_{z,max}}$ has the greatest significance of the introduced criteria.

Single Step Sinusoidal Steering Input

Another open-loop test for objective assessment is the single step sinusoidal input maneuver over one period. The driving speed should at least be 80 km/h. Straight-ahead driving is interrupted to execute the maneuver. The lateral accelerations should be between 2 and 7 m/s² [23]. As it is an open-loop maneuver, the use of a steering robot is necessary for a correct execution. The steering frequency should be within a range from 0.3 to 1.5 Hz [23]. Figure 3.5 provides a qualitative correlation of steering angle δ and the resulting lateral acceleration a_y .

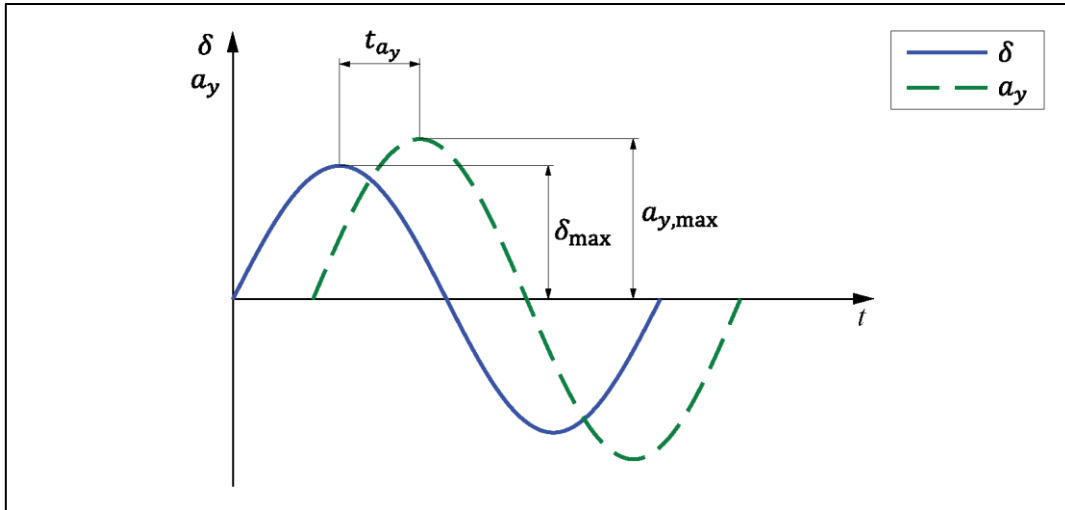


Figure 3.5: Single step sinusoidal input

An assessment criterion for this maneuver is the lateral acceleration gain factor:

$$\frac{a_{y,\max}}{\delta_{\max}}, \quad (3.27)$$

where δ_{\max} is the steering angle amplitude and $a_{y,\max}$ the amplitude of the lateral acceleration. A further criterion for this test is the time delay t_{a_y} between the amplitudes. Table 3.6 provides possible criteria for the assessment of the maneuver.

Table 3.6: Criteria for the single step sinusoidal steering input according to [23]

Criterion	Symbol	Unit
Gain factor	$\frac{a_{y,\max}}{\delta_{\max}}$	$\text{m}/^\circ \cdot \text{s}^2$
Time shift	t_{a_y}	s

Sine with Dwell Test

The range of applications for objective assessment criteria goes beyond the vehicle's tuning phase. Their concurrent relevance concerning legal requirements with regard to vehicle safety is briefly represented at the example of the sine with dwell test. The National Highway Traffic Safety Administration has developed a criterion to evaluate the potential danger of a spinout which can be seen as a criterion for steerability [32]. A spinout occurs if the yaw rate does not decrease fast enough after the steering input is over. The sine with dwell steering input is similar to the single step sinusoidal input. As provided in Figure 3.6 the difference is that there is a steering break at the peak of the second half circle of the sinusoid. This steering break is held for 500 ms [6]. However, the peak values are the same for both sine half circles. The sine with dwell test is usually done to validate the vehicle's electronic stability control.

The criterion F_{S0} can be determined as follows:

$$F_{SO} = \frac{\omega_z(t_0 + 1)}{\omega_{z,max}}. \quad (3.28)$$

According to the NHTSA a spinout occurs, if F_{SO} is higher than 0.6, which would mean that the yaw rate has decreased by less than 40 % in relation to the maximum yaw rate $\omega_{z,max}$ that occurred during the maneuver [32].

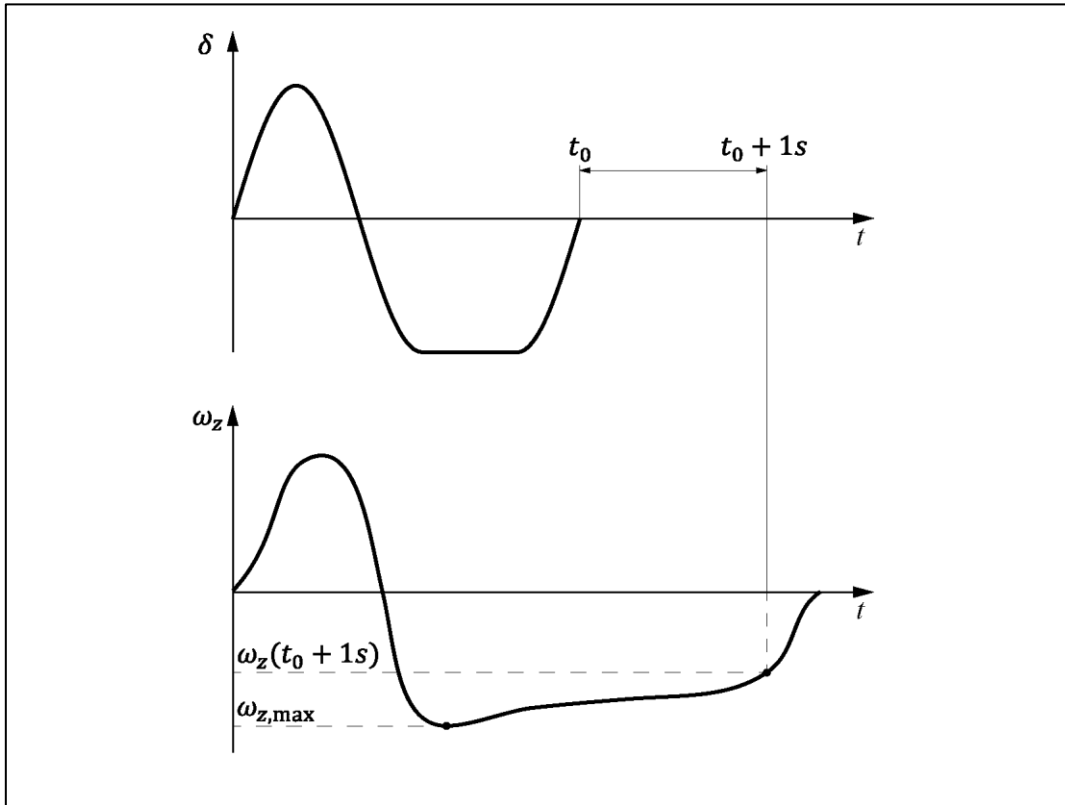


Figure 3.6: Sine with dwell test

A very similar definition can be found in the UN regulation ECE R13-H [31]. In this legislative act, the value an ESC system has to fulfill, is also determined according to equation 3.28.

Due to the circumstance that the ECE R13-H is a legislative provision and has the intention to avoid a spinout in any case, the regulation indicates a more severe limit value. The legislative act determines a limit of $F_{SO} \leq 0.35$ for equation 3.28. This means that the yaw rate has to be reduced by 65 %, 1 s after the steering input is over.

Furthermore, a second limit value is proposed in [31]. It is indicated that the yaw rate should not exceed 20 % of the maximum measured yaw rate $\omega_{z,max}$, 1,75 s after the steering input is over.

3.2 Classification of Driving States

Generally, longitudinal, lateral und vertical dynamics cannot be evaluated separately for a given course. They are rather interrelated with each other.

According to [10], the following driving situations can be critical concerning interactions among longitudinal, lateral and vertical dynamics:

- Braking while cornering
- Accelerating while cornering
- Load Change
- Braking/Starting on inhomogeneous road surfaces

The most standardized criteria are defined for specific driving maneuvers. As the tool was rather designed to evaluate circuit test drives, they cannot be implemented into the expert-tool directly. The use of the tool is not to evaluate specific maneuvers. The expert-tool was originally created to identify particular driving states, such as cornering or braking and analyze these situations by the use of appropriate assessment criteria. Table 3.7 provides an overview of the driving states the tool extracts from a circuit test drive. The driving states standstill and upshift have been added to the tool within the scope of this thesis.

Table 3.7: Extracted driving states

Driving State
Standstill
Driveaway
Upshift
Downshift
Braking
Negative Load Change
Coasting
Positive Load Change
Acceleration
Four-Wheel Drive Anti-Slip Regulation
Cornering
Turning into a curve

Standstill

The standstill state has no significance concerning driving dynamics. Nevertheless, the behavior of an electronically controlled transfer case clutch can be evaluated. The system has to be ready for torque supply in the moment the throttle is applied and a gear is engaged.

Driveaway/Acceleration

At a driveaway test, mainly the vehicle's traction and acceleration ability is evaluated. Tests are usually carried out on dry, wet and icy road surfaces. The wheel load distribution has the major impact

on the traction ability, but also the wheel suspension can have an influence on the traction ability. The traction ability can be evaluated by measuring the pulling force or by measuring time differences. Furthermore, the steering corrections that are required to maintain the vehicle's course (free control) and the vehicle yaw angle at a held steering wheel (fixed control) can be measured [10].

Tests to evaluate the traction ability by the pulling force or by time measurements are defined in DIN 70020-3.

Shifting

The provoked load change due to a shifting event can have influence on the vehicle's driving behavior. From the driving dynamics point of view, a shifting event has to be evaluated similar as a load change event according to the maneuvers and criteria that are suggested to evaluate a load change. Moreover, a shifting event has significant influence on the electronically controlled 4WD system, as the transmission's gear ratio is changed. The torque that is applied by the transfer case clutch has to be changed by the same ratio in order to maintain the same effective torque distribution between the axles.

Braking

An evaluation of the brake situation provides information about the vehicle's deceleration and stability behavior. An important parameter that influences the brake maneuver is the road surface and its coefficient of friction μ that defines the maximum possible deceleration ability. This parameter cannot be influenced, but the impacts can be analyzed. Generally, the braking ability depends on the initial speed and the road surface. The initial speed influences the deceleration as a factor of the driving resistance, the heating of the brakes and the dynamic load distributions along the drivetrain. A brake situation can occur during straight-ahead driving as well as during cornering [23].

In contrast to an improved acceleration behavior due to a four-wheel drive, the braking ability is not improved by a 4WD system, as a standard braking system always brakes all four wheels. Nevertheless, a 4WD system can influence the vehicle's braking ability with its additional weight or can cause instability by locking the drivetrain during a brake event. Therefore, it has to be compatible with ESP systems.

In [23] the following criteria are mentioned to assess the vehicle's deceleration behavior:

- Braking distance s
- Mean deceleration of a_x
- Brake pedal force F_{br}
- Maximum deceleration $a_{x,max}$

Furthermore, it is indicated in [23] that the increase of the braking pressure should happen as quickly as possible at a full braking maneuver. The point where the braking pressure p_{br} reaches 5 % of the destined pressure level is seen as the starting point of the braking action. The elapsed time between the starting point and the ending point, that is determined at 90 % of the destined pressure level, should

not exceed the threshold of 0.4 s. For braking on μ -split, high lateral acceleration values and high yaw rate values have to be expected.

Up to here, braking for straight ahead driving was examined. Furthermore, also the case of braking during cornering has to be discussed. To assess cornering stability and road holding ability, the following assessment criteria are recommended in [23]:

- Course deviation s
- Yaw rate ω_z
- Lateral deceleration a_y
- Maximum Yaw acceleration $\dot{\omega}_{z,\max}$

The assessment of braking while cornering refers in particular to the observation of:

- Steering performance that is described by the lateral deviation referring to the given steering angle and the intended course
- Yaw stability that is described by the occurring yaw and side slip angle

Possible criteria for the assessment of steering performance and yaw stability are listed in Table 3.8. According to [23], these criteria correlate very well with the subjective evaluation of the test driver. Especially the subjective evaluation of an increase of the understeering tendency correlates very well with the maximum value of the yaw rate $\omega_{z,\max}$.

Table 3.8: Possible assessment criteria for braking during cornering according to [23]

Category	Criterion	Symbol
Maximum Values	Yaw rate	$\omega_{z,\max}$
	Yaw acceleration	$\dot{\omega}_{z,\max}$
	Side slip angle	β_{\max}
Integral/mean values	Course deviation	s
	Course angle error	θ
	Course curvature	κ
Values at driver's reaction point (1 s after brake starting point)	Lateral acceleration	$a_{y,1s}$
	Side slip angle	β_{1s}
	Yaw rate	$\omega_{z,1s}$

For the assessment of braking during cornering, low and maximum deceleration have to be distinguished. The wheel load shift, due to a braking action, causes a yaw moment that will reach its maximum at medium decelerations. At high decelerations, the brake force distribution defines the handling characteristics. The brake force distribution also defines the locking order of the wheels. If the rear wheels lock first, a loss in yaw stability occurs and this is normally expressed by high side slip angles. Locked front wheels lead to the limit of steering performance, so that the vehicle is pushed out of the curve straight ahead.

Usually, the driving maneuver braking in a turn, which is defined in ISO 7975, is undertaken to analyze the vehicle's braking behavior during cornering. Initial situation for this maneuver is a steady-state circular motion. An open-loop test method for straight ahead braking on μ -split is provided in ISO 14512 and for straight ahead braking with ABS in ISO 21994.

Load Change

In literature, load change is generally defined as the disconnection of the engine's power supply to the drivetrain. In ISO 9816 a load change is denominated as a power-off reaction. A load change can also occur in the other direction by a resumption of the power supply to the wheels. Therefore, this state was added to the driving states which the expert-tool extracts. In this thesis, the interruption is defined as a negative load change and the resumption as a positive load change. If the single term load change is used, a negative load change is meant in this thesis.

Technically, a load change is the disturbance of the ride due to a change of the longitudinal forces that are applied to the wheels. A load change can be caused by varying the throttle pedal position, engaging the clutch or an automatic gear box shift. A load change affects a change of the mathematical sign of the longitudinal forces on the wheel [23].

In road trials, load changes are evaluated by means of default driving maneuvers. Usually, a load change is carried out as a closed-loop maneuver during a steady-state circular motion with a constant radius. The magnitude of the load change depends on the current lateral acceleration and the actual change of the longitudinal forces. The test's significance for the comparison of different vehicles is limited, as the lateral acceleration for certain radiuses is different for every vehicle. Subjective evaluation returns a positive assessment if the vehicle slightly turns in after a load change [23].

In [23] the following assessment criteria are suggested to evaluate a load change during a steady-state circular motion:

- Yaw rate ω_z
- Yaw acceleration $\dot{\omega}_z$
- Lateral acceleration a_y
- Curve radius R
- Curve curvature κ
- Lane course

Furthermore, a comparison should be done between the disturbed driving situation by a load change and the theoretical behavior, if no disturbance would have occurred.

In ISO 9818 the open-loop evaluation of a load change while cornering is standardized.

Coasting

A vehicle delivers thrust to the engine, if the clutch is engaged and no power is applied by the engine. This state is detected by the expert-tool and occurs logically subsequently to a load change. The state

is detected within the tool, if the state lasts for longer than 0.5 s and continues until the throttle pedal or the clutch pedal is applied.

In comparison to a conventional two-wheel drive, the absorbed torque is divided among both axles at a 4WD. This means, one axle has to absorb less longitudinal forces and has more space left for the absorption of lateral forces in critical driving situations.

Four-Wheel Drive Anti-Slip Regulation

The 4WDASR prevents an axle from spinning. If one axle is located on a low friction surface and the wheels start to spin, the 4WDASR actuates the transfer case clutch and enables a rigid connection between the axles. 4WDASR interventions most likely occur at starting and acceleration situations on low friction surfaces. Basically, 4WDASR interventions during driving and coasting have to be distinguished. A 4WDASR event during coasting for example can occur on low traction surfaces, if the primary axle has to transfer more thrust to the road than the low traction surface's friction coefficient allows. In this case a 4WDASR event prevents the primary axle from overbraking.

4WDASR assessment criteria are related to the reasons for the intervention, as well as to the impact and to the extent of the 4WDASR intervention. Furthermore, actuation measures concerning the system's torque supply are of interest.

Cornering

Cornering behavior describes the yaw behavior and the additional necessary movements that have to be applied due to the influence of lateral and longitudinal accelerations. This behavior is influenced by the wheels that are only able to transfer and absorb lateral and longitudinal forces while slipping.

Typical criteria for the evaluation of a cornering event are the self-steering behavior and the yaw amplification which have been discussed in chapter 3.1.1. Load change and acceleration out of a steady-state circular motion are typical tests to evaluate the vehicle's cornering behavior. Furthermore, the control effort to maintain on the given course can be evaluated [10].

The evaluation of steady-state circular driving behavior is standardized in ISO 4138.

3.3 Stability/Agility

Stability and agility are common terms that occur in professional journals or advertisements to describe the vehicle's performance. A lateral dynamic control system has to be adjusted with regard to a good performance in stability and agility. Nevertheless, these requirements conflict with each other at certain points [32].

A system that is designed to provide high safety will not allow high lateral acceleration values. Consequently, this means less agility, but more stability. On the other hand, high lateral accelerations

can be necessary at fast lateral maneuvers, as driving around obstacles. Therefore, a consensus between these requirements has to be found in the design phase of a vehicle controller.

3.3.1 Stability

The stability of a vehicle is the reaction behavior after the initiation of a disturbance. Disturbances can be influences from the environment, such as cross winds or road unevenness. Inner disturbances can occur due to driver instructions, such as steering wheel modifications or sharp braking actions. An instable vehicle does not follow the applied direction with its longitudinal axis anymore. In the worst case, the car spins out. Controlled oversteering, which could be considered as an instable driving situation, would be drifting as it is done by rally race drivers.

Cornering Stability

A criterion to assess the vehicle's stability is the side slip angle β [16]. Depending on the driving maneuver, there are different speculations on the curve progression of the side slip angle. For a steady-state circular motion, the side slip angle is expected to rise linear with the lateral acceleration. In [32] and [16] it is stated as a general requirement for stability that the peak value of the side slip angle during the maneuver should be as small as possible. According to [1], a vehicle is considered to be stable up to a side slip angle of 5° .

Figure 3.7 explains the justification of the side slip angle as a criterion for stability. Steering a car is expressed in a yaw moment. The yaw moment is responsible for the directional change of the vehicle. However, the severability depends on the side slip angle. As seen in Figure 3.7 the resulting yaw moment vanishes at high side slip angles β depending on the steering angle δ . On high friction surfaces as dry asphalt, this effect occurs late at side slip angles around 12° , but on low friction surfaces as ice, the effects already takes place at low side slip angles around 2° [13].

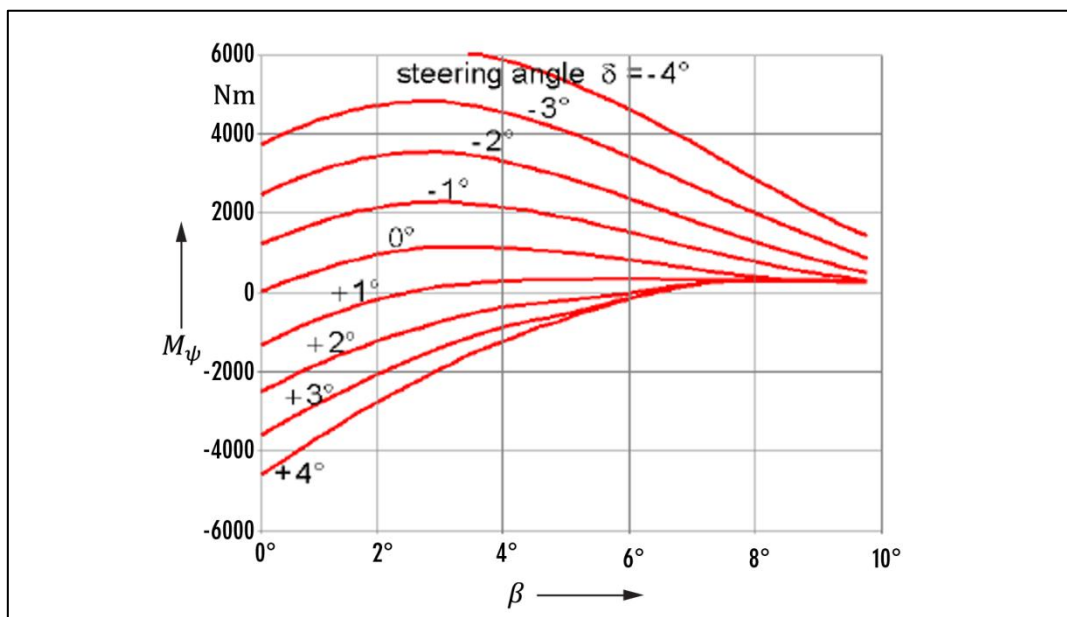


Figure 3.7: Yaw moment over side slip angle on high traction surface, modified from [13]

In [16], Mitschke defines that a vehicle is stable, if the characteristic velocity v_{char} is greater than 0. Therefore, a stable vehicle needs to have understeering layout properties. If the vehicle basically shows oversteering behavior, the vehicle is only stable up to the threshold of the critical velocity v_{crit} .

Braking Stability

Due to stability reasons, the front axle has to be braked stronger. In [16], Mitschke explains the reason for this requirement of an unequal brake force distribution.

At a brake situation, the inertial force F_t occurs. Furthermore, a lateral disturbing force F_y may occur due to the brake application. If the rear wheels block and the front wheels do not, the lateral force can only be compensated by the front wheels as illustrated in Figure 3.8 a). Due to the applied lateral force F_{yf} on the front wheels, a moment $l_f \cdot F_{yf}$ occurs that turns the vehicle away from the direction of the resulting force F_{tot} . The angle γ increases and the vehicle can be considered to be instable. In the worst case, the car would spin out.

On the other hand, the vehicle can be stabilized by braking the front wheels stronger than the rear wheels. If the front wheels block and the rear wheels do not, the lateral disturbance force F_y is compensated by the rear wheels. As provided in Figure 3.8 b), a moment $l_r \cdot F_{yr}$ that stabilizes the vehicle occurs. The occurring moment turns the car in the direction of the resulting force and reduces the angle γ . In this condition, the vehicle continues to move straight ahead, but can be considered to be stable.

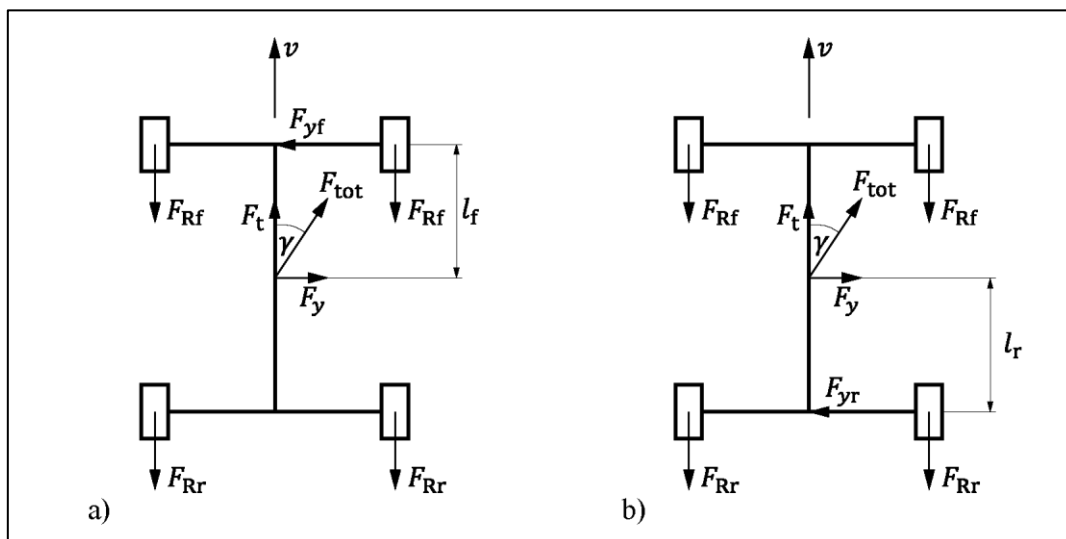


Figure 3.8: Braking with blocked rear wheels in a) and blocked front wheels in b)

For this reason, the wheels on the front axle are automatically braked stronger than the vehicle's rear axle wheels by the brake assistance system. Consequently, an electronically controlled transfer case system has to open the clutch if the braking pressure p_{br} exceeds a default threshold according to the theory of chapter 2.3.5. A rigid connection between the axles tries to prevent rotational speed differences. If the clutch would not relieve the connection between the cardan shafts, the rear axle would be braked the same way as the front axle via the drivetrain.

3.3.2 Agility

According to [3], the term agility is not defined uniformly within the field of automotive engineering. In common linguistic usage, the term agility describes a quick reaction behavior to changes. Concerning vehicle dynamics, the term agility is used to describe longitudinal and lateral dynamic behavior. An agile vehicle is defined by a quick reaction behavior and by smooth and sensitive steering characteristics. In automotive magazines or advertisements of the automotive industry, agility is normally rated as a positive and sportive vehicle property. Diermeyer [3] indicates that a too agile adjustment can have negative impact on the personal driving comfort. Therefore, agility is often used in correlation with subjective driving evaluation. The significance of the term agility as an objective assessment criterion is limited.

Nevertheless, agility can be expressed and quantified by evaluating the vehicle's lateral dynamic reaction behavior. In [32], it is indicated that the vehicle's agility is defined by its maximum allowed lateral acceleration a_y . According to [3], criteria that can be considered additionally to the subjective evaluation of the vehicle's agility are the vehicle's delay and amplitude behavior on the driver's input. If the vehicle follows the driver's input slowly, the vehicle's agility is considered to be inert. If the vehicle reacts unexpectedly strong, the agility behavior is defined as nervous.

Furthermore, Diermeyer [3] defines the following requirements for an optimum vehicle behavior with regard to agility:

- The vehicle has to follow the driver's request exactly and with low side slip angles
- The vehicle reaction has to be quick and the response time has to be short
- The vehicle reaction has to be expectable and controllable

4 Implementation of Substitution Calculations

On the one hand, a high amount of recorded data signals is available for simulation evaluations. Nearly every physical state variable is accessible for the subsequent analysis. On the other hand, the available signals for real road tests depend on the measured variables. Table 4.1 gives an overview of standardly measured data signals at road trials.

Table 4.1: Common measured variables for a road trial

Signal	Symbol	Unit
Longitudinal velocity	v_x	m/s
Lateral acceleration	a_y	m/s ²
Yaw rate	ω_z	°/s, rad/s
Steering wheel angle	δ_S	°, rad
Brake pedal pressure	p_{br}	Pa
Throttle valve opening	th	°, rad
Gear	$gear$	-
Engine speed	n_{mot}	rpm
Engine torque	T_{mot}	Nm
Rotational wheel speeds	ω_i	°/s, rad/s
Torque on front and rear shaft	T_f, T_r	Nm
ESP/ABS flags	-	-
Target torque	T_t	Nm

Certain data signals can easily be reconstructed by substitution calculations to broaden the quantitative amount of the returned information for road tests within the expert-tool.

To receive an overview of the required substitution calculations within the expert-tool, the existing assessment criteria and calculations had to be extracted according to their structure of input signals. The aim was to receive information of imperfect calculations. Furthermore, it had to be evaluated which signals were missing.

The result of this extraction was that the tire slip angle difference $\Delta\alpha$ between the front and rear axle according to the single track model was missing for test drive evaluations. This information can be applied to evaluate the steering tendency. Furthermore, a data signal of the target yaw rate $\omega_{z,t}$ has not been available for test drive evaluations.

4.1 Current Yaw Rate

Combining known kinematic relations of the single track model, which was discussed in chapter 2.1, and the steady-state steering test of chapter 3.1.1 provides a possibility to estimate the current yaw rate $\omega_{z,c}$. For a steady-state circular motion the side slip angle velocity $\dot{\beta}$ is assumed to be zero. Due to this condition the yaw rate ω_z equals the angular velocity and can be calculated as follows:

$$\omega_z = \frac{v}{R}. \quad (4.1)$$

The vehicle's lateral acceleration can be adopted according to the centripetal acceleration provided in equation 2.17. Inserting equation 2.17 in equation 4.1 delivers a possibility to estimate the current yaw rate $\omega_{z,c}$:

$$\omega_{z,c} = \frac{a_y}{v}. \quad (4.2)$$

In Figure 4.1 the current yaw rate signal $\omega_{z,c,sim}$ of evaluated simulation data, that is assumed to be accurate, is compared to the, according to equation 4.2, calculated signal $\omega_{z,c,calc}$. A satisfying result among the original signal, that is assumed to be accurate, and the substitution calculation can be approved.

4.2 Target Yaw Rate

In the current state of the expert-tool the target yaw rate $\omega_{z,t}$ was applied directly from a target yaw rate signal and was therefore only available for driving simulations. To obtain the target yaw rate for road trial signals too, a substitution calculation had to be implemented. The expected yaw rate can be calculated according to [10]:

$$\omega_{z,t} = \kappa_{corr} \cdot v. \quad (4.3)$$

The curvature κ is defined as

$$\kappa = \frac{1}{R}. \quad (4.4)$$

The curvature κ can be obtained from vehicle specific data sheets that provide the associated curvature for the applied steering wheel angle δ_S . To receive the progress of the driven radius this table can be applied to the steering wheel angle's data signal. Furthermore, the curvature has to be corrected by the tire slip angle influence:

$$\kappa_{corr} = \kappa \cdot f_{corr}. \quad (4.5)$$

Therefore, the curvature is multiplied by a correction factor f_{corr} that can be derived by means of the definition of the self-steering behavior. The correction term f_{corr} can be determined by inserting equation 3.25 into equation 3.23:

$$f_{corr} = \frac{1}{1 + \frac{v^2}{v_{char}^2}}. \quad (4.6)$$

Equation 4.6 contains the vehicle specific characteristic speed v_{char} that has to be determined by evaluating the vehicle's steady-state circular driving behavior before. For small angles the radius R can be assumed according to the relations of Figure 2.2 as follows:

$$\tan \delta \approx \delta = \frac{l}{R}. \quad (4.7)$$

In addition the equation to calculate the target yaw rate $\omega_{z,t}$ reads

$$\omega_{z,t} = \frac{v \cdot \delta}{l \cdot \left(1 + \frac{v^2}{v_{\text{char}}^2}\right)}. \quad (4.8)$$

Figure 4.1 provides a comparison between the, according to equation 4.8, calculated target yaw rate $\omega_{z,t,\text{calc}}$ and the target yaw rate $\omega_{z,t,\text{sim}}$ of evaluated simulation data that is assumed to be accurate. As at the verification of the calculated current yaw rate, also the simulation signal of the target yaw rate $\omega_{z,t,\text{sim}}$ is assumed to be accurate. The graphic returns a satisfying result that verifies the application of equation 4.8 to substitute the original signal.

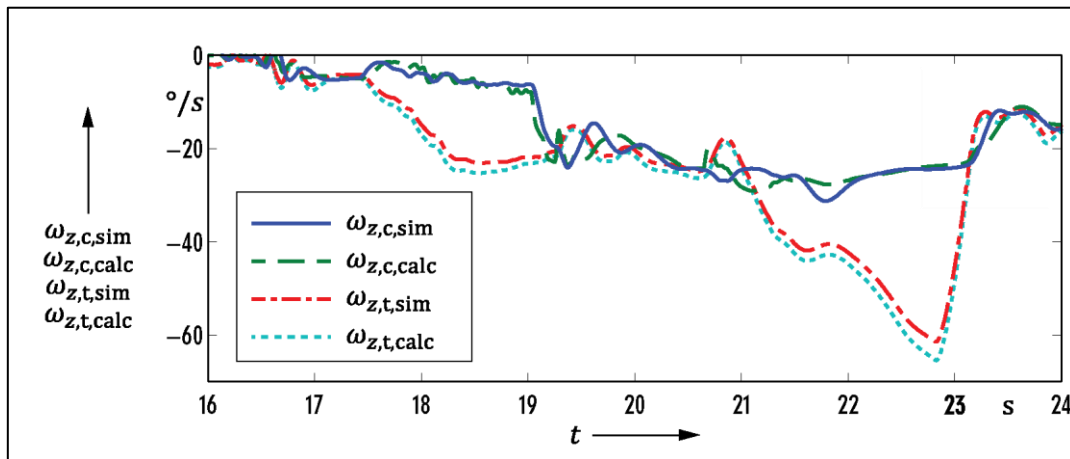


Figure 4.1: Comparison of calculated and accurate yaw rate signals

4.3 Steering Tendency

Vehicle dynamic control systems try to recognize critical driving situations and the optimum moment to interfere. On the one hand, the reaction should take place as long as the vehicle still can be stabilized. On the other hand, the acceptance of the system decreases if the system interferes too early. Due to safety reasons, today's entire standard passenger cars are standardly configured in such a way to show understeering driving behavior during cornering, because uncontrolled swerving of the vehicle's rear, caused by a strongly oversteering vehicle, is considered to be more difficult to control than a straight ahead driving understeering vehicle [10].

There exist distinct ways to evaluate the vehicle's current steering tendency. Many methods base on the linear single track model of chapter 2.1 which is only valid in the linear driving range for lateral accelerations up to 4 m/s^2 . Nevertheless, around 95 % of all lateral accelerations measured at standard road traffic situations are beneath 3.5 m/s^2 [10]. This argument justifies the evaluation of the steering tendency based on the linear bicycle model. Moreover, it is indicated in [32] that this constriction can

be useful for the determination of critical driving situations. The higher the deviations between results of the linear model and measured reference values are, the higher is the risk of a critical driving situation. According to [32], the steering tendency can be evaluated by the following methods:

- Tire slip angle difference
- Yaw rate difference
- Lateral acceleration
- Characteristic speed
- Curve radius
- Self-steering gradient

The determination of the vehicle's steering tendency by evaluating the tire slip angle difference, the self-steering gradient or the characteristic speed are relatively related to each other as the derivation of the self-steering gradient in chapter 3.1.1 shows.

Within the expert-tool, the steering tendency is evaluated according to the tire slip angle difference and the yaw rate difference. The calculation of the steering tendency according to the tire slip angle difference $\Delta\alpha$ is derived in chapter 3.1.1. The calculation is implemented into the expert-tool according to equation 3.19.

Furthermore, the steering tendency is evaluated according to the method of the yaw rate difference within the tool. If a yaw rate sensor is mounted on the road trial's test vehicle, the steering tendency can be evaluated according to the theory of the yaw rate difference. The yaw rate indicates to what extent the vehicle follows the driver's input. To receive the steering tendency the measured yaw rate $\omega_{z,c}$ has to be subtracted from the target yaw rate $\omega_{z,t}$:

$$\Delta\omega_z = |\omega_{z,t}| - |\omega_{z,c}| \begin{cases} > 0, & \text{understeering} \\ < 0, & \text{oversteering} \end{cases} \quad (4.9)$$

If equation 4.9 outputs a result greater than 0 °/s, understeering is detected. If the output is lower than 0 °/s, oversteering is determined. Generally, the sign of the steering angle δ is negative in right curves and positive in left curves [10]. Therefore, also the sign of the current yaw rate is chosen that way. Equation 4.8 for the calculation of $\omega_{z,t}$ contains the steering angle δ . Therefore, the sign of the target yaw rate complies with the signs of steering angle δ and current yaw rate $\omega_{z,c}$. Due to the absolute values in equation 4.9 the output result is not affected by the sign of the curve direction. Nevertheless, equation 4.9 had to be modified within the expert-tool for border cases where the signs of the target and the current yaw rate can be unequal. According to [32], instability can be detected in the case of unequal signs.

Under- or oversteering is only detected if the yaw rate difference exceeds a certain threshold value. According to [32], the choice of this threshold is essential for the quality of the method. Good results could be achieved with threshold values between 2 and 5 °/s.

4.4 Side Slip Angle

As provided in Figure 2.2 the side slip angle β is the angle between the velocity vector of the vehicle in the vehicle's center of gravity and the vehicle's longitudinal axis. As the side slip angle is one of the two degrees of freedom of the simple single-track model it is an important quantity for the assessment

of vehicle dynamics. According to the relations of the single-track model the side slip angle β can be determined by rewriting equation 2.15 and 2.16:

$$\beta = \delta - \alpha_f - \frac{l_f \cdot \omega_z}{v} = \frac{l_r \cdot \omega_z}{v} - \alpha_r . \quad (4.10)$$

However, this approach follows the non-linear simplification of the single-track vehicle model and requires measured tire slip angles as well as a measured yaw rate. Nevertheless, an accurate determination of the side slip angle is not possible with the sensor technology that is available on series-production vehicles. For an exact determination a bi-axial optical sensor for the measurement of the lateral velocity v_y is necessary. With the availability of this parameter the side slip angle β can be calculated according to:

$$\beta = \arctan\left(\frac{v_y}{v_x}\right) . \quad (4.11)$$

Nevertheless, usually the side slip angle is not measured explicitly during a field trial. However, the value of the side slip angle represents an objective criterion for stability and the sense of driving. Also for simulations a way to calculate the side slip angle is needed. In addition, the knowledge of the side slip angle can be very useful for further calculations.

As the direct determination of the side slip angle β via kinematic relations very often is not accurate enough, observation techniques are used to estimate the side slip angle. The objective of a state estimation is the determination of parameters that are not directly measurable, but can be determined by model relations. For this purpose, first of all a vehicle model has to be introduced. This model can be either a kinematic or a physical model. Because of the inaccuracy of pure kinematic models many approaches consider kinetics additionally.

By means of the chosen model the prediction of the new state can be done and the difference between the real measured state and the estimated state can be determined. At last, the required correction has to be calculated. Established observation techniques are for example the Kalman filter or the Luenberger state observer. The state observer approach can be considered simpler than the implementation of a Kalman filter [32]. Also an estimation by using the method of the least squares provides a possibility. The choice of the observation technique is not related to the chosen model.

4.4.1 Side Slip Rate Estimation

A kinematic model to calculate the side slip angle is suggested in [21]. The equations to determine the longitudinal acceleration a_x and the lateral acceleration a_y read

$$a_x = \dot{v} \cdot \cos \beta - v \cdot (\dot{\beta} + \dot{\psi}) \cdot \sin \beta , \quad (4.12)$$

$$a_y = \dot{v} \cdot \sin \beta - v \cdot (\dot{\beta} + \dot{\psi}) \cdot \cos \beta . \quad (4.13)$$

After neglecting the temporal change and linearizing, the equations are rewritten as

$$a_x = \dot{v}_x - \dot{\psi} \cdot v_y , \quad (4.14)$$

$$a_y = \dot{v}_y + \dot{\psi} \cdot v_x . \quad (4.15)$$

The kinematic relations for v_x and v_y are known from equation 2.8 and the side slip angle β can be assumed as being small. This returns

$$v_x \approx v , \quad (4.16)$$

$$v_y \approx v \cdot \beta . \quad (4.17)$$

Applying the product rule on equation 4.17 returns

$$\dot{v}_y = \dot{v} \cdot \beta + v \cdot \dot{\beta} \approx v \cdot \dot{\beta} . \quad (4.18)$$

After inserting equation 4.17 into equation 4.15, the side slip rate $\dot{\beta}$ can be estimated by means of the lateral acceleration a_y , the velocity v and the yaw rate ω_z :

$$\dot{\beta} = \frac{a_y}{v} - \omega_z . \quad (4.19)$$

The side slip angle β can be determined by integrating the side slip rate $\dot{\beta}$ over the time:

$$\beta_{i+1} - \beta_i = \int_{t_i}^{t_{i+1}} \dot{\beta}(t) dt . \quad (4.20)$$

As this function is analytically not solvable, equation 4.20 has to be rewritten and integrated according to a numerical integration rule, such as the trapezoidal rule:

$$\beta_{i+1} = \frac{\dot{\beta}_{i+1} + \dot{\beta}_i}{2} \cdot (t_{i+1} - t_i) + \beta_i . \quad (4.21)$$

The side slip angle β can now be expressed by the yaw rate ω_z , the lateral acceleration a_y and the velocity v . However, the disadvantage of this method is that measurement errors are now added up over the time by the integration. This can lead to bigger errors. Therefore, the estimated side slip angle signal is set to 0 at certain points where straight ahead driving can be assumed. Furthermore, the introduced method to estimate the side slip angle β is only valid for small angles due to the simplifications that have been made.

Figure 4.2 provides the comparison of the estimated side slip angle β_{est} according to equation 4.21 in comparison to the side slip angle signal β_{sim} that has been taken from a simulation with a BMW X3. The side slip angle signal β_{sim} is assumed to be accurate. As seen in Figure 4.2 the approximation is consistent up to mean steering wheel angles δ_s and can be verified for this range. However, as the side slip angle is obtained from the side slip rate by integration, small irregularities falsify the result and grow with the integration. Furthermore, no kinetic relations are considered. As seen in the graph the estimation performs very poorly at extreme cornering situations as it occurs from 77 s to 81 s. However, the estimation provides satisfying results for moderate cornering situations as they occur in the graph for example from 63 s to 65 s.

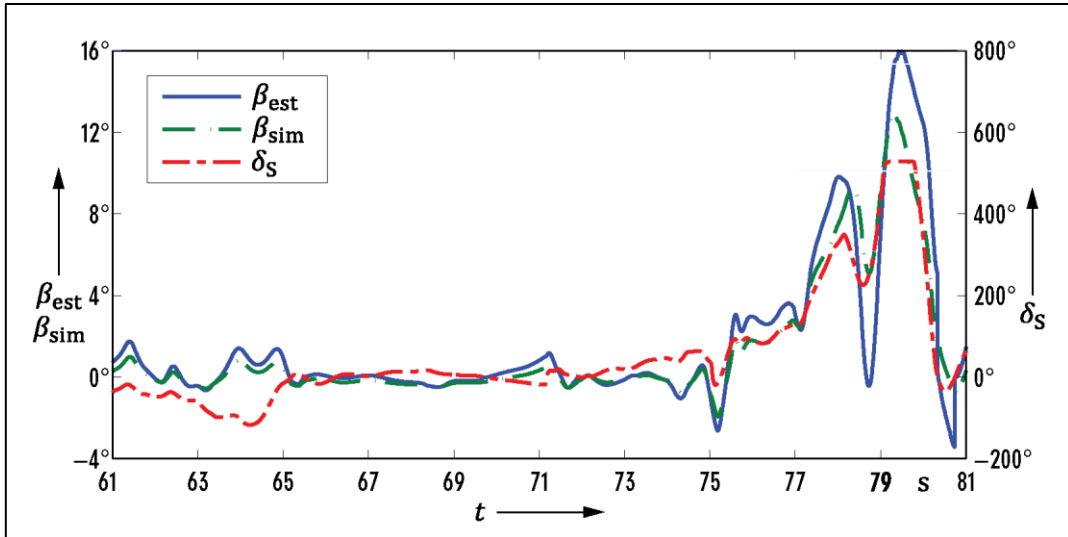


Figure 4.2: Side slip angle estimation

In literature many methods to estimate the side slip angle rely on the use of state observers to compensate noise. In addition, physical models that consider kinetics and not only kinematic relations are used to improve the estimation results.

4.4.2 Luenberger Observer

Observers are applied for the reconstruction of technically difficult or non-measurable state variables. Furthermore, they are applied if the measurement is economically not reasonable.

The idea of an observer relies on David Luenberger from 1964 by connecting an observer parallel to the control system. This structure allows the determination of the difference between a measurement of the system and the observer according to equation 4.24 that is returned to the model. The observer can react on errors or inaccuracies. The standard space state form for a continuous time-invariant system with the state vector \mathbf{x} , the output vector \mathbf{y} and the input vector \mathbf{u} can be expressed as

$$\dot{\mathbf{x}}(t) = \mathbf{A} \cdot \mathbf{x}(t) + \mathbf{B} \cdot \mathbf{u}(t) , \quad (4.22)$$

$$\mathbf{y}(t) = \mathbf{C} \cdot \mathbf{x}(t) + \mathbf{D} \cdot \mathbf{u}(t) , \quad (4.23)$$

where \mathbf{A} is the system matrix, \mathbf{B} the input matrix, \mathbf{C} the output matrix and \mathbf{D} the feedthrough matrix. The state estimation error $\tilde{\mathbf{x}}$ can be determined by subtracting the true value \mathbf{x} from the estimated state $\hat{\mathbf{x}}$:

$$\tilde{\mathbf{x}}(t) = \hat{\mathbf{x}}(t) - \mathbf{x}(t) . \quad (4.24)$$

In [4] a method to estimate the vehicle's lateral velocity v_y is introduced by using a time varying Luenberger state observer that bases on the kinematic model of the equations 4.14 and 4.15. The observer estimates the lateral velocity v_y and the longitudinal velocity v_x . The input parameters to the system are the longitudinal acceleration a_x and the lateral accelerations a_y , as well as the yaw rate ω_z . Measurements of the longitudinal velocity v_x are used to adjust the observation.

The equations can be written down in state space form:

$$\begin{bmatrix} \dot{v}_x(t) \\ \dot{v}_y(t) \end{bmatrix} = \mathbf{A}(\omega_z(t)) \cdot \begin{bmatrix} v_x(t) \\ v_y(t) \end{bmatrix} + \mathbf{B} \cdot \begin{bmatrix} a_x(t) \\ a_y(t) \end{bmatrix}. \quad (4.25)$$

With the system matrix \mathbf{A} :

$$\mathbf{A}(\omega_z) = \begin{bmatrix} 0 & \omega_z(t) \\ -\omega_z(t) & 0 \end{bmatrix}, \quad (4.26)$$

the input matrix \mathbf{B} :

$$\mathbf{B} = \begin{bmatrix} 1 & 0 \\ 0 & 1 \end{bmatrix}, \quad (4.27)$$

and the output matrix \mathbf{C} :

$$\mathbf{C} = [1 \quad 0]. \quad (4.28)$$

The advantage of the kinematic model is that no vehicle parameters are considered. Therefore, the system is unaffected by changes of the vehicle parameters. Furthermore, the model provides estimates throughout the linear handling region. Nevertheless, the estimation results are noisy.

In the model, the measured longitudinal velocity v_x is the feedback variable. The yaw rate, the lateral acceleration and the longitudinal acceleration are the additional parameters. It is required that the measurements of the parameters are very accurate as the feedback of the longitudinal velocity cannot balance the offset of the measured accelerations or the measured yaw rate. Farrelly and Wellstead [4] suggest a state observer in the following form:

$$\begin{bmatrix} \hat{v}_x(t) \\ \hat{v}_y(t) \end{bmatrix} = (\mathbf{A}(\omega_z) - \mathbf{K}(\omega_z(t)) \cdot \mathbf{C}) \cdot \begin{bmatrix} \hat{v}_x(t) \\ \hat{v}_y(t) \end{bmatrix} + \mathbf{B} \cdot \begin{bmatrix} a_x(t) \\ a_y(t) \end{bmatrix} + \mathbf{K}(\omega_z(t)) \cdot v_x(t), \quad (4.29)$$

$$\mathbf{K} = \begin{bmatrix} 2 \cdot \varepsilon \cdot |\omega_z(t)| \\ (\alpha^2 - 1) \cdot \omega_z(t) \end{bmatrix}. \quad (4.30)$$

where \mathbf{K} is the gain matrix and ε is a model design parameter that can be used to reduce the convergence of the estimation error to zero and to decrease the sensitivity to measurement noise [21].

Due to the impreciseness of mere kinematic models the most models additionally include kinetic considerations. Therefore, also a physical model in combination with a state observer is introduced in [4]. The model considers the physical parameters vehicle mass m , the tire cornering stiffness coefficients $c_{\alpha i}$ and the yaw moment of inertia J . A state observer is used to estimate the lateral velocity v_y and the yaw rate ω_z . Therefore, the steering angle δ is the input parameter to the system. The lateral acceleration a_y and the yaw rate ω_z are measurements to adjust the observation. Nevertheless, the model is only valid within the linear operating range, as the tire cornering stiffness coefficients are considered to be constant in the model. Other approaches additionally consider the estimation of the tire cornering stiffness coefficients. A possibility to estimate the cornering stiffness coefficients is to use the magic tire formula [32].

4.4.3 Kalman Filter

A state observer assumes that the model is exact and the measurements are accurate. In contrast to the state observer, the Kalman filter explicitly considers model accuracies and noise. The Kalman filter is based on a stochastic process model and works recursive according to the predictor-corrector method [19].

The Kalman filter can be used for the state estimation of linear models. Nevertheless, very often linear models are not sufficient to describe a real system. In these cases the Extended Kalman Filter (EKF) or the Unscented Kalman Filter (UKF), that base on the principles of the linear Kalman filter, can be applied. The linear Kalman filter works in two steps. The first step is the prediction step. In this step an estimation of the state is calculated by means of a model. In the second step, the correction step, the calculated estimation is compared to the measurement. The quality of the estimation is evaluated to improve the next prediction. The linear Kalman filter relies on a stochastic description of the time-discrete system and the system is defined as

$$\mathbf{x}_{k+1} = \mathbf{A} \cdot \mathbf{x}_k + \mathbf{B} \cdot \mathbf{u}_k + \boldsymbol{\xi}_k, \quad (4.31)$$

$$\mathbf{y}_k = \mathbf{C} \cdot \mathbf{x}_k + \boldsymbol{\theta}_k, \quad (4.32)$$

where \mathbf{x}_{k+1} is the estimated state, \mathbf{u}_k the input variable, $\boldsymbol{\xi}_k$ the system noise and $\boldsymbol{\theta}_k$ the measurement noise. The random variables \mathbf{x}_k , \mathbf{y}_k , $\boldsymbol{\xi}_k$ and $\boldsymbol{\theta}_k$ are assumed to be normally distributed. The noise variables are additionally assumed to be stochastic independent and without mean values. The system and measurement noise are described by the variances $\mathbf{P}_{\boldsymbol{\xi},k}$ and $\mathbf{P}_{\boldsymbol{\theta},k}$.

In the prediction step, $\widehat{\mathbf{x}}_{k+1}^-$ is estimated:

$$\widehat{\mathbf{x}}_{k+1}^- = \mathbf{A} \cdot \widehat{\mathbf{x}}_k^- + \mathbf{B} \cdot \mathbf{u}_k. \quad (4.33)$$

The covariance matrix of the estimation error \mathbf{P}_{k+1}^- can be determined according to:

$$\mathbf{P}_{x,k+1}^- = \mathbf{A} \cdot \mathbf{P}_{x,k} \cdot \mathbf{A}^T + \mathbf{P}_{\boldsymbol{\xi},k}. \quad (4.34)$$

In the correction step, the prediction is corrected by the measurement results. First of all, the correction term, the so-called Kalman amplification \mathbf{K}_{k+1} has to be calculated:

$$\mathbf{K}_{k+1} = \frac{\mathbf{P}_{x,k+1}^- \cdot \mathbf{C}^T}{(\mathbf{C} \cdot \mathbf{P}_{x,k+1}^- \cdot \mathbf{C}^T + \mathbf{P}_{\boldsymbol{\theta},k+1})}. \quad (4.35)$$

By means of the Kalman filter a weighting of the measurement and the estimation can be done:

$$\widehat{\mathbf{x}}_{k+1} = \widehat{\mathbf{x}}_{k+1}^- + \mathbf{K}_{k+1} \cdot (\mathbf{y}_{k+1} - \mathbf{C} \cdot \widehat{\mathbf{x}}_{k+1}^-), \quad (4.36)$$

where \mathbf{y}_{k+1} is the measured data. Now, the new estimation error covariance matrix can be calculated:

$$\mathbf{P}_{x,k+1} = (\mathbf{I} - \mathbf{K}_{k+1} \cdot \mathbf{C}) \cdot \mathbf{P}_{x,k+1}^-. \quad (4.37)$$

The measurement variance $\mathbf{P}_{\boldsymbol{\theta},k}$ can be assumed according to the variance of the sensors' noise that can be determined by a test measurement. The variance of the system noise $\mathbf{P}_{\boldsymbol{\xi},k}$ is not obtainable by direct measurements and has to be assumed according to different recommendations. Furthermore, the starting covariance of the estimation error \mathbf{P}_0 has to be presumed. The choice of \mathbf{P}_0 influences the

filter's behavior during the first cycles. Nevertheless, \mathbf{P}_0 turns into $\mathbf{P}_{x,k+1}$ after some cycles and consequently the influence of \mathbf{P}_0 decreases over time [19].

The predicted covariance matrix of the estimation error $\mathbf{P}_{x,k+1}^-$ grows with the variance of the system noise $\mathbf{P}_{\xi,k}$. This implies, that the predicted estimation values get less reliable with a growing system noise $\mathbf{P}_{\xi,k}$. The Kalman amplification \mathbf{K}_{k+1} grows with the covariance of the estimation error $\mathbf{P}_{x,k+1}^-$. This means that an unsecure model is corrected stronger as the Kalman amplification \mathbf{K}_{k+1} corrects the estimation related to the measurement. With a growing variance of the measurement noise $\mathbf{P}_{\theta,k}$ the correction term \mathbf{K}_{k+1} decreases. This means that the estimated state is less corrected if the measurement is unsecure.

The higher the variance of the system noise $\mathbf{P}_{\xi,k}$, the more relies the Kalman Filter on the model, and the model is more corrected according to the measurement values. The higher the variance of the measurement noise $\mathbf{P}_{\theta,k}$, the less relies the Kalman filter on the measurement values, but rather trusts in the predicted estimation state of the model.

An extensive derivation of the Kalman filter can be found in [35].

Nevertheless, this method is only valid for linear systems. For the observation of non-linear systems the extended Kalman filter can be applied. In [32] the implementation of an Extended Kalman Filter that is based on a kinematic non-linear double-track model is explained. With further growing non-linearity the accuracy of the Taylor series approximation, which the EKF is based on, decreases. Therefore, the Unscented Kalman Filter was developed. In [26] the side slip angle β is estimated by the use of a physical model and an UKF.

4.5 Effective Torque Distribution

To visualize the torque distribution between the axles, two possibilities makes sense in general. From the system's point of view the nominal distribution is significant. Therefore, the target torque T_t is set in relation to the torque that leaves the gear box T_{gb} :

$$x_{\text{dis,nom}} = \frac{T_t}{T_{\text{gb}}} . \quad (4.38)$$

Due to overlocking or thrust reasons the nominal distribution can reach values that exceed 100 %. Such a value is not meaningful from a driving dynamics point of view. For the vehicle dynamic evaluation, the effective distribution $x_{\text{dis,eff}}$ is more significant. Therefore, the torque that really reaches the secondary axle T_{sec} is set in relation to the sum of the torque on the secondary axle T_{sec} plus the torque on the primary axle T_{prim} :

$$x_{\text{dis,eff}} = \frac{T_{\text{sec}}}{T_{\text{sec}} + T_{\text{prim}}} . \quad (4.39)$$

4.6 Binding

Off-road vehicle drivers usually know the feeling of a vibrating drivetrain when turning at low speeds and having the differential lock engaged. This condition is defined as binding. Binding occurs due to a locked drivetrain caused by the absence of an open differential. High tensions will inevitably lead to component failure. This is why a part time 4WD should only be activated in situations when the traction is really needed and not on dry high traction surfaces. Full time 4WD systems are exempted from this danger as a differential balances the differences of the rotational wheel speeds.

Binding occurs due to the non-allowance of different rotational speeds among the axles. The speed difference can occur due to different curve radiuses of the front and rear axle while cornering, but also due to different wheel diameters. During cornering the front wheels pass a higher curve radius than the wheels on the rear axle, which results in faster mean rotational speed on the front and a slower mean velocity on the rear axle.

A locked drivetrain balances the rotational speed of the front axle ω_f and the rear axle ω_r . The mean rotational speed ω_{mean} will result. As the front axle is prevented from rotating at its intended speed ω_f , brake slip occurs as provided in equation 4.40 and the front wheels are braked. The equation to calculate the brake slip s_b reads

$$s_b = \frac{\omega_{\text{mean}} - \omega_f}{\omega_f}. \quad (4.40)$$

The rear wheels are accelerated from ω_r to ω_{mean} which also results in wheel slip s_a :

$$s_a = \frac{\omega_{\text{mean}} - \omega_r}{\omega_{\text{mean}}}. \quad (4.41)$$

The resulting braking action on the front wheels puts the front axle in a thrust absorbing state, whereas the speed difference on the rear axle results in an increased power transmission. An imaginary drag torque T_d is circulating from the rear axle to the front axle via the road. This condition is known as binding.

In Figure 4.3 binding is exhibited. The arrows show the path of the imaginary travelling drag torque T_d . The front axle absorbs thrust from the road that is circulating in the drivetrain via the road. In consequence of this circulating drag torque the vehicle cannot roll out untroubled, but is braked strongly.

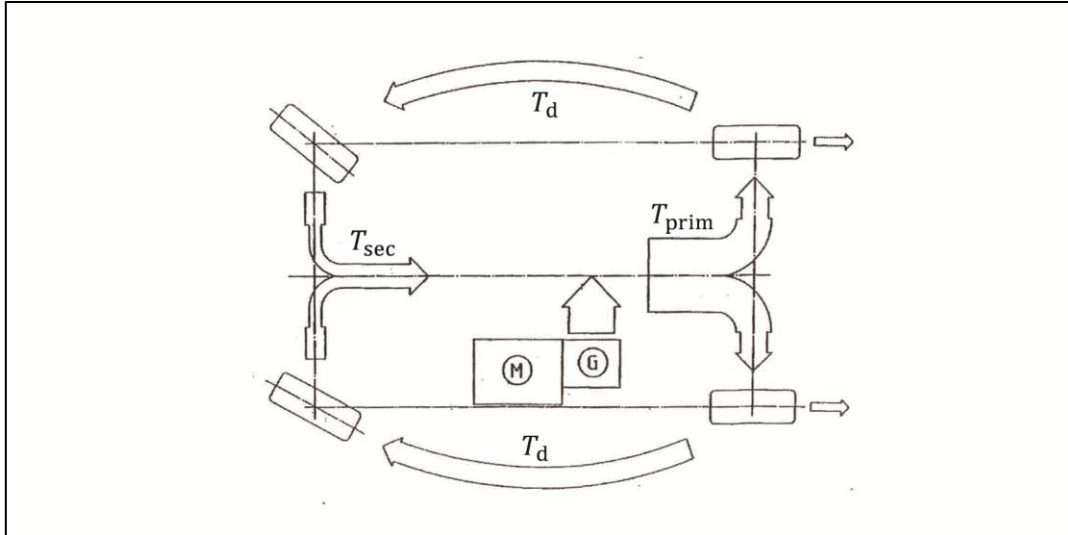


Figure 4.3: Binding in the drivetrain with an imaginary travelling drag torque, modified from [12]

The availability of the measured torque data signals for the front and the rear cardan shaft allow an approach to quantify binding according to equation 4.42. In this thesis the drag torque is defined as the thrust torque that is absorbed by one axle while the other axle is still delivering power to the road. No binding is detected if both axles receive thrust from the road and the engine is apparently coasting:

$$T_d = \begin{cases} T_f, & T_f < 0 \ \& \ T_r > 0 \\ T_r, & T_f > 0 \ \& \ T_r < 0 \\ 0, & T_f < 0 \ \& \ T_r < 0 \ | \ T_f > 0 \ \& \ T_r > 0. \end{cases} \quad (4.42)$$

As mentioned before, binding in the drivetrain can also occur due to rotational speed differences, because of different tire diameters. Thrust may therefore also be absorbed by the rear axle if the front tire diameters are bigger than the rear wheel diameters. In this special case, torque is transferred from the rear of the vehicle via the drivetrain to the front. Therefore, also the case of thrust application via the rear axle has to be considered within the expert-tool.

The drag torque T_d is then evaluated in the expert-tool according to equation 4.43 for the case that the front axle is the primary axle. The equation detects binding only below 50 km/h as experience has shown that binding only occurs at velocities lower than 50 km/h. This statement is justified by equation 4.45, in which the kinematic curve slip sl_{curve} is calculated. Binding will preferably occur at high kinematic curve slip values. However, the higher the vehicle velocity v , the lower the kinematic curve slip sl_{curve} . The equations 4.43 and 4.44 correspond to the Matlab operator logic. The Matlab equation to determine the drag torque T_d for a vehicle where the front axle is the primary axle reads

$$T_d = T_r \cdot (T_r < 0 \ \& \ v_x < \frac{50}{3.6} \ \& \ T_f > 0 \ \& \ T_{gb} > 0) . \quad (4.43)$$

If the rear axle is the primary axle the expert-tool detects the drag torque T_d as follows:

$$T_d = T_f \cdot (T_f < 0 \ \& \ v_x < \frac{50}{3.6} \ \& \ T_r > 0 \ \& \ T_{gb} > 0) . \quad (4.44)$$

Another method to determine the risk of binding is to calculate the kinematic curve slip sl_{curve} . As shown in Figure 4.4 a maximum torque T_{bind} can be applied to the clutch before binding occurs at a certain kinematic curve slip. If the applied torque T_t exceeds the maximum applicable torque T_{bind} , the risk of binding exists. The kinematic curve slip sl_{curve} can be calculated as follows:

$$sl_{\text{curve}} = \frac{\Delta v}{v} = \frac{v_f - v_r}{v}, \quad (4.45)$$

where v_f is the front axle's velocity and v_r the rear axle's velocity.

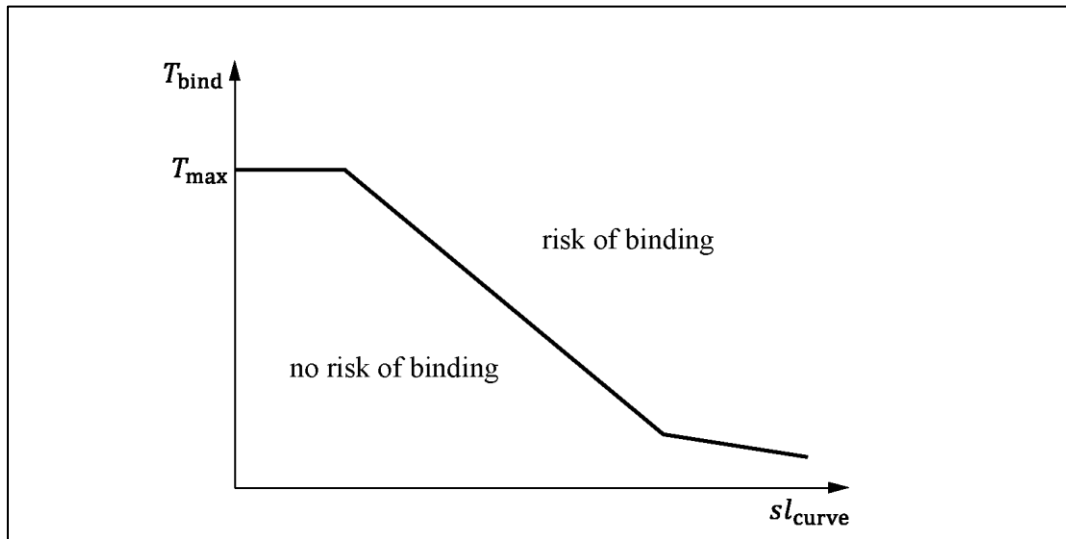


Figure 4.4: Detection of binding in the drivetrain

The velocity difference among the axles Δv can be estimated by making use of the linear bicycle model of chapter 2.1. To calculate the speeds of the combined front and the rear wheels as shown in Figure 2.2 the tire slip angles α_f and α_r can be neglected. The velocities of the vehicle's front, rear and center point can be calculated by means of the angular velocity ω that describes the rotation around the velocity pole O of Figure 2.2:

$$v = \omega \cdot R. \quad (4.46)$$

By calculating the speeds of the front, the rear and the center of gravity, the angular velocity ω drops out and the velocity difference Δv can be written as follows:

$$\Delta v = \frac{v}{R} \cdot (R_f - R_r). \quad (4.47)$$

By assuming that the center of gravity is located exactly centric between the front and the rear wheels the radiuses R_f and R_r can be approximated with the Pythagorean Theorem by assuming Ackermann driving for Figure 2.2:

$$R_r = \sqrt{R^2 - \left(\frac{l}{2}\right)^2}, \quad (4.48)$$

$$R_f = \sqrt{R_r^2 + l^2} = \sqrt{R^2 + \frac{3 \cdot l^2}{4}}. \quad (4.49)$$

Inserting equations 4.48 and 4.49 in 4.47 and applying the binomial formula delivers:

$$\Delta v = \frac{v}{R} \cdot \frac{l^2}{\sqrt{R^2 + \frac{3 \cdot l^2}{4}} + \sqrt{R^2 - \frac{l^2}{2}}}. \quad (4.50)$$

Assuming that the vehicle length l is small in comparison to the radius R simplifies the terms under the root of equation 4.50 as follows:

$$\sqrt{R^2 + \frac{3 \cdot l^2}{4}} + \sqrt{R^2 - \frac{l^2}{2}} \approx 2 \cdot R . \quad (4.51)$$

Equation 4.50 can now simplified be written as

$$\Delta v = \frac{v \cdot l^2}{2 \cdot R^2} . \quad (4.52)$$

The curvature κ can be obtained from vehicle specific data sheets that provide the associated curvature over the applied steering wheel angle δ_S . Finally, the radius R has to be corrected to compensate the neglected tire slip angle influence. With increasing lateral acceleration a_y , the velocity difference among the axles Δv decreases. To consider this circumstance, equation 4.52 can be extended by a correction factor that consists of the square of the velocity v which is divided by the square of a constant term C :

$$\Delta v = \frac{v}{R^2} \cdot \left[\frac{l^2}{2} - \left(\frac{v}{C} \right)^2 \right] . \quad (4.53)$$

The real values of the axes velocity difference Δv , can be considered as adequately approximated with this approach, as company internal experience has shown. In Figure 4.5 the difference of an uncorrected and a correct data signal of the axis velocity difference Δv is provided. The kinematic curve slip sl_{curve} can now be expressed as

$$sl_{\text{curve}} = \frac{1}{R^2} \cdot \left[\frac{l^2}{2} - \left(\frac{v}{C} \right)^2 \right] . \quad (4.54)$$

By determining the maximum applicable torque T_{bind} over the kinematic curve slip sl_{curve} the risk of binding can be quantified. Within the scope of this thesis the risk of binding is detected, if the applied target torque T_t exceeds the maximum applicable torque T_{bind} by 20 %:

$$\frac{T_t - T_{\text{bind}}}{T_{\text{bind}}} > 0.2 . \quad (4.55)$$

At low kinematic curve slip values, thus at straight ahead driving, the maximum clutch capacity T_{max} can be applied without taking the risk of binding. It is shown in the qualitative diagram of Figure 4.4 that no acute risk of binding exists at low kinematic curve slip values. At higher kinematic curve slip values the applicable amount of torque is radically reduced. The provided torque boundary line T_{bind} over the kinematic curve slip sl_{curve} in Figure 4.4 has to be determined by means of empiric values.

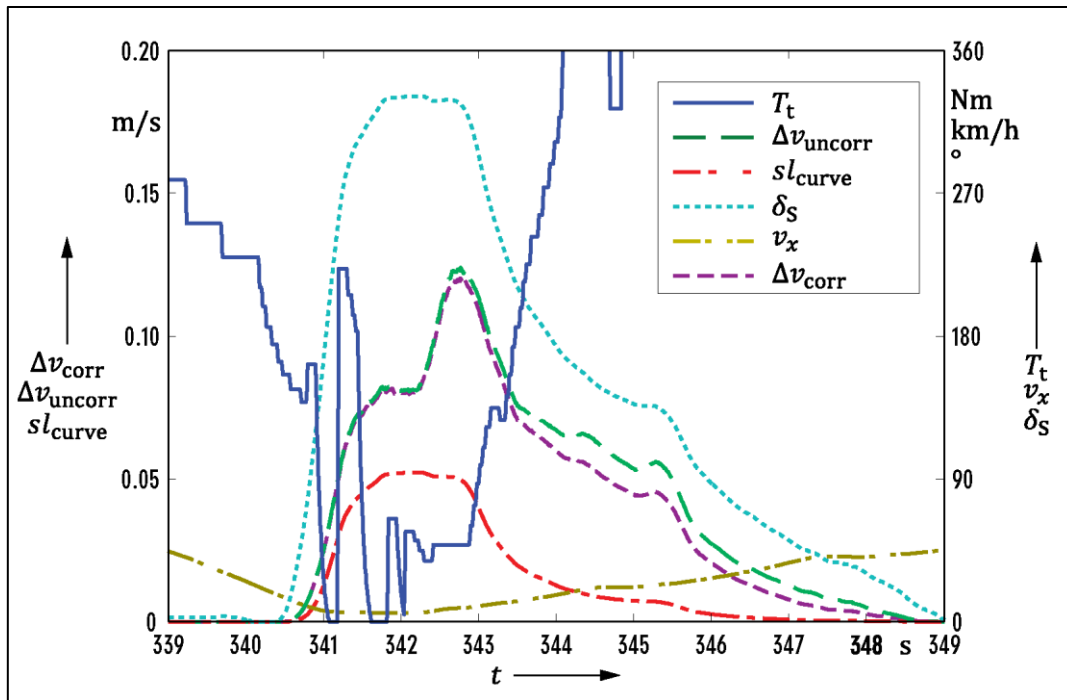


Figure 4.5: Binding at slow cornering

Figure 4.5 shows data of a real road test with a BMW X3 that is equipped with an ATC transfer with a clutch to the front axle. High kinematic curve slip values are recorded from 341 s to 343 s, because the measured velocity v_x is low during this provided cornering event. Acute danger of binding exists as the kinematic curve slip values correspond to the right low area of the T_{bind} target boundary line in Figure 4.4. However, the vehicle controller reacts appropriate and lowers the supplied target torque T_t in this sophisticated cornering event according to the conditions. The target torque T_t only reaches high values for a very short time. Nevertheless, binding in the drivetrain very likely has occurred during this short time period of the test drive.

4.7 Adaption of the Graphical User Interface in Matlab

It was the intention to create a software tool that allows engineers, which have not been integrated in the software's development process, to work with the program. Therefore, easy usability has high priority. With regard to usability, the graphical user interface of the expert-tool has been edited and developed.

A documentation section with explanations and annotations for every assessment criterion has been implemented. The documentation section is accessible within the analysis section of the expert-tool. It contains a short explanation and the designation of the physical unit for every assessment criterion. The documentation supports engineers that are new to the expert-tool, as well as engineers that have been integrated in the software's development process by providing information about the criteria's functionality. Reading the explanation, which is provided in the documentation section, should prevent the engineer from having to read the original Matlab code to understand the functionality of an assessment criterion. The documentation section represents an important measure concerning knowledge management, as it is important to save the knowledge and make it accessible to engineers that will be working with the expert-tool in future.

Furthermore, the possibility to export a list of all output criteria plus their corresponding units and explanations to Microsoft Excel was implemented.

In addition, the graphical user interface was modified by an additional information label that shows the physical units of the returned assessment criteria. As one task of this thesis was to verify the existing assessment criteria of the expert-tool, this measure represented an important step within the verification process, as the plausibility of the output of the criteria had to be rethought and the input parameters were controlled according to their physical unit. Furthermore, the necessity of substitution calculations to evaluate certain signals could be determined with this step, as every criterion had to be extracted according to its structure.

As the expert-tool is based on Matlab and consists of a coherent file structure, it was important to make the expert-tool independent from local data paths. Therefore, a separate m-file has been created that enables the user to open the expert-tool in any folder, at any workstation that has a Matlab version at its disposal.

5 Implementation of new Assessment Criteria

The identification of assessment criteria for the driving states listed in Table 3.7 has priority in this thesis. It is a requirement that the assessment criteria are not specific to certain driving maneuvers, but can be applied independently for every simulation or road trial. The expert-tool's assessment criteria have been classified according to Table 1.1.

The use of the tool is not to evaluate specific maneuvers, as for example the steering step input. The tool originally has been designed to evaluate circuit test drives. The expert-tool identifies particular driving states, such as cornering or braking, and analyzes these states by the use of appropriate assessment criteria. Of course, the tool can not only be used for the analysis of a whole circuit. Also single maneuvers can be recorded and evaluated. This can be necessary within the scope of a tuning process, if single maneuvers are repeated more often and the setup is varied for every start. The tool can support the tuning process by providing a quick overview of the consequences and impacts due to setup changes among the repeated maneuvers.

In this chapter, the assessment criteria that have been added to the expert-tool within the scope of this thesis are listed and explained. The tool is based on Matlab. It is tried to provide the functionality of the algorithms by means of mathematical equations. Therefore, the criteria's mathematical explanations can be considered as incomplete pseudocode that provides the criteria's functionality for the output determination. The operators used in the equations of this chapter correspond to the Matlab operator logic.

Figure 5.1 provides a test drive with a BMW X3 at the Fiorano race circuit in Italy simulated with veDYNA. The simulated vehicle is a BMW X3 3.0i with a 3 liter, 6 cylinder gas engine and a manual gear box. The vehicle is equipped with an ATC transfer case with a clutch to the front axle. Therefore, the rear axle is the primary axle. The expert-tool identifies the driven course and reconstructs the driving route as shown in Figure 5.1 a). The data that was evaluated in the graph only contains a section of the total circuit. Therefore, only the first four curves of the Fiorano circuit are provided in the figure.

An important point is the assessment of the applied torque by the transfer case clutch. Excessive stress on the clutch can be expected for starting and acceleration conditions. To evaluate the system's behavior with particular regard to the system load, test engineers carry out specific driving maneuvers, as for example those that are provided in Table 3.2. Figure 5.1 b) provides the progress of the coupling target torque T_t over the time of the evaluated circuit section of Figure 5.1 a). As seen in Figure 5.1 b) a peak point of the applied torque T_t is recorded around 1.7 s after the start of the record. This peak arises due to a detected 4WDASR event in the first gear, because a 4WDASR intervention tries to enable a rigid connection between the cardan shafts to prevent one axle from slipping. The other target torque peaks in Figure 5.1 b) at 21.5 s, 32.5 s, 38 s and 48.5 s after the start also occur due to 4WDASR interventions. According to the curve progress of the velocity v_x in Figure 5.1 b), it is noticeable that 4WDASR events preferentially occur during acceleration conditions. Disregarding specific driving situations, it can generally be said that the target torque T_t is higher for lower gears, due to a higher transmission ratio.

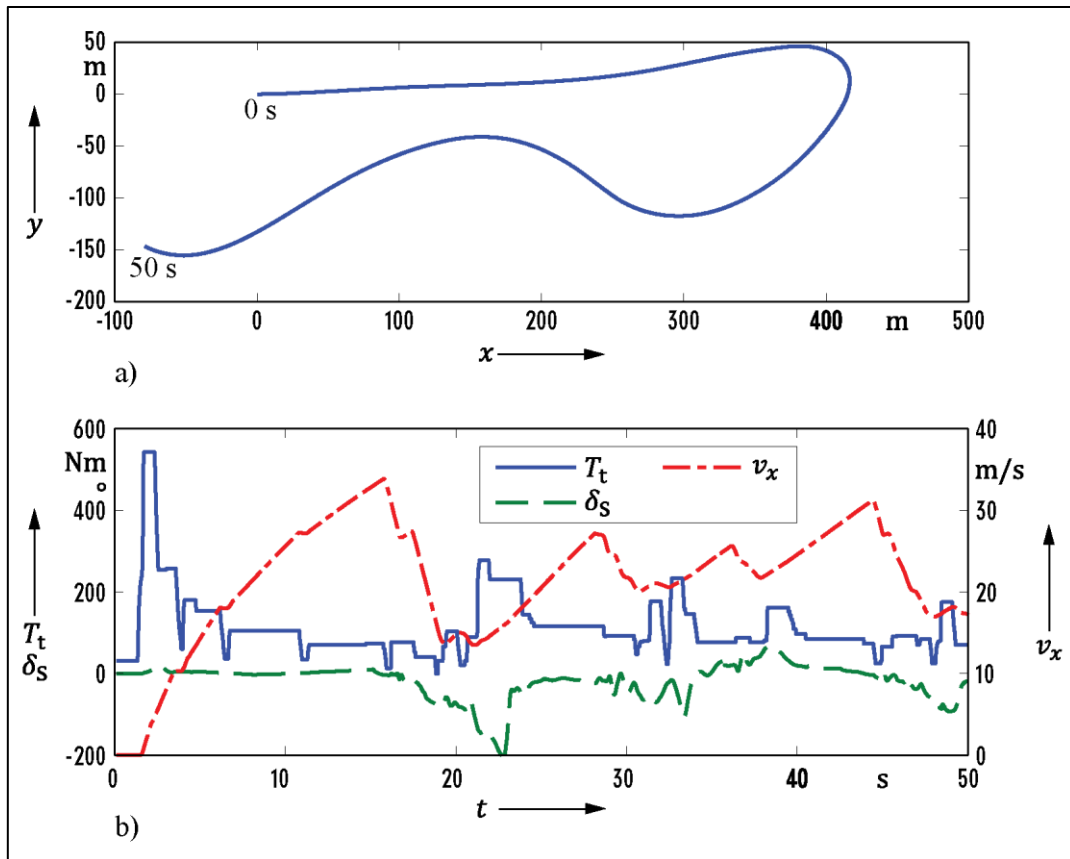


Figure 5.1: Simulated test drive with a BMW X3 at the race circuit Fiorano. a) Driving route coordinates b) Torque/time diagram

5.1 Standstill

Within the scope of this thesis, the driving state standstill has been added to the list of driving states that the software extracts from a data signal. Matlab allows the determination of the standstill state by executing a logical query according to the requirements that are provided in equation 5.1. To determine the time periods where the vehicle has been in the state standstill, the query returns 1 for every sampled data point at which the requirements of equation 5.1 are true, thus the longitudinal velocity v_x has been lower than 0.5 m/s:

$$ss = \begin{cases} 1, & v_x \leq 0.5 \\ 0, & v_x > 0.5 \end{cases} \quad (5.1)$$

The boundary value for the velocity v_x of 0.5 m/s is justified by the veDYNA standstill border which is located between 1.5 and 2 km/h. It is also possible that more than one standstill state is detected within a data file. The absolute indices of the standstill states have to be found by determining the start and end points of the states. Therefore, the Matlab command *find* locates all positive differences between all adjacent elements of the array *ss* to determine the starting points:

$$ss_{on} = \text{find}(\text{diff}(ss) > 0) \quad (5.2)$$

The negative differences have to be located to determine the ending points of the standstill states within the data file:

$$ss_{\text{end}} = \text{find}(\text{diff}(ss) < 0) . \quad (5.3)$$

The absolute indices of the standstill states ss are then determined as follows within the Matlab algorithm:

$$SS = SS_{\text{on}}:SS_{\text{end}} . \quad (5.4)$$

Due to the fact that the vehicle is standing still or moving only very slowly in the state standstill, the assessment criteria that have been found and implemented for this state are referring mostly to the 4WD system and its clutch.

Table 5.1: Added assessment criteria for the driving state standstill

Category	Criterion	Unit
Driver	Event start time, t_{start}	s
	Event end time, t_{end}	s
	Event duration, Δt	s
Vehicle	-	-
System	Clutch work, $W_{\text{cl},ss}$	kJ
	Clutch power, $P_{\text{cl},\text{max}}$	kW
	Mean target torque, $T_{\text{t,mean}}$	Nm
	Braked target torque, $T_{\text{t,brake}}$	Nm
	Target torque gear, $T_{\text{t,gear}}$	Nm
	Target torque no gear, $T_{\text{t,nogear}}$	Nm
	Restbinding, rb	-
	Restbinding gradient, $grad_{\text{rb}}$	Nm/s

Event start time / Event end time / Event duration

First of all, the software extracts the starting and ending time of the standstill state and determines the duration of the state.

Figure 5.2 shows the standstill and driveaway state of the simulated test drive of Figure 5.1. Standstill is detected from to 0.1 s to 1.65 s.

Clutch work / Clutch power

The clutch is working in case of a rotational speed difference between the two cardan shafts according to equation 2.38. For vehicle dynamic reasons, very often a slipping clutch is required. Due to this slip, energy dissipates in the clutch. The clutch is heated and cooling is required. Furthermore, a slipping

clutch causes wear and noise. According to [30], a clutch in on-load operation with a low difference between the rotational shaft speeds, can easily lead to friction oscillations that can be noted acoustically. These oscillations are known as moaning or shuddering.

The tool provides a signal of the work the clutch is applied with over the sampling rate f . This signal W_{cl} is calculated according to equation 2.38 for every sampled data point. The criterion $W_{cl,ss}$ returns the work the clutch has provided during the whole state. The work of the clutch during the state standstill $W_{cl,ss}$ is the sum of the provided work over the whole state:

$$W_{cl,ss} = \sum_{i=ss(1)}^{ss(end)} W_{cl,i} . \quad (5.5)$$

The criterion $P_{cl,max}$ returns the maximum power, the clutch had to provide during the state standstill:

$$P_{cl,max} = \frac{\max(W_{cl}(ss))}{\frac{1}{f}} , \quad (5.6)$$

where attention has to be paid to the sampling rate f that indicates the sampled data points per second. For the example of Figure 5.2 the criterion $W_{cl,ss}$ returns 0.13 kW and the maximum power $P_{cl,max}$ equals 10.33 kW.

Mean target torque

Furthermore, the criterion $T_{t,mean}$ has been implemented in order to calculate the mean target torque T_t that has been applied during the whole state:

$$T_{t,mean} = \text{mean}(T_t(ss)) . \quad (5.7)$$

For the standstill state that is provided in Figure 5.2, the criterion $T_{t,mean}$ outputs 63.83 Nm.

Braked target torque

Unlike a vehicle with a manual transmission, a vehicle that is equipped with an automatic gearbox can carry out a braked start due to the non-existence of a clutch pedal. Therefore, the criterion $T_{t,brake}$ was implemented to recognize a so-called race start and to return the applied coupling torque T_t for this condition. A braked start is determined if the measured braking pressure p_{br} exceeds 30 bar, the throttle pedal was applied with a minimum load at least and a gear has been inserted. Furthermore, it is controlled if a start follows the standstill state by evaluating the sign of the mean acceleration a_x :

$$braking_{ss} = \begin{cases} 1, & th(ss) \geq 0 \ \& \ p_{br}(ss) \geq 30 \ \& \ gear(ss) > 0 \ \& \ \text{mean}(a_x(ss)) > 0 \\ 0, & \text{else} . \end{cases} \quad (5.8)$$

The criterion $T_{t,brake}$ returns the mean applied coupling torque T_t that has been applied for the detected condition of a race start according to:

$$T_{t,brake} = \text{mean}(T_t(\text{braking}_{ss})) . \quad (5.9)$$

Obviously, no real race start has been carried out in the simulation of Figure 5.2. Therefore, $T_{t,brake}$ returns 0 Nm.

Target torque gear / Target torque no gear

Another interesting point is the availability of the transfer case while a gear is inserted, the clutch is closed, but the throttle pedal is not applied. The Matlab equation that controls these requirements reads

$$gear_{ss} = \begin{cases} 1, & (th(ss) == 0 \ \& \ gear(ss) > 0 \ \& \ cl(ss) == 1) \\ 0, & \text{else} . \end{cases} \quad (5.10)$$

If the requirements of equation 5.10 are met during the standstill state, the vehicle controller should output a specified target torque T_t for the detected indices. The criterion $T_{t,gear}$ returns the mean applied coupling torque for the determined period of time according to:

$$T_{t,gear} = \text{mean}(T_t(gear_{ss})) . \quad (5.11)$$

For the case that no gear is inserted, no torque is transmitted from the engine to the powertrain. Consequently, no torque has to be distributed between the axles. The transfer case clutch should not be actuated hence the target torque T_t should be zero. Indices that correspond to these requirements are detected as follows:

$$nogear_{ss} = \begin{cases} 1, & th(ss) < 1 \ \& \ gear(ss) == 0 \\ 0, & \text{else} . \end{cases} \quad (5.12)$$

The criterion $T_{t,nogear}$ returns the mean applied target torque T_t for the data points that are detected according to the requirements of equation 5.12:

$$T_{t,nogear} = \text{mean}(T_t(nogear_{ss})) . \quad (5.13)$$

It can be seen as a control parameter, as the requirement for this condition is that the returned value of $T_{t,nogear}$ should be 0 Nm. For the example of Figure 5.2, the criterion $T_{t,gear}$ returns 0 Nm, because the clutch apparently has not been closed when the throttle opening was 0. The criterion $T_{t,nogear}$ returns 31.07 Nm. As mentioned before, this criterion should not return a value. In this case, the evaluated test drive data has to be analyzed with regard to this illogical assessment result.

Restbinding / Restbinding gradient

Stopping a turned vehicle can leave binding in the drivetrain. It has to be detected, if binding occurs while stopping the vehicle. Therefore, the whole standstill state is scanned for binding. If binding occurs, a flag is set and the risk of binding is returned. The Matlab command *any* returns a logical 1 if any of the evaluated elements is a nonzero number. The criterion also concerns the driveaway state, as tensions in the drivetrain may occur also while driving off. In equation 5.14 binding is detected according to the theory of chapter 4.6. Binding is determined if the target torque T_t has been 20 % higher than the maximum applicable torque T_{bind} in any data point of the standstill state *ss* according

to the theory of Figure 4.4. Furthermore, it is controlled if a drag torque T_d has been detected during the standstill state:

$$rb = \begin{cases} 1, & \text{any}\left(\frac{T_t(ss) - T_{bind}(ss)}{T_{bind}(ss)} > 0.2\right) \mid \text{any}(T_d(ss)) \\ 0, & \text{else.} \end{cases} \quad (5.14)$$

Moreover, the stress on the drivetrain when relieving it is of interest. To analyze this condition, the criterion returns the gradient the clutch is opened with after binding:

$$grad_{rb} = \frac{\Delta T_t}{\Delta t}. \quad (5.15)$$

To avoid loss of comfort, this clutch opening should turn out in a low gradient. If the clutch opens too fast, the driver senses a sudden jerk which reveals in the comfort feeling of the driver. No risk of restbinding is detected in the example of Figure 5.2.

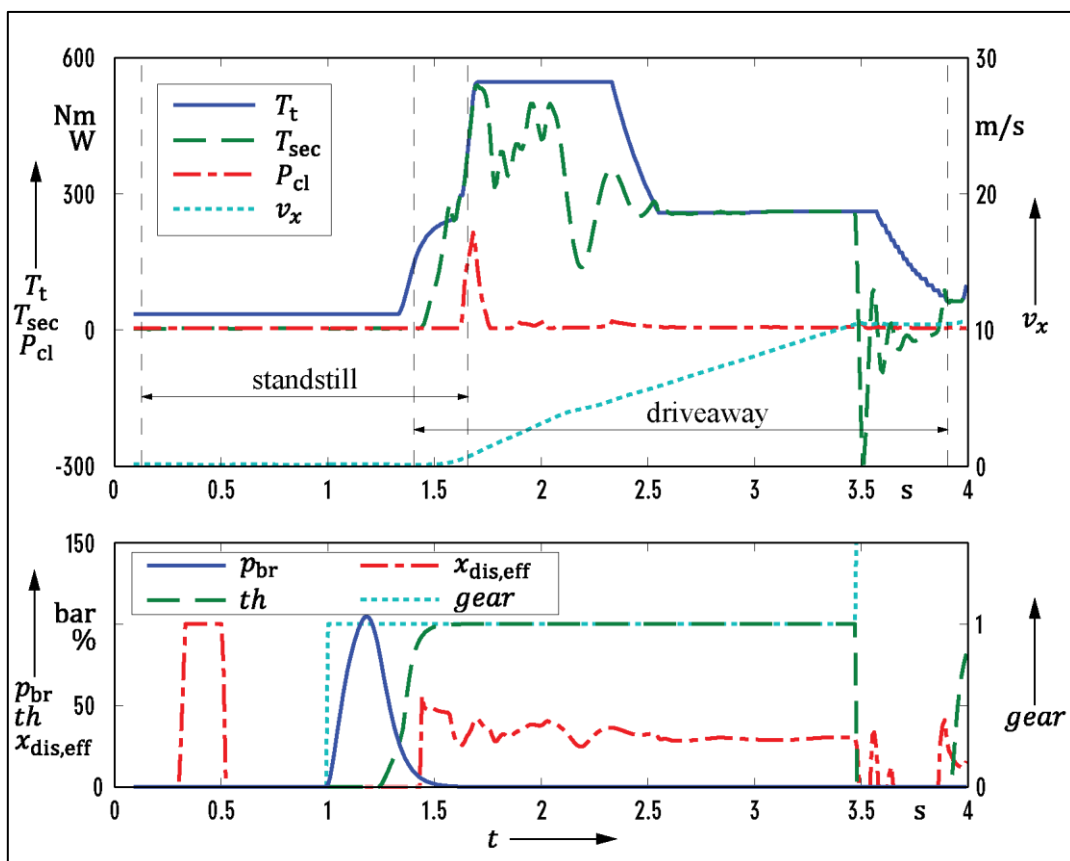


Figure 5.2: Target torque behavior during the standstill and driveaway state of a simulated test drive with a BMW X3

5.2 Driveaway

As the state standstill before, the state driveaway is detected according to a logical query according to the requirements of equation 5.16 or 5.17. For a vehicle with a manual gear box, driveaway is detected if the requirements of equation 5.16 are true. Therefore, the clutch pedal signal has to be between 0 and 1. Furthermore, the signal br should return that the brake is not applied. The signal br contains 1

if the brake pedal is applied with any force, and 0 for a non-applied brake pedal. Moreover, the longitudinal velocity v_x does not exceed 10 km/h in equation 5.16 and the engine speed is higher than 500 rpm. If the requirements are true for a data point, equation 5.16 returns 1:

$$da = \begin{cases} 1, cl > 0 \ \& \ cl < 1 \ \& \ br < 0.1 \ \& \ v_x < \frac{10}{3.6} \ \& \ n_{mot} > 500 \\ 0, \text{else.} \end{cases} \quad (5.16)$$

For a vehicle equipped with an automatic gear box, the requirements to detect the state driveaway are nearly the same. As no clutch pedal signal can be evaluated for a vehicle equipped with an automatic gear box, this requirement is replaced by the requirement that a gear is engaged at least:

$$da = \begin{cases} 1, br < 0.1 \ \& \ v_x < \frac{10}{3.6} \ \& \ n_{mot} > 500 \ \& \ gear > 0 \\ 0, \text{else.} \end{cases} \quad (5.17)$$

The absolute indices of the driveaway states within the sampled data are then determined the same way as for the state standstill according to the equations 5.2, 5.3 and 5.4.

For the evaluation of four-wheel drive systems, driving maneuvers are carried out on different road surfaces. Very common are starting tests on μ -split and μ -jump surfaces. For the development engineer it is of interest to know how the transfer case clutch system behaves at a normal driveaway and during a driveaway on μ -split or μ -jump.

To feed the development engineer with useful information, the state driveaway has been extended by further criteria within the scope of this thesis. Table 5.2 provides a full overview of the added assessment criteria for the state driveaway.

Table 5.2: Added assessment criteria for the driving state driveaway

Category	Criterion	Unit
Driver	Race start, rs	-
	Clutch closing, $grad_{cl}$	rpm/s
Vehicle	Engine dying, $\Delta\omega_{ed}$	rpm
System	Drag torque, $T_{d,min}$	Nm
	Pre-control torque, $T_{t,abs}$	Nm
	Effective distribution, $x_{dis,eff,da}$	%

Race start

Similar to the standstill criterion $T_{t,brake}$, the criterion rs returns the information if a race start has been carried out or not. A race start is detected according to the requirements of equation 5.18. The brake pressure p_{br} should be beyond 30 bar. Simultaneous, the throttle pedal should be applied with a minimum value at least. Furthermore, a gear should be engaged and the longitudinal measured vehicle velocity v_x should be beneath 1 m/s to ensure that the vehicle is nearly still standing when brake and

throttle pedal are applied simultaneously. The criterion returns 1 in case a race start is detected according to the requirements of equation 5.18 and 0 if not:

$$rs = \text{any}(p_{br}(da) > 30 \ \& \ v_x(da) < 1 \ \& \ th(da) > 0 \ \& \ gear(da) > 0) . \quad (5.18)$$

Additional to the standstill state, Figure 5.2 also provides the time period of the detected driveway state for the example of Figure 5.1. Driveway is detected from 1.43 s to 3.93 s. As for the state standstill, no race start has been detected within the driveway state.

Clutch closing

When engaging the clutch at a driveway, the engine speed and the vehicle speed are balanced. As seen in Figure 5.3, the engine speed can fall temporarily due to the balance activity. Figure 5.3 provides the same driveway state as Figure 5.2. To restrict the observed area, the criterion limits the evaluated data within the driveway state according to the following requirements:

$$clutchclosing = (gear(da) == 1 \ \& \ cl(da) \sim = 0) . \quad (5.19)$$

Within the time period *clutchclosing*, the start point at t_1 and the end point at t_2 of the engine speed reduction are detected. Furthermore, the current engine speeds of the start point $n_{mot}(t_1)$ and the end point $n_{mot}(t_2)$ are determined. Then the gradient of the engine speed reduction is returned:

$$grad_{cl} = \frac{n_{mot}(t_2) - n_{mot}(t_1)}{t_2 - t_1} . \quad (5.20)$$

For the example of Figure 5.3 the criterion returns a gradient of -1139.82 rpm/s. However, the engine speed does not necessarily have to fall during engaging the clutch. This depends on the way the clutch was closed. The criterion recognizes if no temporary engine speed reduction has occurred. In this case the criterion returns the least occurred gradient of the observed area.

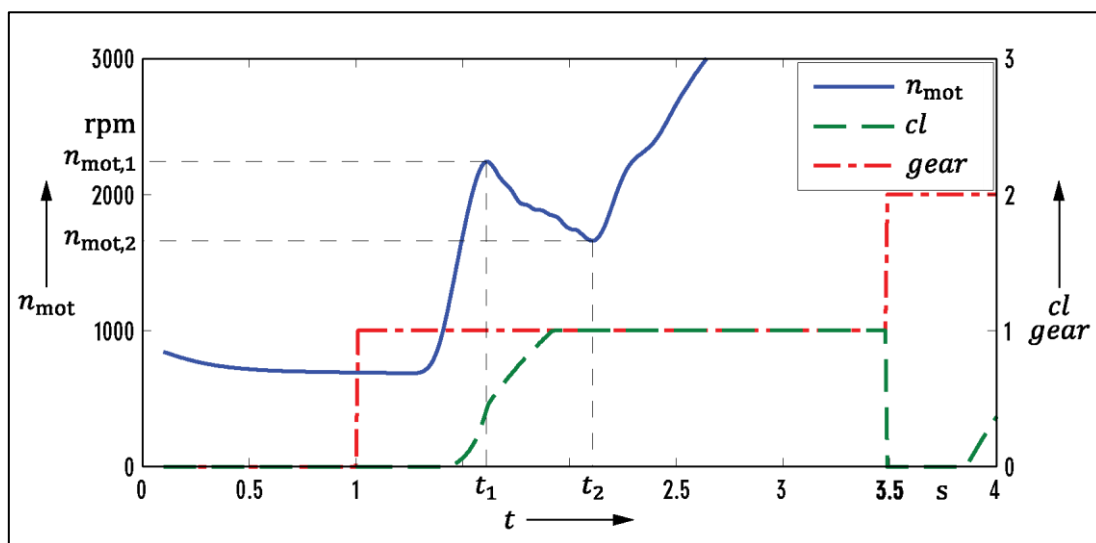


Figure 5.3: Clutch closing

Engine dying

During engaging the clutch the speed difference between the engine and the transmission is balanced. The engine speed can reach very low values in this situation as seen in Figure 5.3. The criterion returns the gap between the minimum engine speed n_{mot} that has occurred during the starting state and the idle speed n_{idle} . Logically, the engine speed should not fall below the engine specific idle speed n_{idle} to avoid engine dying. The criterion $\Delta\omega_{\text{ed}}$ evaluates the gap between the lowest measured engine speed n_{mot} during the driveaway state and the engine specific idle speed n_{idle} :

$$\Delta\omega_{\text{ed}} = \min(n_{\text{mot}}(da) - n_{\text{idle}}) . \quad (5.21)$$

For the driveaway example in Figure 5.3, the criterion returns a gap $\Delta\omega_{\text{ed}}$ of 300.94 rpm. The idle speed of the provided BMW engine is 850 rpm.

Drag torque

To provide the optimum traction during driveaway, the transfer case will try to balance the torque distribution among the front and the rear axle. However, a turned steering wheel and a locked transfer case clutch may provoke binding in the drivetrain. In that case, the transfer case system has to open the clutch. The criterion $T_{\text{d,min}}$ returns the maximum arisen drag torque T_{d} :

$$T_{\text{d,min}} = \min(T_{\text{d}}(da)) . \quad (5.22)$$

The drag torque signal T_{d} has been calculated according to equation 4.42 or 4.43. The risk of binding has been detected for the example of Figure 5.2 according to the theory of chapter 4.6. The criterion $T_{\text{d,min}}$ returns a value of -60.92 Nm. The cause for this unwanted output has to be analyzed.

Pre-control torque

This criterion returns the maximum target torque T_{t} that is applied to the clutch by the vehicle controller during the starting state:

$$T_{\text{t,max}} = \max(T_{\text{t}}(da)) . \quad (5.23)$$

For the driveaway state in Figure 5.2 a maximum target torque $T_{\text{t,max}}$ of 542.28 Nm is returned. As shown in Figure 5.2 this value obviously occurs due to a four-wheel drive anti-slip regulation event.

Effective distribution

The best possible traction at a driveaway on a high traction surface can be reached with a power distribution to the axles according to the dynamic wheel load distribution. The criterion $x_{\text{dis,eff,da}}$ returns the mean effective torque distribution $x_{\text{dis,eff}}$ which is defined in equation 4.39:

$$x_{\text{dis,eff,da}} = \text{mean}(x_{\text{dis,eff}}(da)) \cdot 100 . \quad (5.24)$$

On heterogeneous road surfaces the transfer case system tries to distribute the higher amount of torque to the axle that has the better friction coefficient available. This means, the criterion should return very low values of around 0 % for a μ -jump start if the secondary axle is standing on ice. For a μ -jump start where the primary axle is on ice, the criterion can return values of up to 100 %, if the primary axle is not able to transfer torque to the road. For the example of Figure 5.2 the criterion $x_{\text{dis,eff,da}}$ returns 27.79 %.

5.3 Upshift

Shifting up one gear lowers the gear ratio and affects a lower engine speed at the same driving velocity. Furthermore, less torque is supplied from the gear transmission to the drivetrain. This means that the transfer case should reduce the locking torque T_t in the same relation as the torque that leaves the gear transmission T_{gb} has been lowered.

The state upshift has been added additionally to the list of driving states, the expert-tool extracts from a sampled data file and is detected according to the requirements of 5.25 for an automatic gear box. In equation 5.25 the Matlab command *diff* determines the differences between all adjacent elements of the array i_{sync} that contains the gear ratio values. If a change of the gear ratio is detected at a velocity v_x above 2 m/s, the array $shift_{\text{up}}$ is filled with a 1:

$$shift_{\text{up}} = \begin{cases} 1, & (\text{diff}(i_{\text{sync}}) < 0 \ \& \ v_x > 2) \\ 0, & \text{else.} \end{cases} \quad (5.25)$$

For a manual gear box shifting is detected if the clutch pedal signal cl is beneath 0.1 which indicates an applied clutch pedal. As for the automatic gear box it is ensured that the velocity v_x is above a minimum value of 2 m/s:

$$shift_{\text{up}} = \begin{cases} 1, & (cl < 0.1 \ \& \ v_x > 2) \\ 0, & \text{else.} \end{cases} \quad (5.26)$$

Furthermore, it has to be controlled if a gear shift has really taken place, if shifting is detected for a manual gear box according to equation 5.26. To distinguish upshifting and downshifting, a logical query controls if the inserted gear before the shift event was lower than the selected gear after the shift event. The absolute indices of the detected upshift events within the sampled data are then determined the same way as for the other states according to the equations 5.2, 5.3 and 5.4.

Table 5.3: Added assessment criteria for the driving state upshift

Category	Criterion	Unit
Driver	-	-
Vehicle	-	-
System	Pre-control torque, $T_{t,\text{abs}}$	Nm
	Torque reduction, ΔT_t	Nm
	Actuation time, Δt	s
	Actuation gradient, $grad_{\text{us}}$	Nm/s

Pre-control torque / Torque reduction / Reduction time

The criterion $T_{t,abs}$ returns the absolute value the transfer case torque T_t was decreased to due to the upshifting event:

$$T_{t,abs} = T_t(t_2) . \quad (5.27)$$

Furthermore, the relative torque reduction is determined:

$$\Delta T_t = T_t(t_2) - T_t(t_1) . \quad (5.28)$$

The actuation speed of the torque reduction is defined as follows:

$$\Delta t = t_2 - t_1 . \quad (5.29)$$

Figure 5.4 shows the target torque behavior for a clean upshift event of a test simulation. The figure shows a section of another simulation on the Fiorano race circuit. However, the simulated vehicle is the same BMW X3 with the same ATC transfer case as in the example of Figure 5.1. Again, the rear axle is the primary axle. In Figure 5.4 an upshift event from the 3rd into the 4th gear has taken place. The expert-tool determines an upshift event from 8.95 s to 9.52 s. The criterion ΔT_t outputs -45.72 Nm. The absolute value $T_{t,abs}$ at t_2 is 82.22 Nm.

Reduction gradient

This criterion returns the gradient calculated from the two criteria before and provides a measure for the actuation speed of the transfer case controller:

$$grad_{us} = \frac{\Delta T_t}{\Delta t} . \quad (5.30)$$

For the shifting example of Figure 5.4, the criterion Δt returns 0.09 s. This results in a gradient $grad_{us}$ of -508.08 Nm/s.

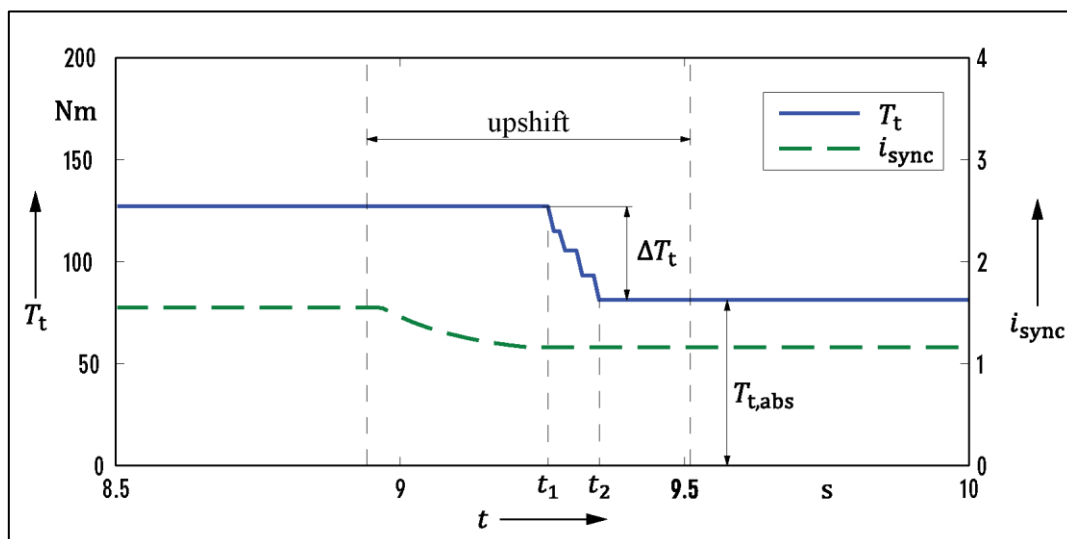


Figure 5.4: Upshift event from the 3rd into the 4th gear with an automatic gearbox

5.4 Downshift

After shifting down one gear, the torque that leaves the transmission T_{gb} increases due to a higher transmission ratio. Subsequently, the transfer case's target torque T_t has to increase by the same percentage the transmission torque has increased with. Special requirements for the transfer case may occur due to a braking action or a load change during the downshift event. A simultaneous braking event has more impact on a downshifting event, as the torque is lowered anyway at an upshift event due to a lower gear ratio. As discussed in chapter 3.3.1, the distributed amount of torque should not be increased in case of braking to avoid stability problems. The clutch should rather be opened if the ESP orders to and the axles should not be connected if a certain deceleration threshold is exceeded.

The indices of the state downshift $shift_{down}$ are detected according to the same requirements as for the state upshift $shift_{up}$ according to the equations 5.21 and 5.22. To distinguish the state downshift from the state upshift, a logical query is added that controls if the engaged gear before the downshift event was higher than the selected gear after the downshift event. Table 5.4 provides an overview of the added assessment criteria for the state downshift.

Table 5.4: Added assessment criteria for the driving state downshift

Category	Criterion	Unit
Driver	Braking, $braking_{ds}$	-
	Thrust downshift, $thrust_{ds}$	-
Vehicle	-	-
System	Pre-control torque, $T_{t,abs}$	s
	Torque difference, ΔT_t	Nm
	Actuation time, Δt	Nm
	Actuation gradient, $grad_{ds}$	Nm/s
	Holding time, t_{hold}	s
	Braking torque, $T_{t,brake}$	Nm

Braking

To provide a short explanation for a decreased target torque T_t despite a downshift event, the criterion $braking_{ds}$ returns 1 if braking has occurred during the downshift maneuver or 0 if not. Therefore, the indices within the downshift state at which braking has occurred have to be determined. According to equation 5.31 braking during the downshift state is determined for data points at which the braking pressure p_{br} exceeds the critical braking pressure p_{crit} :

$$shift_{down,br} = (p_{br}(shift_{down}) > p_{crit}), \quad (5.31)$$

where p_{crit} is the critical braking pressure which is explained in chapter 5.5. The criterion detects a brake event if at least one array entry of the array $shift_{down,br}$ is true:

$$braking_{ds} = any(shift_{down,br}). \quad (5.32)$$

Thrust downshift

Engaging the clutch after a shifting event can be done by just releasing the clutch pedal or by applying the throttle pedal simultaneously. The existence of a manual or an automatic gearbox has to be considered while evaluating this criterion. According to equation 5.33 the criterion returns 0, if the throttle pedal has been applied with more than 5 % at any data point during the downshift event. If the throttle pedal has not been applied with more than 5 % during the downshift event, the criterion returns 1 and indicates a downshift event during coasting:

$$thrust_{ds} = \sim any(th(shift_{down}) > 5). \quad (5.33)$$

Holding time

If the vehicle controller applies a certain locking torque due to a 4WD anti-slip regulation intervention or a downshift event, the applied torque is held for a certain time to avoid irritations within the system. The criterion t_{hold} returns the time the torque was held:

$$t_{hold} = t_3 - t_2. \quad (5.34)$$

The criterion was implemented that way that it analyzes the locking torque progress and only returns a value if the holding time exceeds the threshold of 0.5 s. Furthermore, it is controlled if the held torque value occurs due to a downshifting event. The criterion also returns the holding time of the locking torque if the torque is decreased.

Pre-control torque / Torque difference / Actuation time / Actuation gradient

The pre-control torque $T_{t,abs}$ returns the absolute value, the locking torque T_t was raised to due to a downshift event. The criterion returns the target torque value T_t at the moment t_2 according to equation 5.27. In case of a clean downshift event, the torque should be raised to a certain value. If it did not increase, apparently special conditions, like e.g. braking, occurred during the downshift event. In that case, the criterion returns the value the target torque was decreased to.

Moreover, not only the absolute value the clutch torque was raised to is of interest, but also the relative increase related to the initial locking torque. Therefore, the torque difference ΔT_t is determined as for the state upshift according to equation 5.28. The criterion also returns a value if the locking torque was decreased. As for the upshift state, criteria that return the time difference Δt and the gradient of the actuation $grad_{ds}$ have been implemented. A reference value for the gradient can be found in [33]. There it is written that the torque build-up gradient should not be beneath 5000 Nm/s for SUVs. Generally, the gradient should not be too low, as this can affect the subjective traction sensation. On the other hand, a too high gradient leads to a loss of comfort, if an actuation jerk is sensed.

Braking torque

If braking is detected by the criterion $braking_{ds}$, the criterion $T_{t,brake}$ returns the difference between the maximum applied target torque T_t during the detected braking period $shift_{down,br}$ and the target torque T_t of the first detected data point of the array $shift_{down,br}$:

$$T_{t,brake} = \max\left(T_t(shift_{down,br})\right) - T_t\left(shift_{down,br}(1)\right). \quad (5.35)$$

According to the theory of chapter 3.3.1, the clutch should be opened in case of strong braking events as in the example of Figure 5.5 b) and $T_{t,brake}$ should therefore return a negative value. The necessity of this criterion additional to the criterion $T_{t,abs}$ is justified as very irregular torque progresses may occur due to sophisticated driving situations.

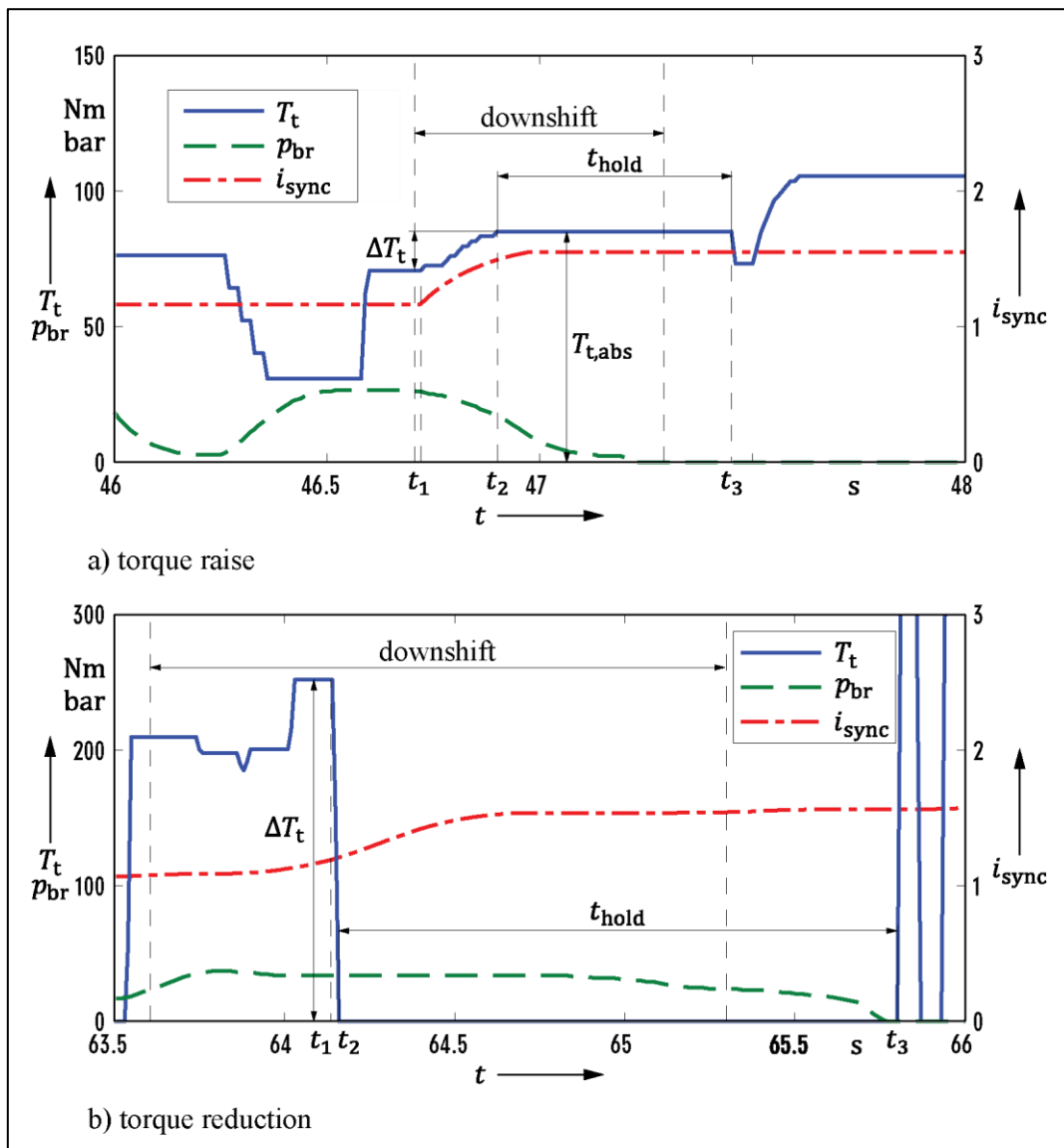


Figure 5.5: Diagram a) provides a clean torque rise, diagram b) shows a torque reduction due to a braking event

Figure 5.5 provides examples of downshifting events. Figure 5.5 a) provides a target torque rise ΔT_t and b) a target torque reduction ΔT_t due to a brake event. Although a brake application is obviously recognized in Figure 5.5 a) too, the torque is raised anyway, because the maximum applied brake pressure apparently does not exceed the threshold to lower the torque.

In Figure 5.5 a), a downshift event is returned from 46.70 s to 47.27 s. The diagram shows a section of the same simulated data that has been provided in Figure 5.4. The criterion t_{hold} outputs 0.55 s at a pre-control torque $T_{t,\text{abs}}$ of 85.07 Nm. The vehicle controller actuation Δt is carried out in 0.19 s and the torque difference ΔT_t is 14.43 Nm. This equals a gradient $grad_{\text{ds}}$ of 75.93 Nm/s.

In Figure 5.5 b), a torque reduction is provided due to a parallel running braking event. Figure 5.5 b) provides data of a real test drive carried out with the same BMW X3 that has been simulated in Figure 5.1 and Figure 5.4. Moreover, the transfer case is an ATC system again and the primary axle is the rear axle. The expert-tool detects a downshift state from 63.58 s to 65.31 s. The torque difference ΔT_t is -251.80 Nm and is lowered to a pre-control torque $T_{t,\text{abs}}$ of 0 Nm. The zero value is held for 1.64 s. The vehicle controller actuation has been carried out in 0.02 s in this example. This equals a gradient $grad_{\text{ds}}$ of -12 589.84 Nm/s. This high gradient can be explained, due to the circumstance that the threshold of the critical deceleration has been exceeded and the clutch has been opened immediately.

5.5 Braking

The vehicle's braking ability is not improved by a four-wheel drive. In contrast to an acceleration event, at which the 4WD system improves the available traction, standard braking systems always distribute the braking power to all four wheels. Therefore, it is not interesting if a 4WD system can improve the vehicle's braking ability, but rather how the system does not affect the braking loop. The tool detects braking according to the requirements of equation 5.36. Braking is detected for a data point if the brake pressure p_{br} is at least 5 bar or the brake pedal signal br indicates that the brake was applied. Furthermore, the velocity v_x should be beyond 2 m/s. If these requirements are true for a data point the array *brake* is filled with a 1:

$$brake = \begin{cases} 1, & ((p_{\text{br}} > 5 \mid br > 0.1) \& v_x > 2) \\ 0, & \text{else.} \end{cases} \quad (5.36)$$

The absolute indices of the braking states within the sampled data are then determined the same way as at the other states according to the equations 5.2, 5.3 and 5.4. Table 5.5 provides an overview of the added criteria for the state braking.

Table 5.5: Added assessment criteria for the driving state braking

Category	Criterion	Unit	
Driver	-		
Vehicle	Oversteering increase, oi	°/s	
	Instability, $T_{t,inst}$	Nm	
	Engine brake, $engine_{brake}$	%	
	System	Pre-control torque, $T_{t,abs}$	Nm
		Torque reduction, ΔT_t	Nm
Actuation time, Δt		s	
	Actuation gradient, $grad_{br}$	Nm/s	
	Holding time, t_{hold}	s	

Oversteering increase

Due to a braking event a vehicle can be led in an oversteering driving situation. The steering tendency can be quantified by the difference of the target yaw rate $\omega_{z,t}$ and the current yaw rate $\omega_{z,c}$ according to the theory of chapter 4.3. The criterion oi evaluates if the yaw rate difference $\Delta\omega_z$, which has been calculated according to equation 4.9, has increased due to the braking action or not. Therefore, the steering tendency of the first data point of the braking event is subtracted from the lowest yaw rate difference value $\Delta\omega_z$ that occurs during the further braking event. Then the criterion returns the absolute value, the yaw rate difference $\Delta\omega_z$ has increased due to the braking event:

$$oi = \text{abs} \left(\min \left(\Delta\omega_z \left(\text{brake}(10:\text{brake}(\text{end})) \right) \right) \right) - \text{abs} \left(\Delta\omega_z \left(\text{brake}(1) \right) \right). \quad (5.37)$$

If equation 5.37 returns a negative value, oversteering has increased due to the braking event and if a positive value is returned, understeering has increased. Attention has to be paid to the sign of the yaw rate difference $\Delta\omega_z$. Equation 5.37 is only valid for the case that the yaw rate difference $\Delta\omega_z$ at the first data index of the braking event has the same sign as the minimum occurring yaw rate difference $\Delta\omega_z$ of the further braking event. Within the tool, unequal signs of the yaw rate differences are considered and equation 5.37 is adapted to the circumstances.

In Figure 5.7 the same measured data of a real test drive on a high traction road surface as in Figure 5.5 b) is provided. The figure shows a target torque reduction due to a braking event. Braking is detected from 104.98 s to 109.23 s. No oversteering increase has been detected for this example.

Instability

Due to dynamic wheel load and stability reasons, that are discussed in chapter 3.3.1, the front wheels are braked more intensively than the rear wheels. In this situation the rear axle rotates faster than the

front axle. For safety reasons it is even legally established that the braking efficiency on the rear wheels is not entirely used. In certain situations the transfer case clutch has to be opened so that the clutch cannot try to balance the different rotational speeds of the axles to avoid instability. To detect situations in which the system does not act as it should, a criterion has been implemented. Therefore, every data point within the braking event, at which the braking pressure p_{br} exceeds the critical braking pressure p_{crit} and the transfer case clutch is applied with at least 10 % of the maximum clutch capacity T_{max} is detected and marked with a 1 within the array *instability*:

$$instability = \begin{cases} 1, & (p_{br}(brake) > p_{crit} \ \& \ T_t(brake) > 0.1 \cdot T_{max}) \\ 0, & \text{else.} \end{cases} \quad (5.38)$$

The vehicle specific critical braking pressure p_{crit} , which appears in equation 5.38, has to be determined for every vehicle and is defined by the critical deceleration. A threshold for the critical deceleration is defined at -2 m/s^2 . This threshold originates from the friction coefficient of snow that is approximately $0.2g$.

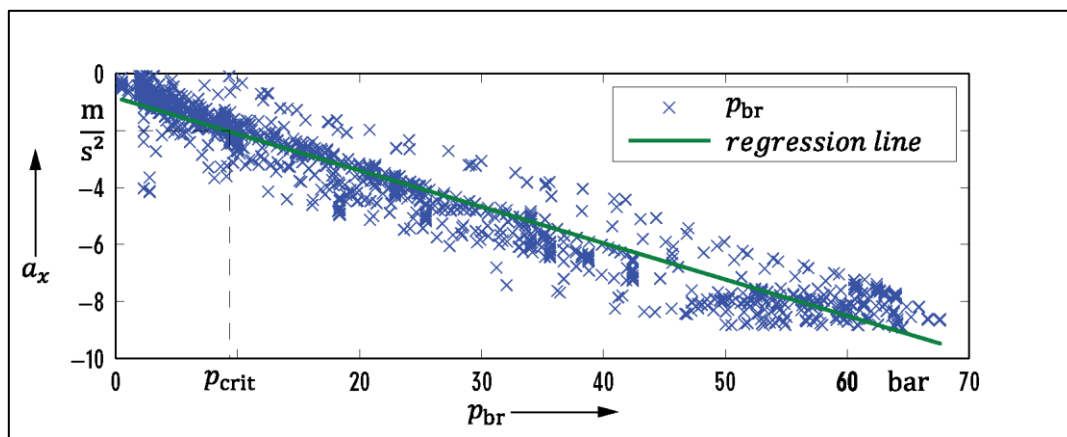


Figure 5.6: Determination of the critical braking pressure

The critical braking pressure p_{crit} is evaluated within the expert-tool by plotting every deceleration event due to a braking action of the whole sampled data file over the applied braking pressure p_{br} . The critical braking pressure p_{crit} , that corresponds to the critical deceleration, can be determined by means of the obtained regression line as shown in Figure 5.6. To reduce the data volume, the braking pressure values p_{br} and the values of the longitudinal acceleration a_x exclude data points that correspond to a braking pressure beneath 0.05 bar and a deceleration higher than -0.05 m/s^2 . The regression line rl of the selected data points can be created by means of the internal Matlab function *polyfit*:

$$rl = \text{polyfit}(p_{br}(a_x < -0.05 \ \& \ p_{br} > 0.05), a_x(a_x < -0.05 \ \& \ p_{br} > 0.05), 1) \quad , \quad (5.39)$$

where the 1 at the end of equation 5.39 means that the regression line is of first order. For the example of Figure 5.5 a critical braking pressure of 9.51 bar is determined.

The variables $inst_{end}$ and $inst_{on}$ are the data indices of the starting and ending points of the determined instability events that have been determined according to equation 5.38 within the braking state. The absolute indices of the starting points $inst_{on}$ and the ending points $inst_{end}$ can be detected according to the same principle as the starting and ending points of the driving states are determined according to the equations 5.2, 5.3 and 5.4. If the requirements of equation 5.38 are detected for a greater time period than 0.2 s, the position of this state is determined:

$$position = \text{find}((inst_{end} - inst_{on}) > 20), \quad (5.40)$$

where a time period of 0.2 s equals 20 data points at a sampling rate f of 10 ms. The criterion $T_{t,inst}$ now returns the maximum target torque T_t that has been applied to the transfer case clutch during the detected instability periods. Equation 5.41 only considers the start and end points of time periods that exceed 0.2 s according to equation 5.40:

$$T_{t,inst} = \max(T_t(inst_{on}(position):inst_{end}(position))). \quad (5.41)$$

With regard to a clean torque reduction in case of a braking situation, this criterion should return very low or even no values. For the test drive in Figure 5.7, the criterion instability does not detect the risk of instability due to a deferred torque reduction, as the torque is lowered according to the theory and $T_{t,inst}$ returns 0 Nm.

Engine brake

The vehicle's deceleration ability can be strengthened by the engine braking effect. The criterion returns the information, if engine braking simultaneously has occurred during a braking event by doing a simple query if the clutch was engaged or not:

$$engine_{br} = (cl(brake) == 1). \quad (5.42)$$

The criterion returns the percentage of the time that the clutch was engaged in relation to the total braking time:

$$engine_{brake} = \left(\frac{\text{length}(engine_{br}(engine_{br} \sim 0))}{brake(end) - brake(1)} \right) \cdot 100. \quad (5.43)$$

If the clutch was engaged during the whole braking event, the criterion returns 100 %. For the example of Figure 5.7 the criterion returns 67.14 %.

Pre-control torque

For the explained instability reasons of chapter 3.3.1, the connection between the front and the rear cardan shaft has to be interrupted during a braking maneuver in certain situations if the ESP orders to. According to defined pre-control characteristics the vehicle controller then reduces the target torque T_t to lower values in case of braking. The criterion $T_{t,abs}$ returns the value the target torque was reduced to due to a braking action.

The tool tries to find the value at which the target torque is held for a defined holding time. Therefore, the code controls if the torque rises or falls. If the torque rises, an irregular event apparently takes place and $T_{t,abs}$ returns 0 Nm. If a falling slope is detected, the tool determines the initiation of the torque reduction progress at t_1 . The program detects the reduction endpoint at t_2 , from whereon the torque is held at a certain value. For the example of Figure 5.6 the criterion $T_{t,abs}$ returns 0 Nm, as the clutch is completely opened.

Torque reduction / Actuation time / Actuation gradient / Holding time

Furthermore, criteria that evaluate the relative torque reduction ΔT_t and the actuation time Δt as at the upshift state according to the equations 5.28 and 5.29 have been implemented. Depending on the product, the transfer case should not exceed actuation times of 300 to 500 ms to reduce the torque. In addition to the relative torque reduction ΔT_t and the actuation time Δt , a criterion that returns the gradient of the actuation $grad_{br}$, as in equation 5.30 has been implemented.

For the braking example that is provided in Figure 5.7, the criterion ΔT_t outputs a reduction of -200.51 Nm within 0.02 s. This equals a gradient of -10 025.39 Nm/s. As for the state downshift, a criterion has been implemented that returns the time, the reduced target torque was held, due to the braking event. For the braking event of Figure 5.7 the criterion returns a holding time t_{hold} of 4.16 s.

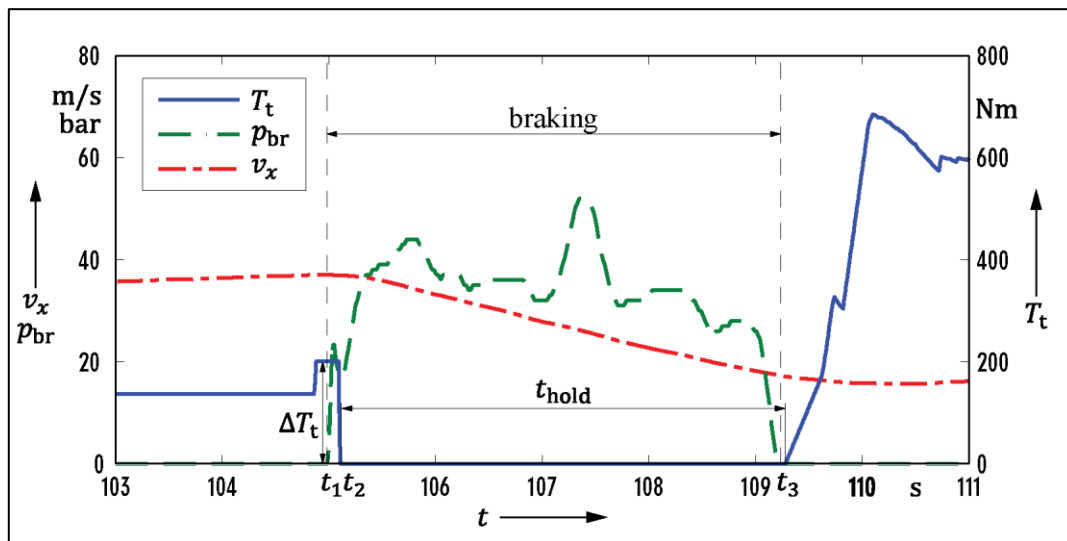


Figure 5.7: Target torque reduction due to a braking event

5.6 Acceleration

A four-wheel drive provides advantages concerning traction. However, due to the additional weight of the transfer case and friction within the additional components, the acceleration ability is not automatically improved in comparison to a rear-drive vehicle on a high traction road surface. Nevertheless, the more power the engine provides that cannot be transferred to the road with two drive wheels, the better performs the four-wheel drive system. An acceleration state is determined according to the requirements of equation 5.45. Acceleration is detected, if the longitudinal velocity v_x equals at least 10 km/h and the brake signal br indicates that the brake has not been applied. Furthermore, either the throttle pedal has to be applied by more than 20 % or the longitudinal acceleration a_x has to be beyond 0.8 m/s^2 :

$$acc = \begin{cases} 1, & \left(v_x > \frac{10}{3.6} \ \& \ (th > 20 \ | \ a_x > 0.8) \ \& \ br == 0 \right) \\ 0, & \text{else.} \end{cases} \quad (5.45)$$

The absolute indices of the detected acceleration states within the sampled data are then determined the same way as for the other states according to the equations 5.2, 5.3 and 5.4. Table 5.6 provides an overview of the added criteria for the driving state acceleration.

Table 5.6: Added assessment criteria for the driving state acceleration

Category	Criterion	Unit
Driver	-	-
Vehicle	Maximum velocity, $v_{x,max}$	km/h
	Acceleration duration, t_{accel}	s
	Elasticities, Δt	s
System	Rear drive, $v_{x,rd}$	km/h

Maximum velocity

This criterion $v_{x,max}$ returns the maximum speed that has been reached at the end of the acceleration event:

$$v_{x,max} = \max(v_x(acc)) \cdot 3.6 . \quad (5.46)$$

The maximum speed logically occurs at the last sampled data point of the acceleration event from whereon the velocity stays constant or falls again. Figure 5.8 provides the graphical representation of an acceleration event from 0 to 249.89 km/h, which is the value the criterion for the maximum velocity $v_{x,max}$ returns. The acceleration event in Figure 5.8 represents a real test drive acceleration event with a Maserati Quattroporte. The vehicle is equipped with an ATC transfer case with a clutch to the front cardan shaft. Hence the rear axle is the primary axle. The engine has a maximum power output of 400 hp.

Acceleration duration / Elasticities

This criterion returns the time that was needed to accelerate the vehicle from the initial state of the acceleration event up to the maximum detected speed of the acceleration event, which logically is the elapsed time of the whole identified acceleration event. Therefore, the start point of the acceleration event is subtracted from the point in time where the maximum velocity is reached within the observed acceleration event:

$$t_{accel} = t \left(acc \left(\min \left(\text{find} \left(\max(v_x(acc)) == v_x(acc) \right) \right) \right) \right) - t(acc(1)) . \quad (5.47)$$

Furthermore, criteria have been implemented in form of a separate Matlab function file that returns the acceleration elasticities for the categories that are listed in Table 5.7. In addition, the mean acceleration values for the provided ranges are returned.

Due to the differentiation of the states driveaway and acceleration, the tool detects the beginning of an acceleration event at 10 km/h as provided in equation 5.45. Nevertheless, for the correct output of the elasticity criteria and t_{accel} the absolute beginning of the acceleration event has to be considered.

Therefore, a simple *while* loop displaces the starting position of the acceleration event for the elasticity criteria and the acceleration duration t_{accel} to the point where the acceleration really starts.

The acceleration duration t_{accel} returns 37.92 s for the example of Figure 5.8. The values for the determined elasticities of the represented acceleration event in Figure 5.8 are listed in Table 5.7. It has to be taken into account that the acceleration event of Figure 5.8 is not a full-load acceleration.

Table 5.7: Acceleration results

Category	Δt [s]	$meana_x$ [m/s ²]
0 - 40 km/h	4.83	2.18
0 - 80 km/h	9.81	2.21
0 - 100 km/h	12.35	2.20
0 - 130 km/h	16.07	2.21
0 - 160 km/h	19.89	2.21

Rear drive

At high driving speeds, the advantages of a four-wheel drive are not as crucial anymore for the vehicle performance as at lower driving speeds. Therefore, many vehicle controllers open the clutch at a certain driving speed and interrupt the torque distribution if the rear axle is the primary axle. This measure protects the clutch from heavy loads in high speed situation and allows longer lifetimes. A criterion has been implemented that evaluates the speed $v_{x,\text{rd}}$ at which the interruption takes place. Therefore, low points within the target torque data progress due to brake applications, load changes, shifting events or other torque lowering causations have to be considered and ignored. An example for such a low point is provided in Figure 5.8 from 21.75 s to 22.86 s, where the target torque is momentarily reduced due to a load change. Another short torque reduction that has to be ignored is visible at 12.4 s. The tool tries to find the point at which the torque is permanently reduced to 0 Nm or a low value as in the example of Figure 5.8 as a result of a high driving speed. Therefore, it is controlled if the rear axle is the primary axle. Furthermore, a torque reduction due to high velocities is only detected if the vehicle is accelerated beyond 100 km/h. The torque has to be lower than the defined threshold of 5 % of the maximum clutch capacity T_{max} :

$$reardrive = (T_t < 0.05 \cdot T_{\text{max}}) . \quad (5.48)$$

The criterion only outputs a result, if the condition according to equation 5.48 is held for more than 2 s. In this case, the criterion returns the vehicle's velocity at the first detected data point of the condition:

$$v_{x,\text{rd}} = v_x(reardrive(1)) . \quad (5.49)$$

For the example of Figure 5.8 the criterion returns 169.39 km/h.

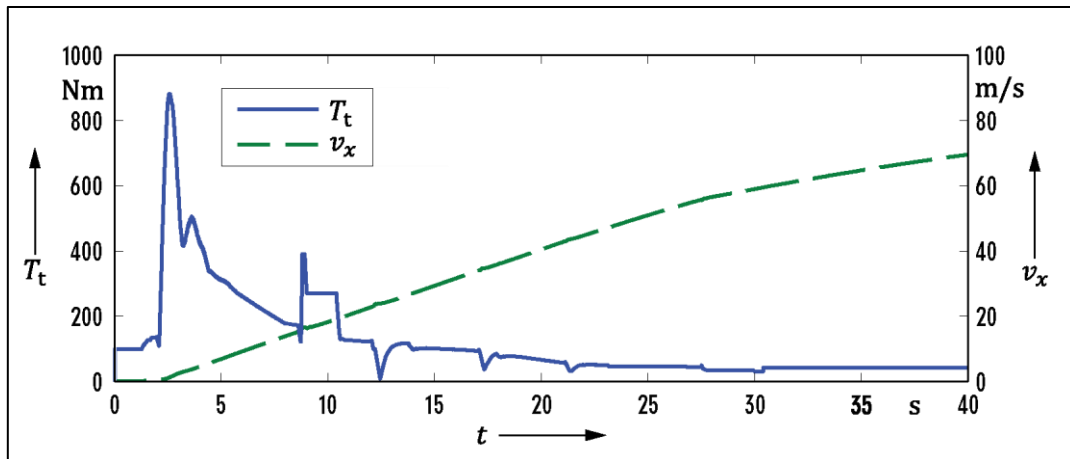


Figure 5.8: Acceleration from 0 to 249.89 km/h

5.7 4WDASR

The four-wheel drive anti-slip regulation comes into action if the rotational speed difference between the front and the rear axle exceeds a certain threshold, and a balancing of the rotational speeds is obviously required due to the current driving situation. In this case, the 4WDASR locks the axles to prevent the axle that has less traction available from slipping.

For the engineer, the behavior of the anti-slip regulation and the impact on the drivetrain and the driving situation is of interest. Table 5.8 shows an overview of all added criteria for the 4WDASR state. Mostly, the four-wheel drive anti-slip regulation is active during driveaway and acceleration states. Generally, a data signal that returns the information if the anti-slip regulation was switched on or not is always available. The variable *4wdasr* contains the absolute indices of the observed 4WDASR event within the sampled data.

Table 5.8: Added assessment criteria for the driving state 4WDASR

Category	Criterion	Unit
Driver	-	-
Vehicle	-	-
System	Restbinding, rb	-
	Overlocking time, $lock_{sr}$	%
	Overlocking torque, $lock_{srmean}$	%
	Axle, $axle$	-
	Holding time, t_{hold}	s
	Pre-control torque, $T_{t,abs}$	Nm

Restbinding

A non-desired secondary effect of a locked drivetrain is binding. Binding may occur during cornering when the clutch is closed and affects the driving comfort. Furthermore, binding will inevitably lead to component failure. Due to a 4WDASR event, the cardan shafts are connected rigidly and therefore the danger of binding exists. The criterion returns the information if binding is detected subsequently to the current 4WDASR event. The criterion observes a time period of 0.2 s after the 4WDASR event, as 0.2 s equal 20 data points at a sampling rate f of 10 ms:

$$bind_{after} = 4wdasr(end):4wdasr(end) + 20 . \quad (5.50)$$

A logical query as provided in equation 5.51 is executed for the evaluated time period $bind_{after}$, to detect the risk of binding according to the theory of chapter 4.6. The criterion restbinding rb returns 1, if a risky condition is detected and 0, if not:

$$rb = \text{any} \left(\frac{T_t(bind_{after}) - T_{bind}}{T_{bind}} > 0.2 \right) \mid \text{any}(T_d(bind_{after}) \sim = 0) . \quad (5.51)$$

Figure 5.9 shows an example of a 4WDASR event of the same simulation data that has been provided in Figure 5.4. Figure 5.9 shows a detected 4WDASR event from 63.75 s to 63.94 s. Although the 4WDASR event takes place simultaneously to a cornering and an acceleration event, no restbinding is detected in the example of Figure 5.9.

Overlocking time

It is not reasonable to actuate the transfer case clutch with more torque than the secondary axle is able to transfer to the road. This condition would lead to excessive load on the clutch and to a waste of energy. The condition when the clutch provides more torque than the secondary axle is maximally able to transfer to the road is called overlocking. For the case that the front axle is the primary axle, overlocking is detected according to:

$$x_{over} = \max \left(\frac{T_t - \text{abs}(T_r)}{\text{abs}(T_r)}, 0 \right) . \quad (5.52)$$

In equation 5.52 the variable x_{over} returns the percentage of the excessive target torque amount T_t , in relation to the effective torque on the rear axle T_r . The absolute values in the equations 5.52 and 5.53 consider the case that the vehicle is coasting. Also during coasting overlocking can be quantified. The equations 5.52 and 5.53 return 0, if no overlocking is detected.

If the rear axle is the primary axle, overlocking is detected according to equation 5.53. In equation 5.53 the variable x_{over} returns the percentage of the excessive target torque amount T_t , in relation to the effective torque on the front axle T_f :

$$x_{over} = \max \left(\frac{T_t - \text{abs}(T_f)}{\text{abs}(T_f)}, 0 \right) . \quad (5.53)$$

The array ind_{lock} contains the indices at which overlocking is determined. Overlocking is determined only if the overlocking variable x_{over} returns a value that exceeds 5 % and the applied target torque T_t exceeds a threshold of 20 Nm:

$$ind_{lock} = \text{find}(x_{over}(4wdasr) > 0.05 \& T_t(4wdasr) > 20) . \quad (5.54)$$

The overlocking time criterion $lock_{sr}$ returns the percentage of the time the clutch was overlocked, in relation to the total time of the 4WDASR event:

$$lock_{sr} = \frac{\text{length}(ind_{lock})}{\text{length}(4wdasr)} \cdot 100 . \quad (5.55)$$

According to [33] the clutch should not be overlocked. An overlocked clutch equals a rigid connection among the axles and yields in a torque distribution corresponding to the dynamic wheel load distribution. This limits the individual distribution to the secondary axle.

Figure 5.9 provides a visual example of overlocking, as the target torque T_t is held due to a 4WDASR event at 230.3 Nm from 63.80 s to 64.40 s, but the secondary torque T_{sec} does not utilize the provided transfer case torque capacity. In the example of Figure 5.9, the overlocking time criterion $lock_{sr}$ returns 10 % overlocking for the 4WDASR event that already ends at 63.94 s. An extension of this criterion could be to analyze the overlocking behavior over the whole holding time t_{hold} , as a detected 4WDASR event is usually over while the torque is still held at a constant value.

Overlocking torque

In addition to the criterion that computes the percentage of the locked time, it is as important to have the information about the absolute magnitude the clutch was overlocked during the event. Due to general inconstant characteristics of the torque distribution during a 4WDASR event and hence an inconstant progress of the overlocking value x_{over} , the criterion $lock_{srmean}$ returns the mean overlocking value x_{over} of the total sampled 4WDASR event:

$$lock_{srmean} = \text{mean}(x_{over}(4wdasr(ind_{lock}))) \cdot 100 . \quad (5.56)$$

The overlocking torque criterion $lock_{srmean}$ returns a mean overlocking of 5.68 % for the detected overlocking indices ind_{lock} of the example in Figure 5.9.

Axle

This criterion returns the information if the front or the rear axle is slipping:

$$axle = (v_f(4wdasr(1)) > v_r(4wdasr(1))) . \quad (5.57)$$

The criterion $axle$ returns 1 if the front axle slipped and 0 if the rear axle slipped. Therefore, the criterion returns 0 for the example of Figure 5.9 as the rear axle speed v_r is higher than the front axle speed v_f .

Pre-control torque / Holding time

Figure 5.9 provides a typical target torque curve progression of a 4WDASR event, as the torque is raised for a certain period of time to strengthen the connection between the axles. The criterion pre-control torque $T_{t,abs}$ returns the value of the held torque, which is generally the maximum torque that occurred during the 4WDASR event:

$$T_{t,abs} = \max(T_t(4wdasr)) . \quad (5.58)$$

At the 4WDASR event of Figure 5.9 the pre-control torque $T_{t,abs}$ returns 230.34 Nm. To prevent irritations and inconsistencies the applied torque is held for a minimum time, also if the speed differences are already balanced. The criterion holding time t_{hold} returns the length of the time period the torque was held:

$$t_{hold} = t_2 - t_1 . \quad (5.59)$$

As the 4WDASR can be over before the applied torque is reduced again, a *while* loop determines the ending point t_2 of the held time period. For the example of Figure 5.9 the criterion holding time t_{hold} returns 0.61 s.

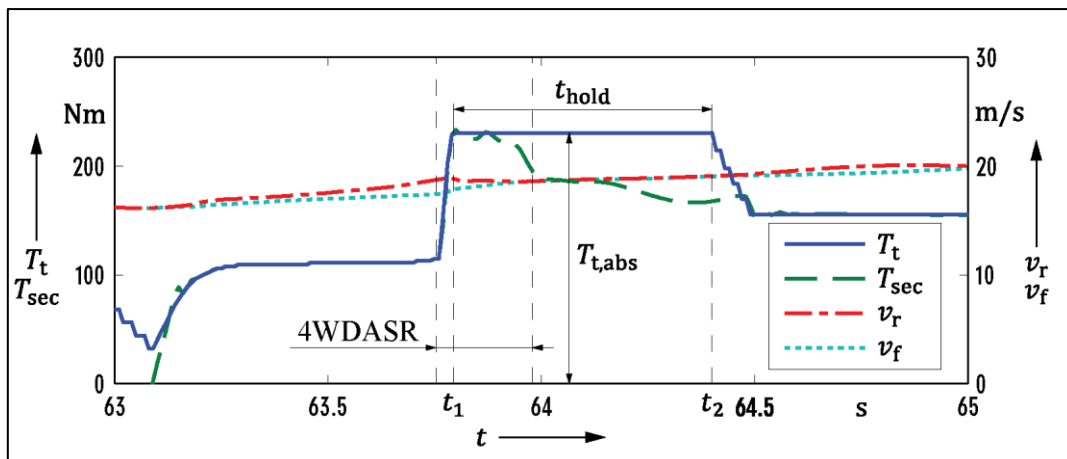


Figure 5.9: Four wheel drive anti-slip regulation event

5.8 Cornering

A very important topic considering vehicle dynamics is cornering. Lateral dynamics can be influenced by the transfer case by varying the torque distribution between the axles. As described in chapter 2.3.4, the transfer case is able to balance unwanted under- and oversteering events. Therefore, the transfer case system's behavior during cornering is of interest for the engineer that analyzes a driven curve. The expert-tool detects the driving state cornering by evaluating if the absolute value of the steering wheel angle δ_s is higher than 20° and the absolute value of the lateral acceleration a_y is beyond 1.5 m/s^2 :

$$cornering = \begin{cases} 1, & (\text{abs}(\delta_s) > 20 \ \& \ \text{abs}(a_y) \geq 1.5) \\ 0, & \text{else.} \end{cases} \quad (5.60)$$

The absolute indices of the detected cornering states within the sampled data file are then determined the same way as for the other states according to the equations 5.2, 5.3 and 5.4. Table 5.9 provides a list of the added assessment criteria for the driving state cornering.

Table 5.9: Added assessment criteria for the driving state cornering

Category	Criterion	Unit
Driver	Shifting, $\Delta gear$	-
	Braking, $braking_{curve}$	-
Vehicle	Stability, β_{max}	°
System	Slip inner front wheel, $slip_{ifw}$	1/0
	Drag torque, $T_{d,min}$	Nm

Shifting

Changes in the dynamic wheel load distribution during cornering can have huge effects on the stability of the vehicle that are expressed by under- or oversteering events. Dynamic wheel load changes can be caused by accelerating, braking, shifting or a load transfer. Therefore, this criterion returns the information if shifting or multiple shifting has occurred during the observed cornering state. The criterion $\Delta gear$ returns the difference between the gear that has been engaged at the beginning and the gear that is engaged at the end of the cornering event:

$$\Delta gear = gear(cornering(1)) - gear(cornering(end)) . \quad (5.61)$$

Braking

As mentioned before, the knowledge about possible influences on the dynamic wheel load distribution can be necessary. This criterion returns the simple information, if braking has occurred or not during the examined cornering state. The detected braking states of chapter 5.5 are numbered and listed. The variable $brake_{on}$ contains the starting points of all detected braking events and the variable $brake_{end}$ contains the ending points of all detected braking events. In equation 5.62 the starting points of all braking states are compared to the first point in time of the currently observed cornering event. Furthermore, the ending points of all braking events are compared to the end point in time of the currently observed cornering event. If the start point in time and the end point in time of a brake event are within the temporal boundaries of the observed cornering event, the Matlab command *find* returns the number of the detected braking state. If more braking states are detected for the current observed cornering event, equation 5.62 returns the number of the first detected braking event by applying the Matlab command *min*:

$$braking_{curve} = \min \left(\text{find} \left(brake_{on} > t(cornering(1)) \ \& \ brake_{end} < t(cornering(end)) \right) \right) . \quad (5.62)$$

Stability

According to chapter 3.3.1, the side-slip angle β can be considered as a measure for the vehicle's stability. An estimation of the side slip angle signal can be calculated according to the suggestions of chapter 4.4. Within the scope of this thesis, the side slip angle β was estimated according to the kinematic model of chapter 4.4.1. An accurate signal of the side slip angle β is available for simulated test drives.

Different literature entries suggest different ways to use the information of the side slip angle β . In this thesis, the requirement for a small maximum side slip angle β_{\max} over the cornering state was adapted. The side slip angle β is the angle between the velocity vector of the vehicle in the vehicle's center of gravity and the vehicle's longitudinal axis. According to [10], the sign of the side slip angle β changes when a vehicle is accelerated from low to high velocities, due to the tire slip angle influence on the wheels. The side slip angle β is assumed to be negative for low velocity values and positive at high velocity values in left curves. Therefore, positive values of the side slip angle β can be considered for oversteering situations in left curves. The criterion β_{\max} has been implemented that returns the side slip angle's maximum value that occurred during the cornering event. If a left curve is detected, the maximum side slip angle β that occurred during the event is returned:

$$\beta_{\max} = \max(\beta(\text{cornering})) . \quad (5.63)$$

If the evaluated curve is a right curve, the minimum side slip angle β is returned:

$$\beta_{\max} = \min(\beta(\text{cornering})) . \quad (5.64)$$

Slip inner front wheel

Due to the effect of lateral acceleration, wheel load is transferred to the curve outer wheels during cornering. If the dynamic wheel load of the inner front wheel falls below a certain threshold, the wheel will start to slip if it is a powered wheel. Moreover, it will lose its lateral guidance. Naturally, this describes a non-desired situation. The vehicle tends to understeer and traction ability is lost. Limited slip differentials provide a mechanical solution to prevent the inner front wheel from slipping. An electronic solution can be provided by replacing the LSD by a cheaper open differential system that simulates the function of a LSD by targeted wheel brake interventions. The disadvantage of such a system is that brake interventions consume energy.

A criterion has been implemented that returns the information, if the unwanted condition of a slipping inner front wheel has occurred during the examined curve. The criterion recognizes, if the left or the right wheel is the inner wheel. Furthermore, it compares the wheel speed of the identified inner wheel with the vehicle's velocity and the speed of the other front wheel. Logically, the speed of the inner front wheel should be lower than the others. The variable $sifw_{\text{on}}$ contains the chronological starting point indices of the states where the inner front wheel was turning faster than the outer front wheel. The variable $sifw_{\text{end}}$ contains the ending point indices of these states. If slipping of the inner front wheel is detected for more than 0.1 s the criterion $slip_{\text{ifw}}$ returns a brief 1:

$$slip_{\text{ifw}} = \text{any}(\text{find}(sifw_{\text{end}} - sifw_{\text{on}} > 10)) . \quad (5.65)$$

The time period of 0.1 s equals 10 data points at a sampling rate f of 10 ms.

Drag torque

If a drag torque T_d has circulated in the drivetrain during the cornering event, this criterion returns the maximum drag torque T_d that has occurred during the examined cornering state. The criterion is calculated according to the same way as the maximum drag torque $T_{d,min}$ has been calculated for the state driveaway in chapter 5.2.

5.9 Turning into a Curve

Before the real cornering state begins, the state turning into the curve is determined.

Table 5.10: Added assessment criteria for the driving state turning into a curve

Category	Criterion	Unit
Driver	-	-
Vehicle	-	-
System	Drag torque, $T_{d,min}$	Nm

Drag torque

The determination of an occurring drag torque has been implemented for the state turning into a curve the same way, as for the states driveaway in chapter 5.2 and cornering in chapter 5.8.

6 Summary

During the last decades, four-wheel drive systems have changed from pure mechanical traction systems, which were mainly designed for off-road use, to complex mechatronic solutions. Due to the possibility of 4WD systems to provide a positive impact on the vehicle's driving behavior, they are more and more applied for everyday road traffic.

The variety of different transfer case systems is huge. On this point, different OEMs rely on distinct concepts. Generally, transfer case systems can be classified into active, semi-active or passive systems. Active systems in general base on the principle of actuated multi-plate clutches which are actuated by a vehicle controller. Passive systems do not require external energy for actuation. The distributed torque arises as a result of internal friction in the system. Semi-active systems represent a mixture between active and passive transfer case systems.

Magna Powertrain offers a wide range of different transfer cases with various torque distribution alternatives to their customers. Most of these concepts rely on an active torque distribution between the front and the rear axle by an externally controlled multi-plate wet clutch. This technology can be seen as the company's core competence.

Due to their controllability, externally controlled transfer case systems can function as an additional vehicle dynamic control component. The ESP's control concept usually exists out of the two control loops engine management and brake management. An externally controlled transfer case system extends the control concept with a further control loop, the longitudinal torque management.

The adjustment of drivetrain systems of modern motor vehicles requires expert knowledge and experience. Magna Powertrain made the attempt to integrate specific knowledge of the fields pre-adjustment, analysis and fine-tuning into an applicable expert-tool.

Within the scope of this thesis, assessment criteria have been added to the already existing expert-tool. Already implemented criteria have been verified. As the tool had to be prepared for series utilization, the compatibility of the assessment criteria had to be assured for real test drives and simulation tests. To guarantee an accurate evaluation process, substitution calculations have been added to the tool. These are especially important for the evaluation of road test data, as not every signal is available. Substitution calculations have been added to determine the vehicle's steering tendency, binding in the drivetrain and the effective torque distribution. Furthermore, a method has been implemented to estimate the side slip angle.

The expert-tool originally has been designed to evaluate circuit test drives. The expert-tool identifies particular driving states, such as cornering or braking and analyzes these states by the use of appropriate assessment criteria. The tool subdivides the sampled data of a test drive into the driving states standstill, driveaway, upshift, downshift, braking, coasting, load change, acceleration, four-wheel drive anti-slip regulation, turning into a curve and cornering. The states upshift and standstill have been added additionally to the existing states within the scope of this thesis.

Within the design and adjustment stage of a four-wheel drive system, conflicting goals occur between traction, driving dynamics, comfort, system load and efficiency requirements. Due to this conclusion, the assessment criteria have been classified according to these categories. Furthermore, the criteria

have been distinguished according to their causation. Therefore, the criteria have been classified into driver-, vehicle- and system-related criteria. Criteria have been found for all three categories. However, as the development and production of externally controlled transfer cases is a core competence of Magna Powertrain, the evaluation of these systems has also stayed the main focus of this thesis. Therefore, mainly system-related criteria have been implemented.

Moreover, it was the intention to create an expert-tool that allows engineers, which have not been integrated in the software's development process, to work with the program. Therefore, easy usability has high priority. With regard to usability, the graphical user interface of the expert-tool has been edited and developed. A documentation section with explanations and annotations for every assessment criterion has been implemented. The section contains a short explanation and the designation of the physical unit for every assessment criterion. As the expert-tool is based on Matlab and consists of a coherent file structure, it was important to make the software tool independent from local data paths. Therefore, a separate m-file has been created that enables the user to open the tool at any workstation in any folder.

Future Work

Technical literature that deals with the objective assessment of transfer case systems is relatively rare, considering the dimension of the automotive industry. The evaluation of transfer case systems by means of objective measurement criteria seems to be a topic, the big automotive groups treat internally only. Therefore, a research topic to continue could be the finding of transfer case specific driving maneuvers, including associated objective performance criteria.

Considering the expert-tool, further work could be done with regard to the side slip angle estimation by determining the side slip angle according to a more accurate physical model and by implementing a Luenberger observer or a Kalman filter to enhance the quality of the estimation. The expert-tool originally has been designed to evaluate simulated circuit test drives. However, especially concerning real road trials, very often only a single test maneuver is executed. Development engineers take the vehicle and evaluate a single vehicle parameter by undertaking the same maneuver more times in a row. Therefore, the extension of the expert-tool with regard to the evaluation of standardized and company internal driving maneuvers could be a further task for the future.

List of Figures

Figure 1.1: Configuration and environment of the expert-tool [34].....	2
Figure 2.1: Typical characteristic of the lateral force F_y over the tire slip angle α	6
Figure 2.2: Kinematic relations of the bicycle model, modified from [25].....	7
Figure 2.3: Forces while accelerating (simplified case).....	10
Figure 2.4: Circle of forces.....	12
Figure 2.5: 2WD and 4WD traction performance on off-road surface, modified from [30].....	13
Figure 2.6: Active Transfer Case 450 [15].....	17
Figure 2.7: Functionality of the BMW's DSC control loops.....	20
Figure 2.8: Oversteering and understeering, modified from [13].....	21
Figure 3.1: Steering tendency according to the self-steering gradient and the tire slip angle difference	32
Figure 3.2: Yaw rate amplification factor over velocity.....	33
Figure 3.3: Non-steady-state steering inputs.....	34
Figure 3.4: Steering step input.....	35
Figure 3.5: Single step sinusoidal input.....	37
Figure 3.6: Sine with dwell test.....	38
Figure 3.7: Yaw moment over side slip angle on high traction surface, modified from [13].....	44
Figure 3.8: Braking with blocked rear wheels in a) and blocked front wheels in b).....	45
Figure 4.1: Comparison of calculated and accurate yaw rate signals.....	49
Figure 4.2: Side slip angle estimation.....	53
Figure 4.3: Binding in the drivetrain with an imaginary travelling drag torque, modified from [12]...	58
Figure 4.4: Detection of binding in the drivetrain.....	59
Figure 4.5: Binding at slow cornering.....	61
Figure 5.1: Simulated test drive with a BMW X3 at the race circuit Fiorano. a) Driving route coordinates b) Torque/time diagram.....	64
Figure 5.2: Target torque behavior during the standstill and driveaway state of a simulated test drive with a BMW X3.....	68
Figure 5.3: Clutch closing.....	70
Figure 5.4: Upshift event from the 3rd into the 4th gear with an automatic gearbox.....	73
Figure 5.5: Diagram a) provides a clean torque rise, diagram b) shows a torque reduction due to a braking event.....	76
Figure 5.6: Determination of the critical braking pressure.....	79
Figure 5.7: Target torque reduction due to a braking event.....	81
Figure 5.8: Acceleration from 0 to 249.89 km/h.....	84
Figure 5.9: Four wheel drive anti-slip regulation event.....	87

List of Tables

Table 1.1: Assessment criteria classification.....	3
Table 2.1: Advantages of 4WD Systems [14]	14
Table 2.2: Four-wheel drive systems [30].....	15
Table 3.1: Examples of ISO-standard tests for the assessment of lateral dynamics.....	27
Table 3.2: Examples of specific maneuvers for the transfer case assessment.....	27
Table 3.3: Influential factors on assessment categories	28
Table 3.4: Assessment criteria to evaluate steady-state circular driving behavior according to [23] ...	29
Table 3.5: Criteria and reference values for the steering step input according to [23].....	36
Table 3.6: Criteria for the single step sinusoidal steering input according to [23].....	37
Table 3.7: Extracted driving states	39
Table 3.8: Possible assessment criteria for braking during cornering according to [23]	41
Table 4.1: Common measured variables for a road trial	47
Table 5.1: Added assessment criteria for the driving state standstill	65
Table 5.2: Added assessment criteria for the driving state driveaway	69
Table 5.3: Added assessment criteria for the driving state upshift.....	72
Table 5.4: Added assessment criteria for the driving state downshift.....	74
Table 5.5: Added assessment criteria for the driving state braking.....	78
Table 5.6: Added assessment criteria for the driving state acceleration.....	82
Table 5.7: Acceleration results	83
Table 5.8: Added assessment criteria for the driving state 4WDASR	84
Table 5.9: Added assessment criteria for the driving state cornering.....	88
Table 5.10: Added assessment criteria for the driving state turning into a curve	90

Bibliography

- [1] Breuer, B. and Bill, K.H.: *Bremsenhandbuch: Grundlagen, Komponenten, Systeme, Fahrdynamik*, Springer, Berlin, 4th edition, 2012
- [2] Die Presse, *Zu Premium gehört immer mehr auch Allrad*, Available at <http://diepresse.com/home/leben/motor/1323814/Zu-Premium-gehört-immer-mehr-auch-Allrad/>, 2012, Accessed on April 29th 2013
- [3] Diermeyer, F.: *Methode zur Abstimmung von Fahrdynamikregelsystemen hinsichtlich Überschlagsicherheit und Agilität*, TU München, Dissertation, 2008
- [4] Farelly, J. and Wellstead, P.: *Estimation of Vehicle Lateral Velocity*, In *Proceedings of the 1996 IEEE International Conference on Control Applications*, September 1996, Dearborn, USA
- [5] Fischer, G.; Pfau, W.; Braun, H. and Billig, C.: *xDrive – Der neue Allradantrieb im BMW X3 und BMW X5*, In *ATZ-Automobiltechnische Zeitschrift 02 (2004)*, pp. 92-102
- [6] Forkenbrock, G.J.; Elsasser, D. and O’Harra, B.: *NHTSA’S light vehicle handling and esc effectiveness research program*, Paper No. 05-0221, In *Proceedings of the 19th International Technical Conference on the Enhanced Safety Vehicles*, 2005, Washington DC, USA
- [7] German Federal Motor Vehicle and Transport Authority, *Anzahl der allradgetriebenen Pkw in Deutschland nach Bundesländern (Stand: 1. Januar 2009)*. Available at <http://de.statista.com/statistik/daten/studie/156190/umfrage/allradgetriebene-pkw-in-deutschland/>, 2009, Accessed on April 29th 2013
- [8] German Federal Motor Vehicle and Transport Authority, *Der Fahrzeugbestand im Überblick am 1. Januar 2013*, Available at http://www.kba.de/cln_033/nn_125398/DE/Statistik/Fahrzeuge/Bestand/2012__b__ueberblick__pdf,templateId=raw,property=publicationFile.pdf/2012_b_ueberblick_pdf.pdf/, 2013, Accessed on April 29th 2013
- [9] Grote, J. H. and Feldhusen, J.: *Dubbel: Taschenbuch für den Maschinenbau*, Springer, Berlin, 23rd edition, 2011
- [10] Heiing, B.; Ersoy, M. and Gies, S.: *Fahrwerkhandbuch: Grundlagen, Fahrdynamik, Komponenten, Systeme, Mechatronik, Perspektiven*, Vieweg+Teubner, Wiesbaden, 3rd edition, 2011
- [11] Henze, R.: *Beurteilung von Fahrzeugen mit Hilfe eines Fahrermodells*, Shaker, Herzogenrath, 1st edition, 2004
- [12] Lanzer, H.: *Vergleich verschiedener Allradsysteme*, Magna Powertrain, 2005
- [13] Liebemann, E.K.; Meder, K.; Schuh, J. and Nenninger, G.: *Safety and Performance Enhancement: The Bosch Electronic Stability Control (ESP)*, In *SAE Paper 2004-21-0060*, 2004

- [14] Meißner, T.C.: *Verbesserung der Fahrzeugquerdynamik durch variable Antriebsmomentenverteilung*, TU München, Dissertation, 2008
- [15] Magna Powertrain, *Products & Services*, Available at <http://www.magnapowertrain.com/capabilities/powertrain-systems/products-services>, 2013, Accessed on May 5th 2013
- [16] Mitschke, M. and Wallentowitz, H.: *Dynamik der Kraftfahrzeuge*, Springer, Berlin, 4th edition, 2004
- [17] Mohan, S.: *All-Wheel Drive/Four-Wheel Drive Systems and Strategies*, In *FISITA World Automotive Congress*, June 2000, Seoul, South Korea
- [18] Motor Trend, *4WD vs AWD. What's the Diff?*, Available at http://www.motortrend.com/features/consumer/1105_4wd_vs_awd/viewall.html/, 2011, Accessed on 05.05.2013
- [19] Obermüller, A.: *Modellbasierte Fahrzustandsschätzung zur Ansteuerung einer aktiven Hinterachskinematik*, TU München, Dissertation, 2012
- [20] Panzani, G.; Corno, M.; Tanelli, M.; Zappavigna A.; Savaresi, S.M.; Fortina, A. and Campo, S.: *Combined performance and stability optimization via central transfer case active control in four-wheeled vehicle*, In *Joint 48th IEEE Conference on Decision and Control and 28th Chinese Control Conference*, December 2009, Shanghai, P. R. China
- [21] Panzani, G.; Corno, M.; Tanelli, M.; Zappavigna A.; Savaresi, S.M.; Fortina, A. and Campo, S.: *Designing On-Demand Four-Wheel-Drive Vehicles via Active Control of the Central Transfer Case*, In *IEEE Transactions on intelligent transportation systems Vol. 11 No. 4 (2010)*, pp. 931 – 941
- [22] Pfeffer, P. and Harrer, M.: *Lenkungs-handbuch: Lenksysteme, Lenkgefühl, Fahrdynamik von Kraftfahrzeugen*, Vieweg+Teubner, Wiesbaden, 1st edition, 2011
- [23] Rompe, K. and Heißing, B.: *Objektive Testverfahren für die Fahreigenschaften von Kraftfahrzeugen*, TÜV Rheinland, Köln, 1st edition, 1984
- [24] Reif, K.: *Bosch Grundlagen Fahrzeug- und Motorentechnik: Konventioneller Antrieb, Hybridantriebe, Bremsen, Elektronik*, Vieweg+Teubner, Wiesbaden, 1st edition, 2011
- [25] Reif, K.: *Kraftfahrtechnisches Taschenbuch*, Vieweg+Teubner, Wiesbaden, 27th edition, 2011
- [26] Reif, K.; Renner, K. and Saeger, M.: *Fahrzustandsschätzung auf Basis eines nichtlinearen Zweispurmodells*, In *ATZ-Automobiltechnische Zeitschrift 07-08 (2007)*, pp.682 - 687
- [27] Schindler, E.: *Fahrdynamik: Grundlagen des Lenkverhaltens und ihre Anwendungen für Fahrzeugregelsysteme*, Expert, Renningen, 1st edition, 2007
- [28] Schramm, D.; Hiller, M. and Bardini, R.: *Modellbildung und Simulation der Dynamik von Kraftfahrzeugen*, Springer, Berlin, 1st edition, 2010
- [29] Stocker, M.: *Analyse erreichbarer Funktionsvorteile für Fahrdynamik-Regelsysteme durch eine online Reibwertabschätzung*, FH Joanneum, Master's thesis, 2008

- [30] Stockmar, J.: *Das große Buch der Allradtechnik*, Pietsch, Stuttgart, 1st edition, 2004
- [31] United Nations Economic Commission for Europe: *ECE Regulation No. 13-H*, 2010
- [32] Vietinghoff, A. von: *Nichtlineare Regelung von Kraftfahrzeugen in querdynamisch kritischen Fahrsituationen*, Karlsruhe Institute of Technology, Dissertation, 2008
- [33] Vockenhuber, M. and Ehmann, M.: *Dimensionierung einer Allradkupplung im Zielkonflikt zwischen verbesserter Fahrdynamik und Fahrzeuggewicht*, In *Systemanalyse in der KFZ-Antriebstechnik IV Vol. 79 (2007)*, pp. 42-51
- [34] Vockenhuber, M.; Ehmann, M. and Ruckenbauer, T.: *Funktionsapplikation für Allrad-Traktionsregelsysteme – Ein Expertentool für die klassische und modellbasierte Applikation verschiedener 4WD Traktionssystem-Architekturen*, 1. Automobiltechnisches Kolloquium, Garching, April 2009, Garching, Germany
- [35] Wendel, J.: *Integrierte Navigationssysteme: Sensordaten, GPS und Inertiale Navigation*, Oldenbourg, Munich, 2nd edition, 2011